Indirect Dark Matter Detection

Pierre Salati – Université de Savoie & **LAPTH**

1) The messengers of DM annihilation

2) High energy photons and the Galactic center

3) Hunting for neutrinos in the ice cap

4) Cosmic ray transport : a short overview

5) TeV antiprotons : a new window

6) Uncertainties i … ropagation

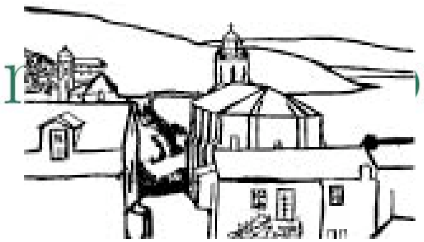

Cosmology and Particle Physics Beyond the Standard Models – Cargese – August 7, 2007

Indirect Dark Matter Detection

Pierre Salati – Université de Savoie & **LAPTH**

1) The messengers of DM annihilation

2) High energy photons and the Galactic center

3) Hunting for neutrinos in the ice cap

4) Cosmic ray transport : a short overview

5) TeV antiprotons : a new window

6) Uncertainties … propagation

Cosmology and Particle Physics Beyond the Standard Models – Cargese – August 7, 2007

The messengers of DM annihilation

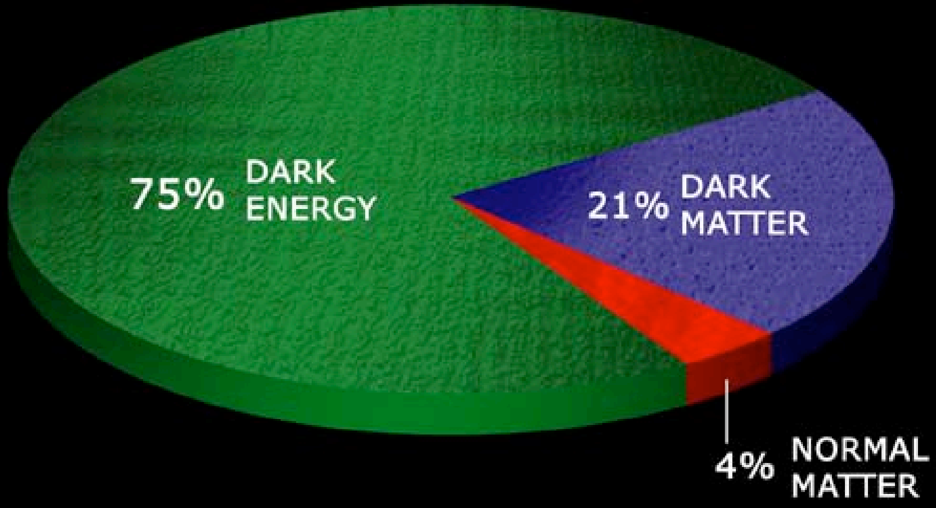

$$\chi + \chi \rightarrow f\bar{f}, W^+W^-, \ldots \rightarrow \bar{p}, \bar{D}, e^+, \gamma \;\&\; \nu\text{'s}$$

Weakly Interacting Massive particles – WIMPs – could be the major component of the haloes of galaxies. Their mutual annihilations would produce extra high–energy cosmic rays : the DM messengers

The messengers of DM annihilation

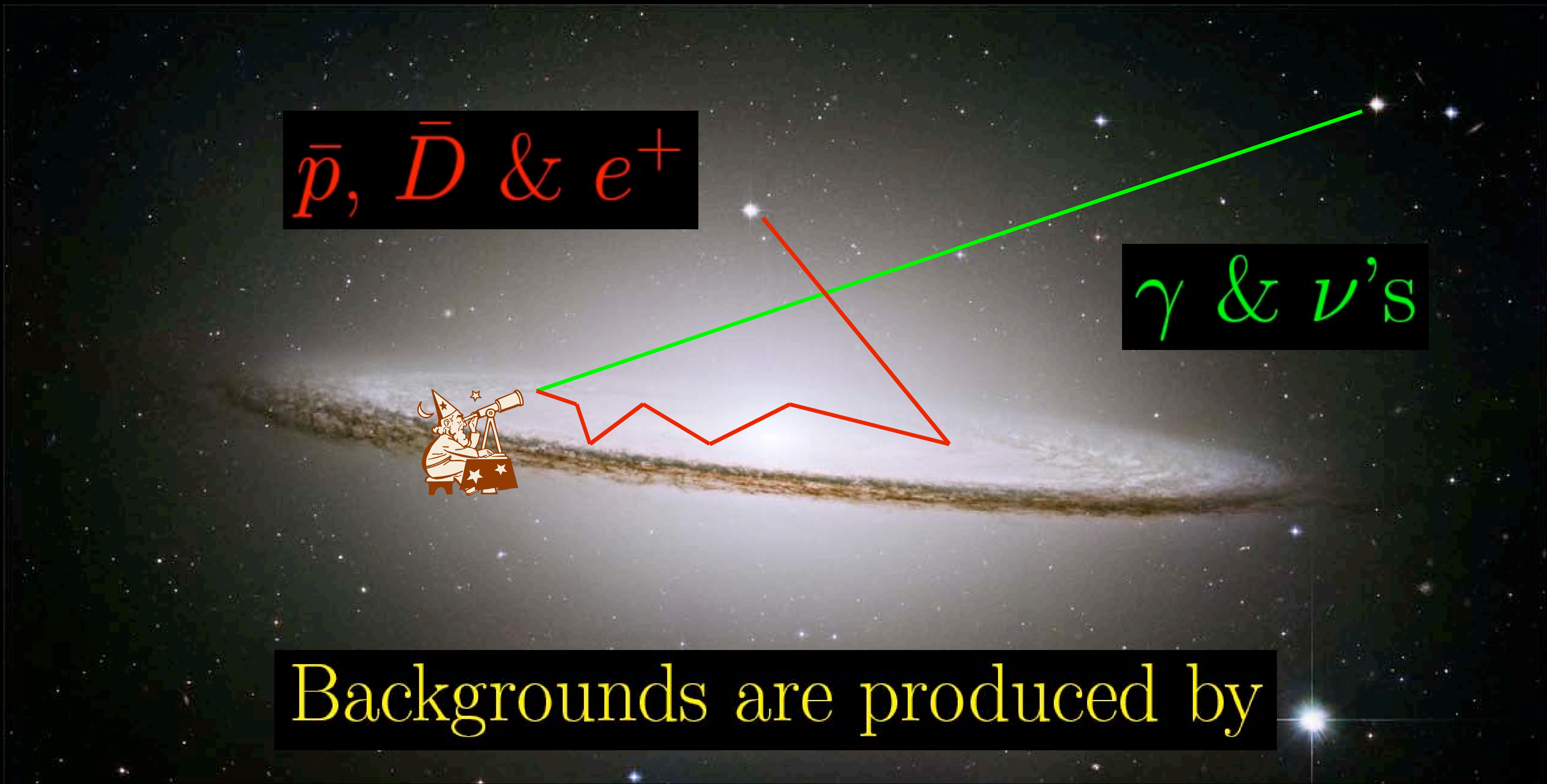

Backgrounds are produced by
standard processes within the Galactic disk !

Photons & Neutrinos

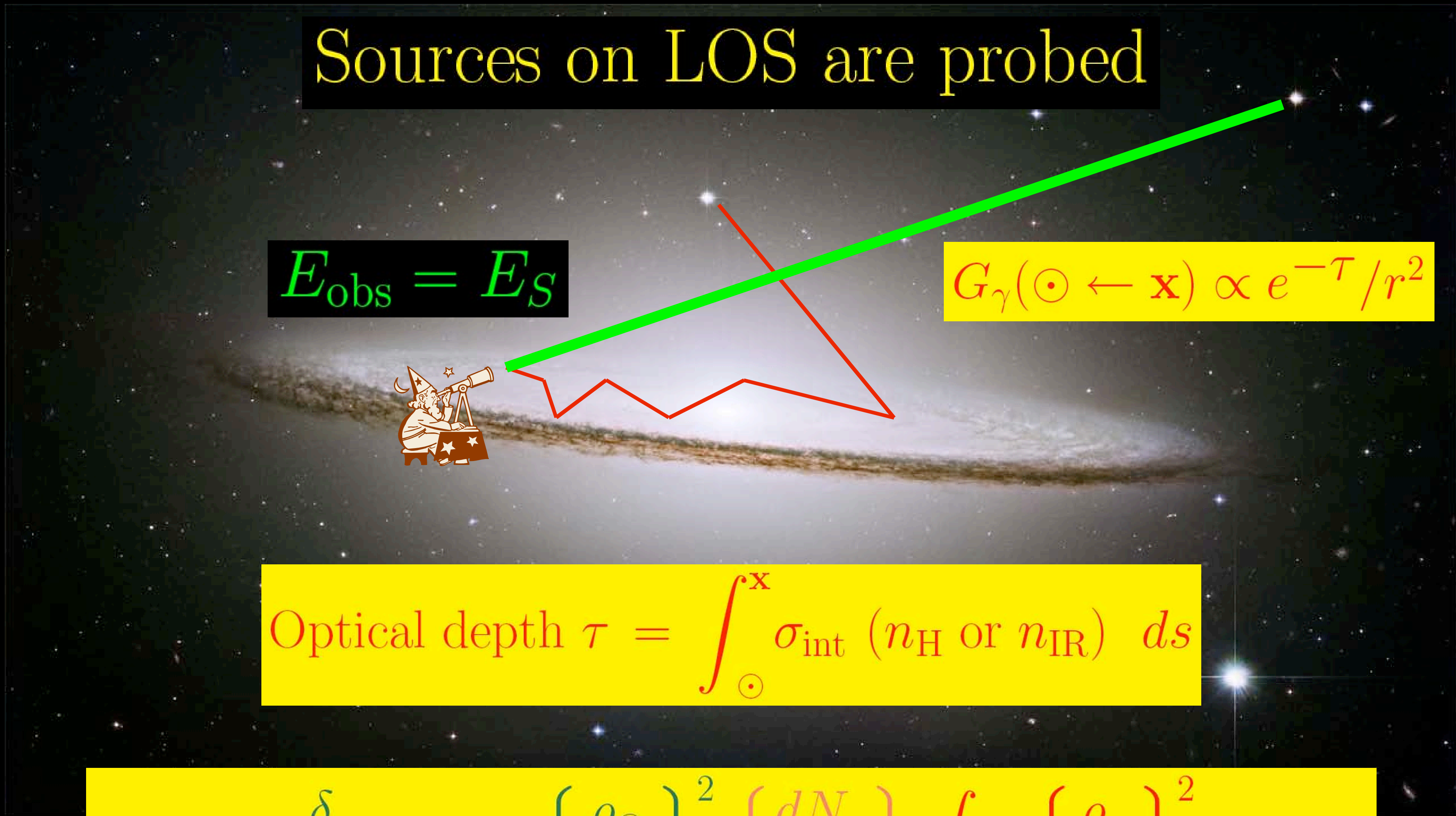

$E_{\rm obs} = E_S$

$G_\gamma(\odot \leftarrow \mathbf{x}) \propto e^{-\tau}/r^2$

$$\text{Optical depth } \tau = \int_\odot^{\mathbf{x}} \sigma_{\rm int}\,(n_{\rm H} \text{ or } n_{\rm IR})\; ds$$

$$\Phi_\gamma^{\rm DM} = \frac{\delta}{4\pi}\langle\sigma_{\rm ann} v\rangle \left\{\frac{\rho_\odot}{m_\chi}\right\}^2 \left\{\frac{dN_\gamma}{dE_\gamma}\right\} \int_{\rm los} \left\{\frac{\rho_\chi}{\rho_\odot}\right\}^2 e^{-\tau}\, ds$$

Cosmic Ray Antiprotons

A large portion of the MW is probed

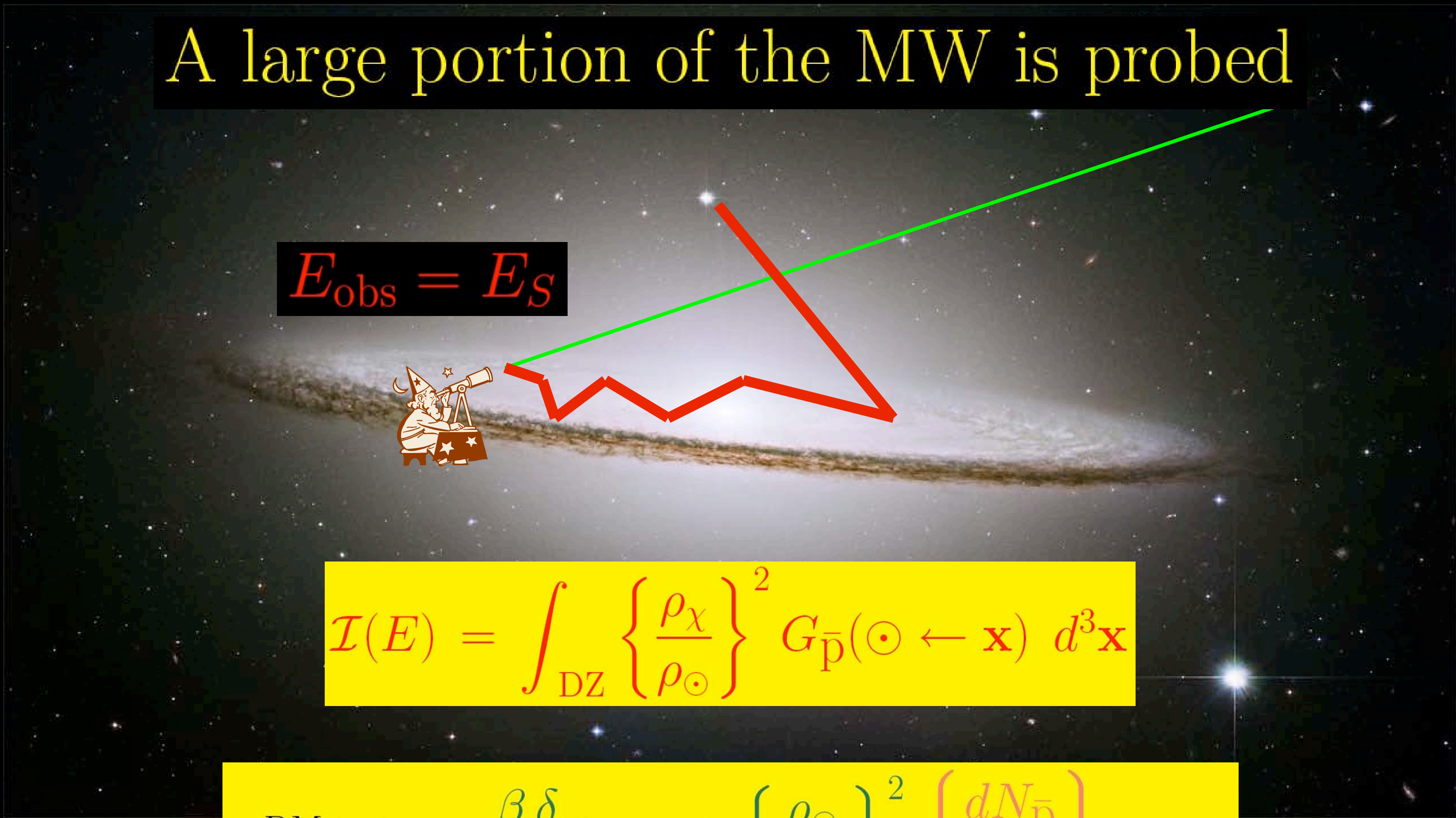

$E_{\rm obs} = E_S$

$$\mathcal{I}(E) \; = \; \int_{\rm DZ} \left\{ \frac{\rho_\chi}{\rho_\odot} \right\}^2 G_{\bar{\rm p}}(\odot \leftarrow \mathbf{x}) \;\; d^3\mathbf{x}$$

$$\Phi_{\bar{\rm p}}^{\rm DM}(E) \; = \; \frac{\beta\,\delta}{4\pi} \langle \sigma_{\rm ann} v \rangle \; \left\{ \frac{\rho_\odot}{m_\chi} \right\}^2 \; \left\{ \frac{dN_{\bar{\rm p}}}{dE_{\bar{\rm p}}} \right\} \; \mathcal{I}(E)$$

Cosmic Ray Positrons

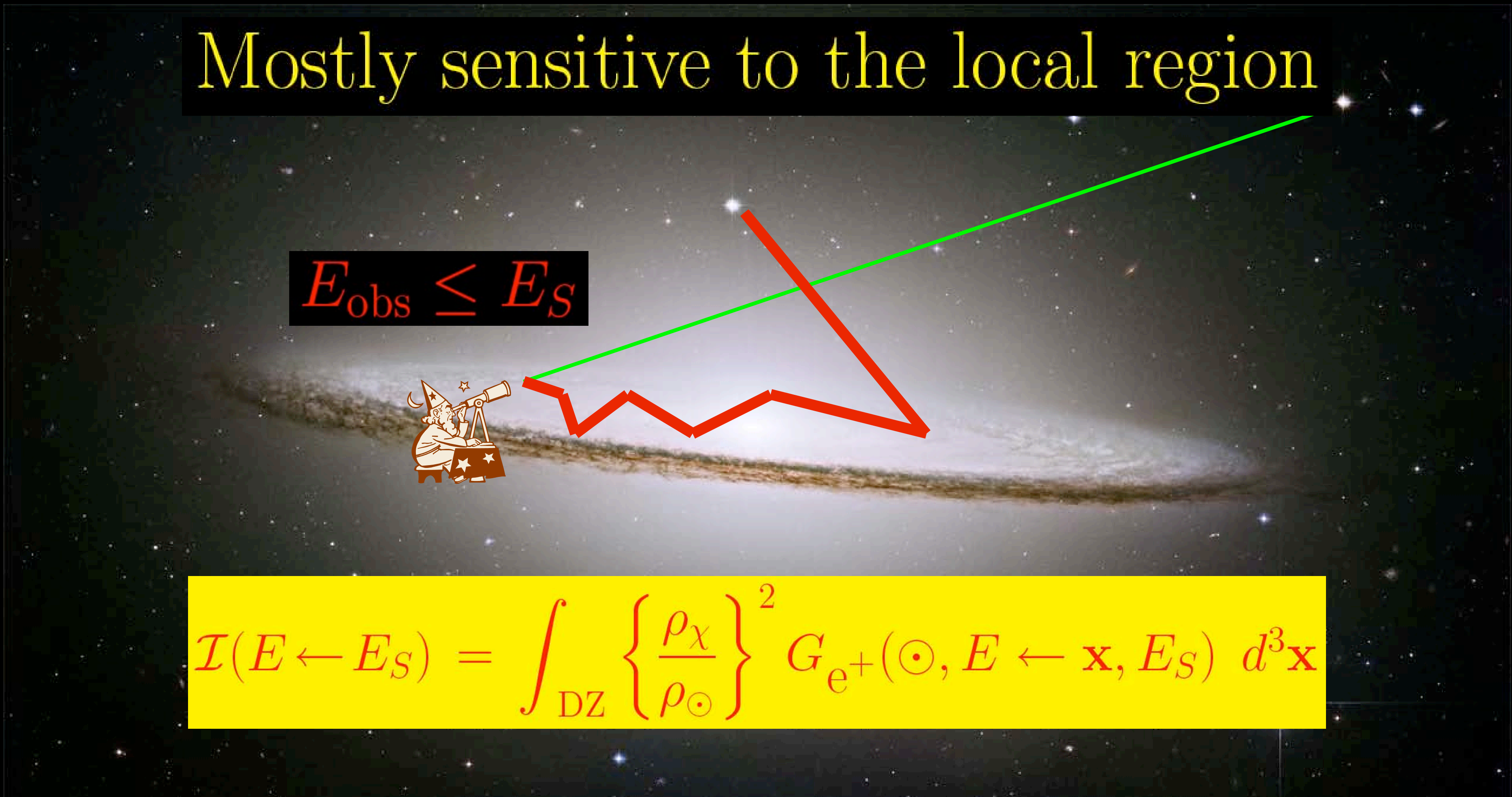

$$\mathcal{I}(E \leftarrow E_S) \;=\; \int_{\rm DZ} \left\{ \frac{\rho_\chi}{\rho_\odot} \right\}^2 G_{\rm e^+}(\odot, E \leftarrow \mathbf{x}, E_S)\; d^3\mathbf{x}$$

$$\Phi_{\rm e^+}^{\rm DM}(E) \;=\; \frac{\beta\,\delta}{4\pi} \langle \sigma_{\rm ann} v \rangle \left\{ \frac{\rho_\odot}{m_\chi} \right\}^2 \int_E^{m_\chi} dE_S \; \left\{ \frac{dN_{\rm e^+}}{dE_{\rm e^+}} \right\}_{E_S} \mathcal{I}(E \leftarrow E_S)$$

Indirect Dark Matter Detection

Pierre Salati – Université de Savoie & **LAPTH**

1) The mechanisms of DM annihilation

2) High energy photons and the Galactic center

3) Hunting for neutrinos in the ice cap

4) Cosmic ray transport : a short overview

5) TeV antiprotons : a new window

6) Uncertainties … propagation

Neutralino annihilations lead to

- A continuous spectrum of photons through the hadronization of quark–antiquark pairs :

$$\chi + \chi \rightarrow q\bar{q}, W^+W^-, \ldots \rightarrow \gamma + \ldots$$

- Monochromatic γ–rays through box–diagrams :

$$\chi + \chi \rightarrow \gamma + \gamma \;\&\; \gamma + Z^0$$

The corresponding flux at the Earth is

$$\Phi_{\gamma}^{\rm DM} = \frac{\delta}{4\pi} \langle \sigma_{\rm ann} v \rangle \left\{ \frac{\rho_{\odot}}{m_{\chi}} \right\}^2 \left\{ \frac{dN_{\gamma}}{dE_{\gamma}} \right\} \int_{\rm los} \left\{ \frac{\rho_{\chi}}{\rho_{\odot}} \right\}^2 ds$$

$$\Phi_{2\gamma\,{\rm line}}^{\rm DM} = 3.8 \times 10^{-13} \text{ photons cm}^{-2}\text{ s}^{-1}\text{ sr}^{-1} \frac{\langle \sigma v \rangle_{29}}{m_{100}^2} J(\vec{u})$$

Bergström, Ullio & Buckley, Astropart. Phys. 9 (1998) 137

$$\text{where} \quad J(\vec{u}) = \left\{ \rho_{\odot}^2 \, r_{\odot} \right\}^{-1} \int_{\rm los} \rho_{\chi}^2 \, ds$$

Black hole at the center of the Milky Way

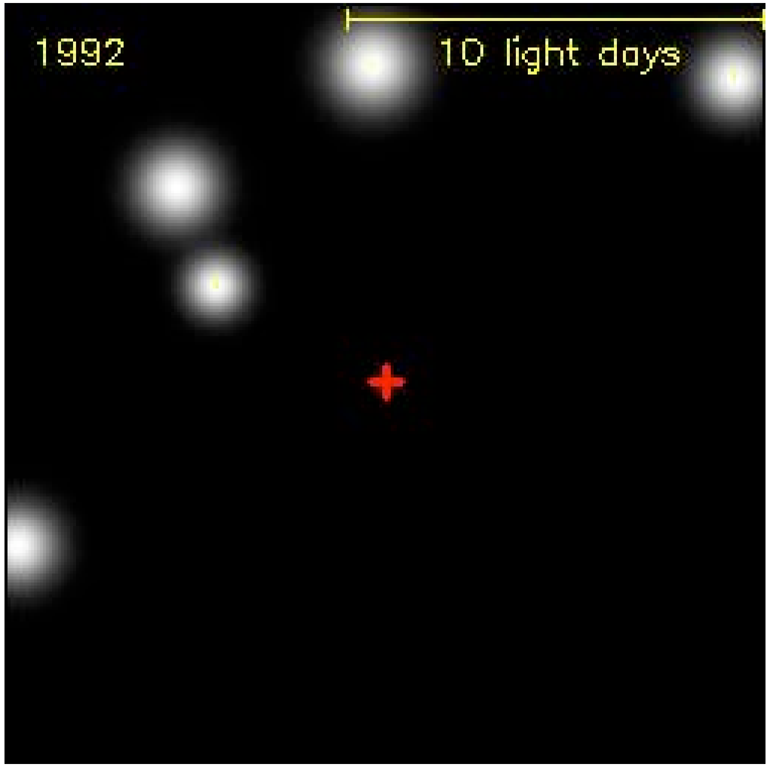

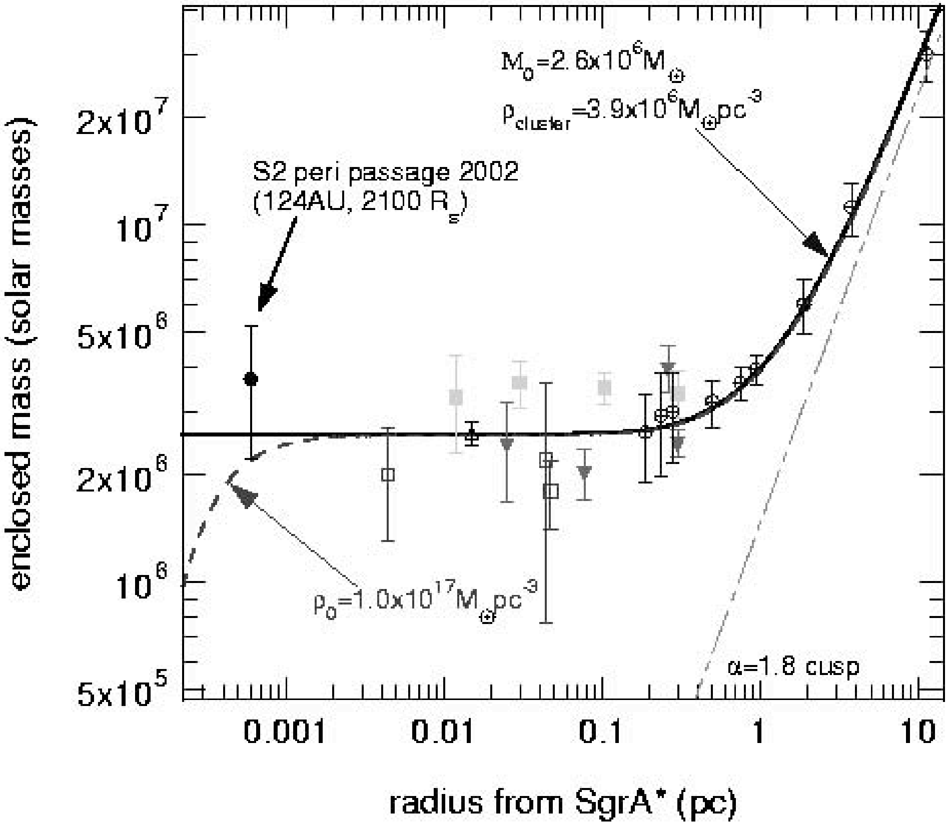

$$M_{\rm BH} = 4.1\,(\pm\,0.6) \times 10^6\ M_\odot$$

$$L_i = L_f$$
$$\Downarrow$$
$$r_i \, M_i \{r_i\} = r_f \, M_f \{r_f\}$$
$$\Downarrow$$
$$r_i \, M_i^{\rm h} = r_f \, M_{\rm BH}$$
$$\Downarrow$$
$$r_f \propto r_i^{4-\gamma}$$

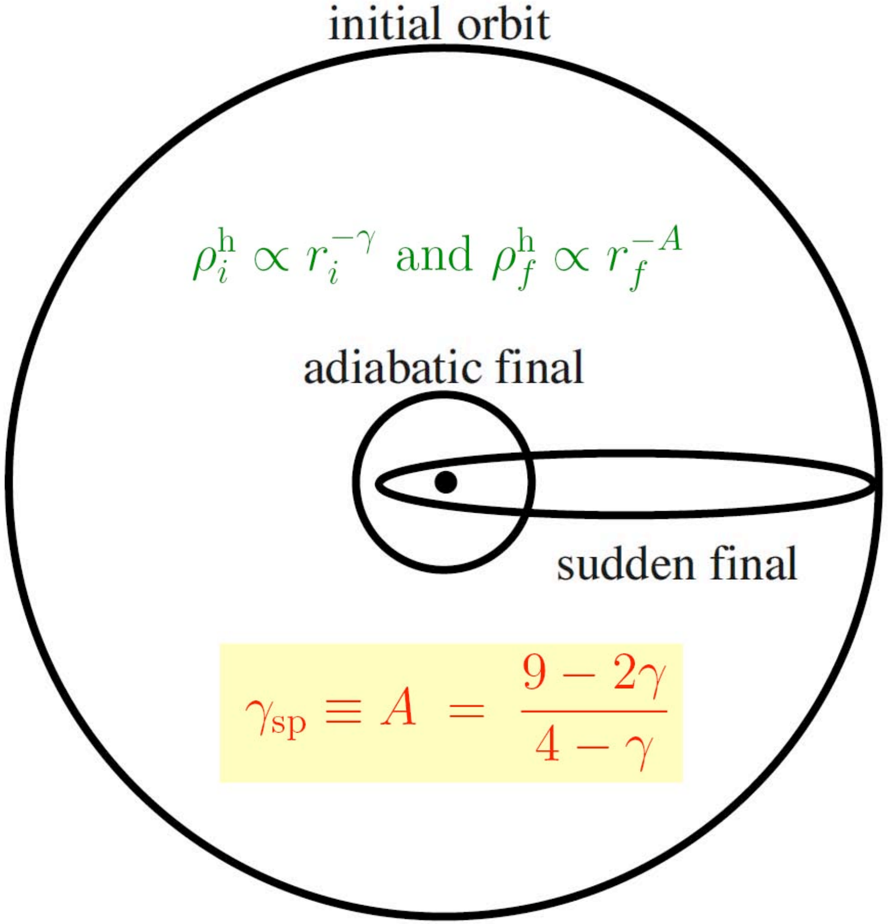

$$\rho_i^{\rm h} \propto r_i^{-\gamma} \text{ and } \rho_f^{\rm h} \propto r_f^{-A}$$

$$\gamma_{\rm sp} \equiv A = \frac{9 - 2\gamma}{4 - \gamma}$$

$$M_i^{\rm h} \{r_i\} = M_f^{\rm h} \{r_f\}$$
$$\Downarrow$$
$$r_i^{3-\gamma} \propto r_f^{3-A}$$

• The angular momentum $\vec{L} = \vec{r} \wedge \vec{v}$ is always conserved.

• If the black hole formation is slow – adiabatic – compared to the orbital period, the radial action is also conserved

$$J_r \, (E, L) = \frac{1}{\pi} \int_{r_-}^{r_+} dr \, \sqrt{2 \, \{E - \Phi(r)\} - \frac{L^2}{r^2}}$$

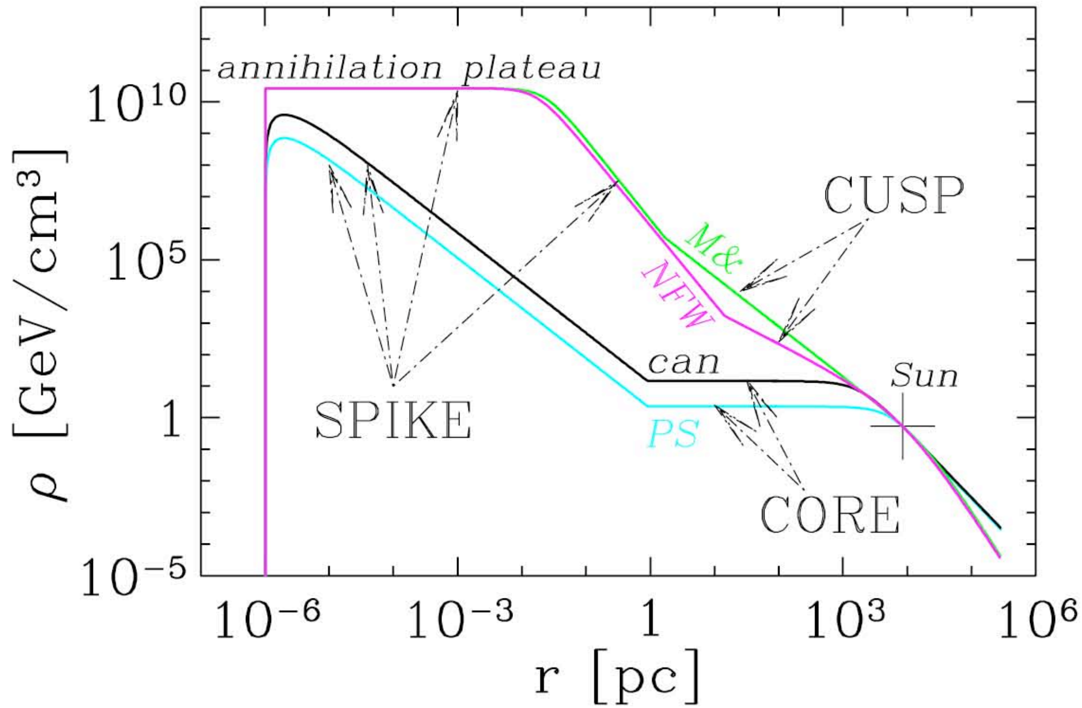

FIG. 12: Dark matter density as a function of distance from the galactic center, showing spikes, cusps, and cores. Four density models are shown: canonical ("can"), Persic–Salucci ("PS"), Navarro–Frenk–White ("NFW") and Moore-et-al. ("M&"). The models are normalized to the same rotation velocity and the same density at the Sun's position (marked by a cross).

- For $\gamma > 0$ and $1 \leq \alpha \leq 2 \quad \Rightarrow \quad \gamma_{sp} = \dfrac{9-2\gamma}{4-\gamma}$
- For $\gamma = 0$ and $1 \leq \alpha < 2 \quad \Rightarrow \quad \gamma_{sp} = \dfrac{9-\alpha}{4}$
- For $\gamma = 0$ and $\alpha = 2 \quad \Rightarrow \quad \gamma_{sp} = 3/2$

Halo profile is unknown

$$\rho_{\rm CDM}(r) \;=\; \rho_{\rm CDM\,\odot} \left\{\frac{r_\odot}{r}\right\}^{\gamma} \left\{\frac{1 + (r_\odot/a)^{\alpha}}{1 + (r/a)^{\alpha}}\right\}^{(\beta-\gamma)/\alpha}$$

Halo model	a (kpc)	r_0 (kpc)	α	β	γ	$\bar{J}(10^{-5}\mathrm{sr})$
isothermal cored	3.5	8.5	2	2	0	30.4
NFW	20.0	8.0	1	3	1	1.26×10^4
NFW+ac	20.0	8.0	0.8	2.7	1.45	1.02×10^7
Moore	28.0	8.0	1.5	3	1.5	9.68×10^6
Moore+ac	28.0	8.0	0.8	2.7	1.65	3.12×10^8

Various models for the DM distribution within the Milky Way

$$\Phi_\gamma(\Delta\Omega) = \int_{E_{\rm th}}^{m_\chi} dE_\gamma \, d\Phi_\gamma/dE_\gamma(E_\gamma, \Delta\Omega)$$

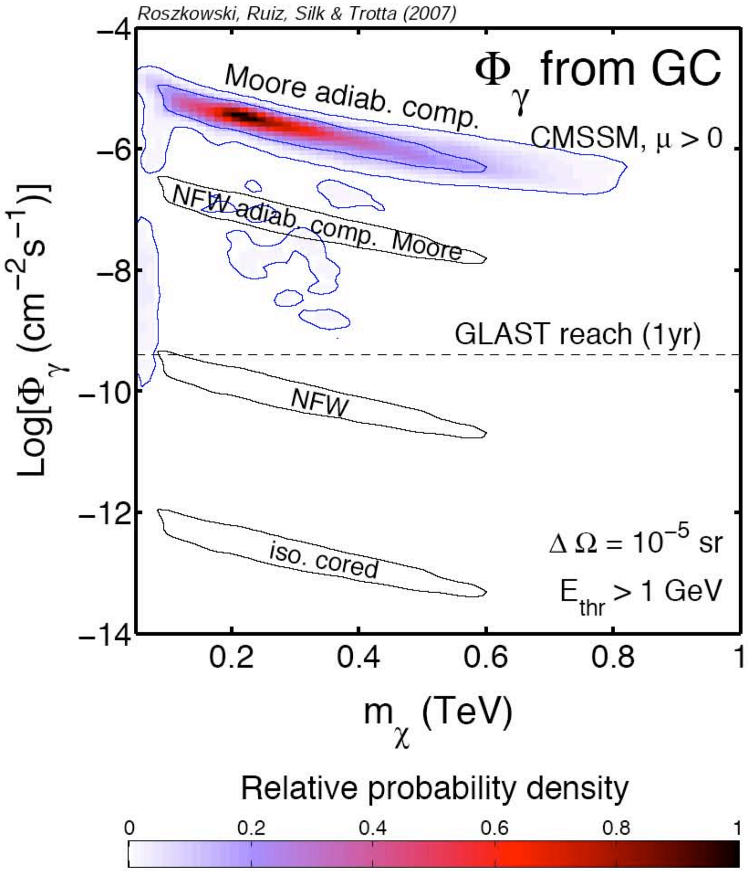

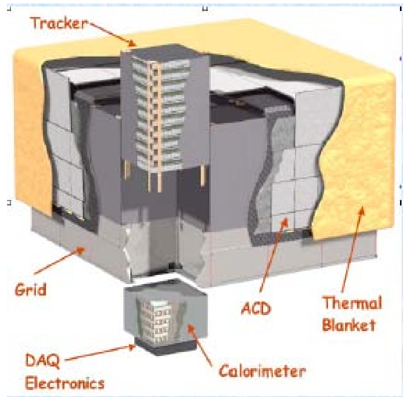

FIG. 1: The joint probability distribution for the γ–ray flux Φ_γ from the Galactic center vs. the neutralino mass m_χ for some popular halo profile models. The inner (outer) solid contours delimit the predicted regions containing 68% and 95% total probability, respectively. We also plot the expected reach of GLAST after 1 year of operation.

$$\text{Bayesian approach} \quad p(m|d) = \frac{p(d|\xi)\pi(m)}{p(d)}$$

Various foregrounds need to be considered

• A γ–ray diffuse emission from the Milky Way itself is produced as primary cosmic rays interact on the atoms of the interstellar medium. This foreground results from the convolution

$$\Phi_{\gamma}^{\rm diffuse}(E) \; = \; \int_{\rm los} I_{\rm H}(E,s)\, n_{\rm H}(s)\, ds$$

between the gamma–ray emissivity per hydrogen atom and the hydrogen density.

$$I_{\rm H}(E_{\gamma}, s) \; = \; \int_{E_{\gamma}}^{+\infty} \sigma_{\rm pp}\,(E_{\rm p})\, \frac{dN_{\gamma}}{dE_{\gamma}}\, \Phi_{\rm p}\,(E_{\rm p}, s)\; dE_{\rm p}$$

$$\Downarrow$$

$$I_{\rm H}(E_{\gamma}, \odot) \; = \; \left(2 \times 10^{-35}\ {\rm GeV}^{-1}\,{\rm s}^{-1}\,{\rm sr}^{-1}\right)\ \left(E/1\,{\rm TeV}\right)^{-2.73}$$

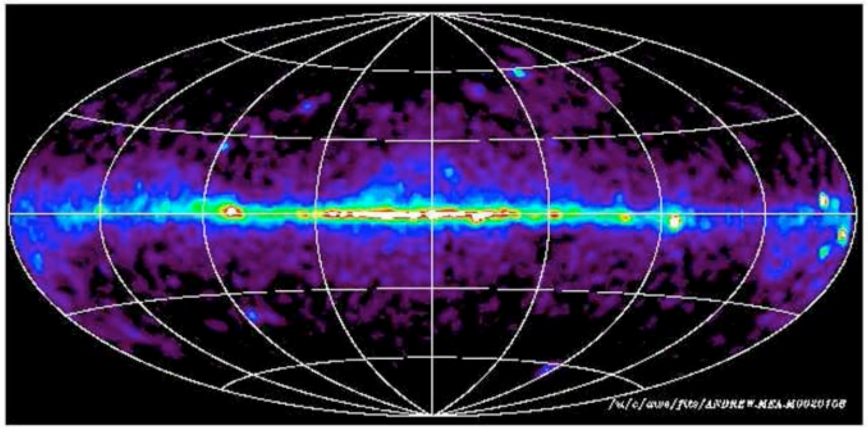

Figure 1. EGRET all-sky map in continuum γ-ray emission for energies >100 MeV (A. W. Strong, unpublished).

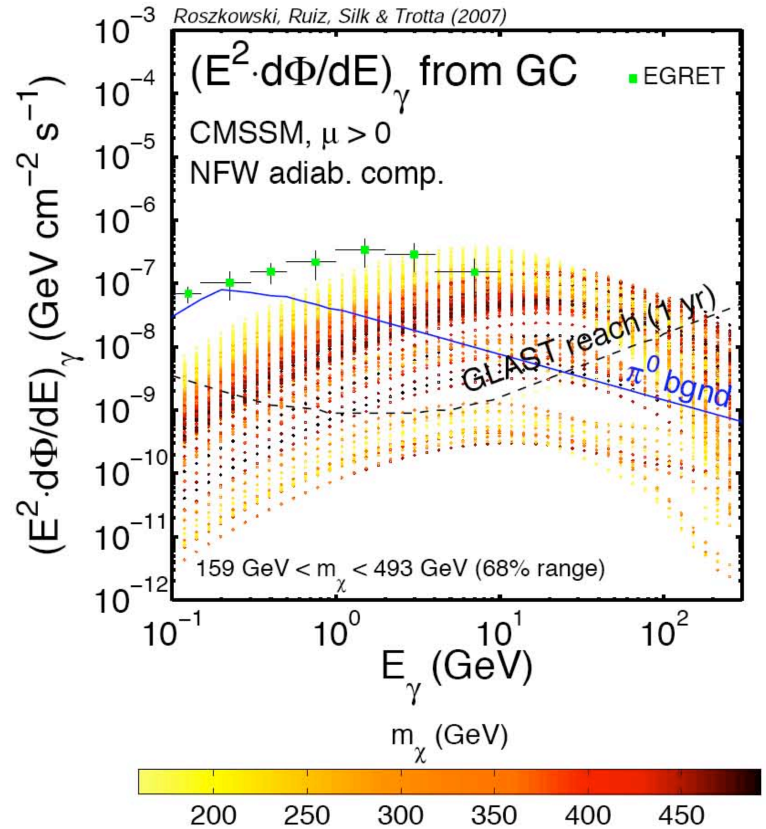

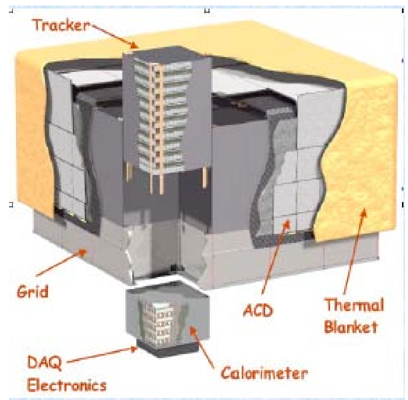

FIG. 2: Predicted γ–rays energy spectrum, for the parameter region encompassing 68% of probability for the neutralino mass (values given by the color coding). This spectrum is for an NFW profile with adiabatic compression, all other cases can be obtained by rescaling it by the factors $\bar{J}$ given in Table I. The normalization of the π^0 background has been normalized here to the EGRET data but it is otherwise arbitrary.

Gianfranco Bertone,[1] Torsten Bringmann,[2] Riccardo Rando,[1] Giovanni Busetto,[1] and Aldo Morselli[3]

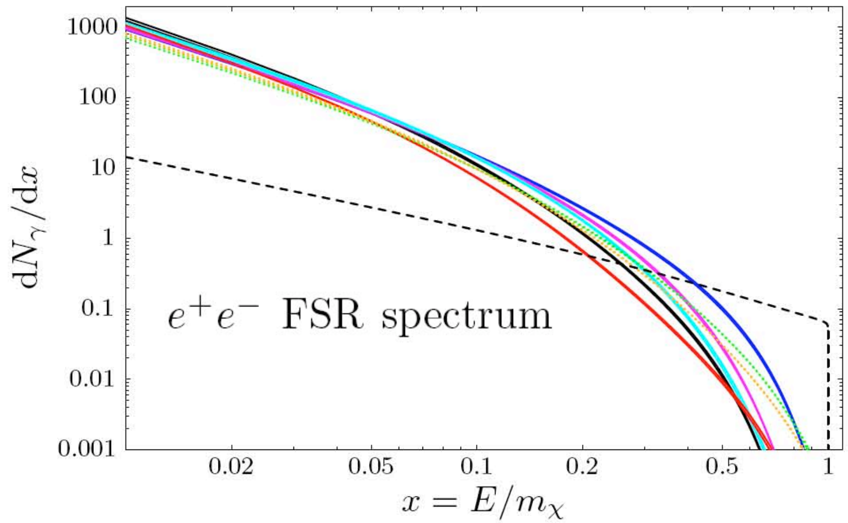

FIG. 1: Photon multiplicity for various final states. The (blue,magenta,cyan,black,red) solid lines show the ($u\bar{u}/d\bar{d}$, $s\bar{s}$, $c\bar{c}$, $b\bar{b}$, $t\bar{t}$) quark spectra, while the (green,blue) dotted lines give the contributions from (WW, ZZ) gauge bosons. The (black) dashed line, finally, is the FSR spectrum from e^+e^- final states. All spectra are plotted for both $m_\chi = 500\,\mathrm{GeV}$ and $m_\chi = 1000\,\mathrm{GeV}$.

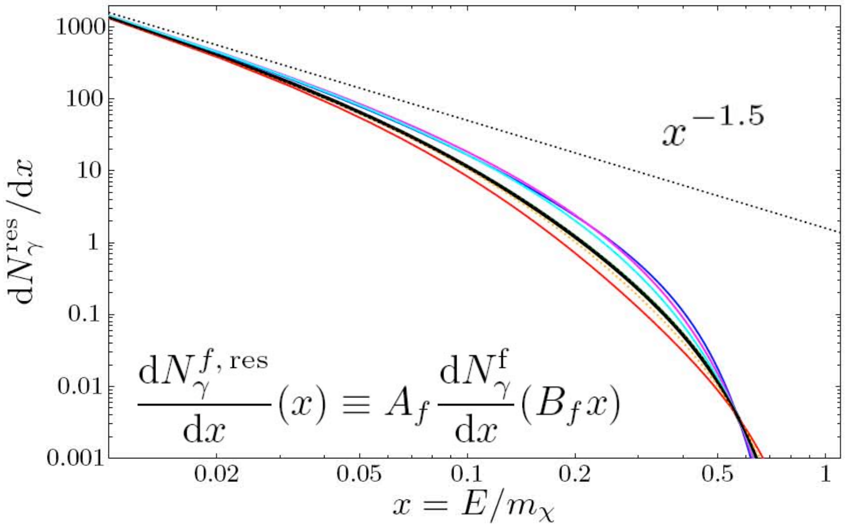

FIG. 2: Same as Fig. 1 (for $m_\chi = 500$ GeV and without the e^+e^- FSR case), but with spectra rescaled as in (5) and scaling parameters as given in Tab. I. The straight dotted line represents the extrapolated, asymptotic $x^{-1.5}$ behaviour of the photon spectrum from $b\bar{b}$ final states. The thick black line shows the (not rescaled) $b\bar{b}$ spectrum that we will use for reference.

	$b\bar{b}$	$u\bar{u}$	$d\bar{d}$	$s\bar{s}$	$c\bar{c}$	$t\bar{t}$	WW	ZZ
A_f	1.00	2.74	2.74	1.83	1.38	1.36	3.56	3.02
B_f	1.00	1.47	1.47	1.16	1.07	1.05	1.52	1.45

Ground based imaging detectors
Air–shower Cerenkov Telescopes

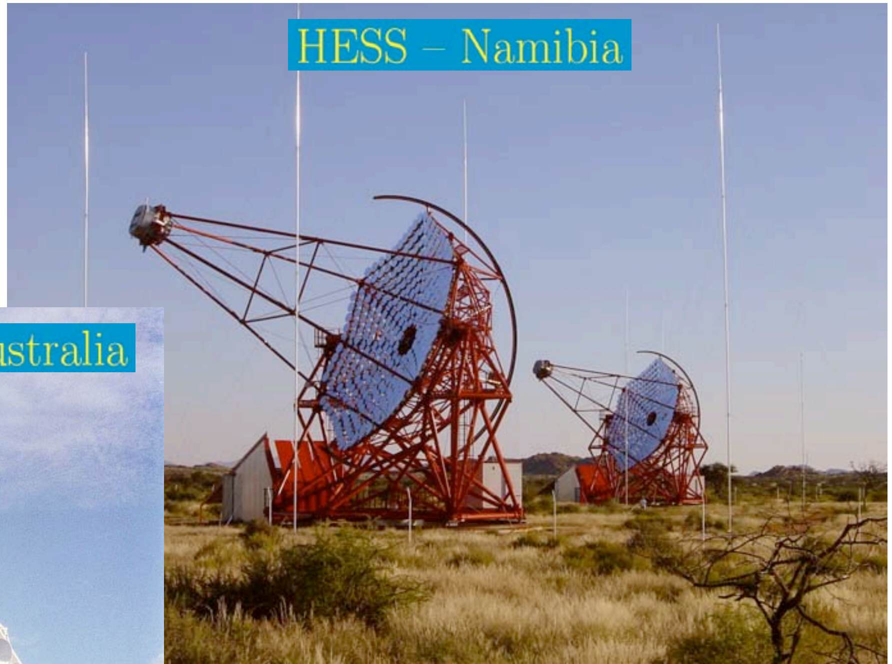

Detection principle

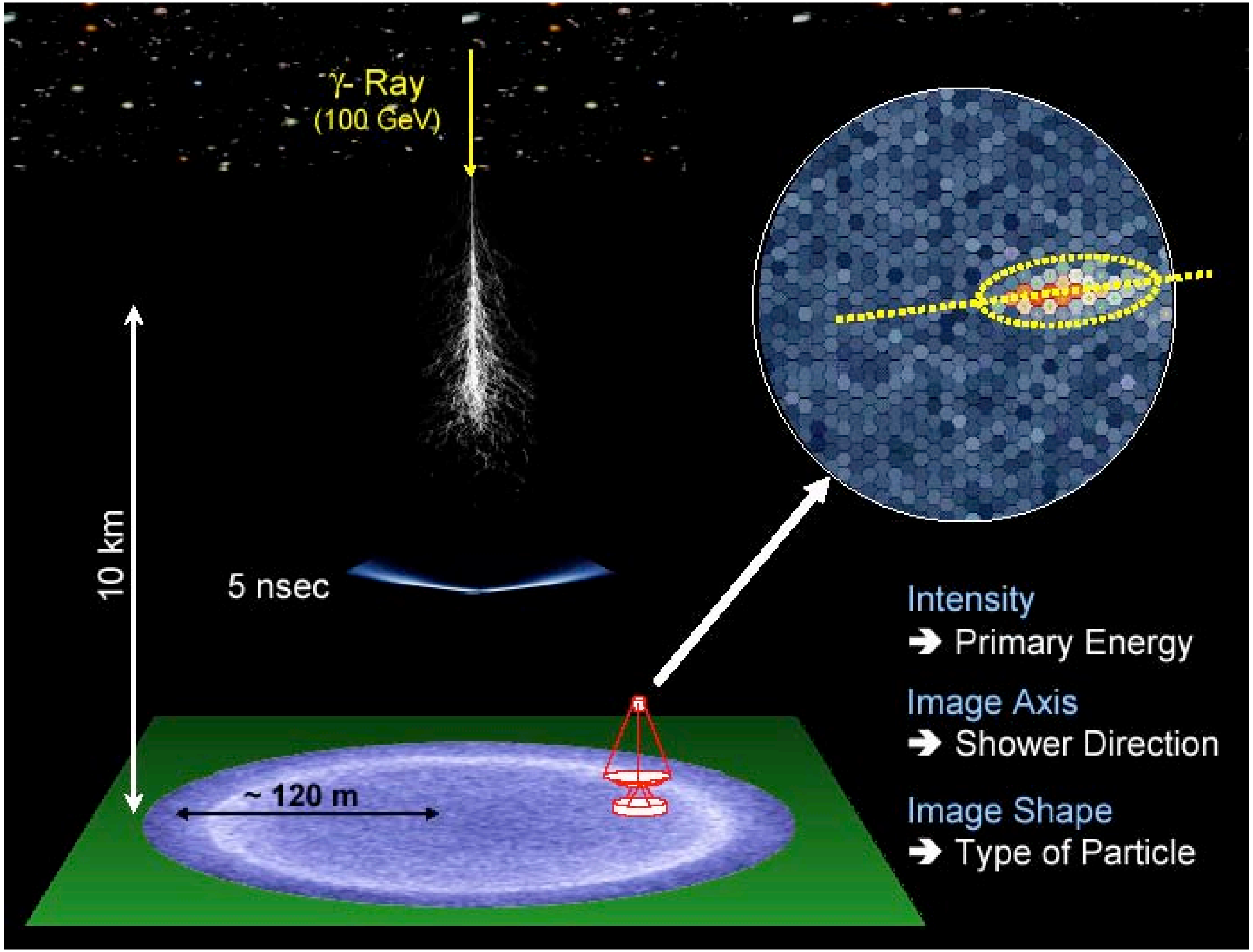

Detection principle

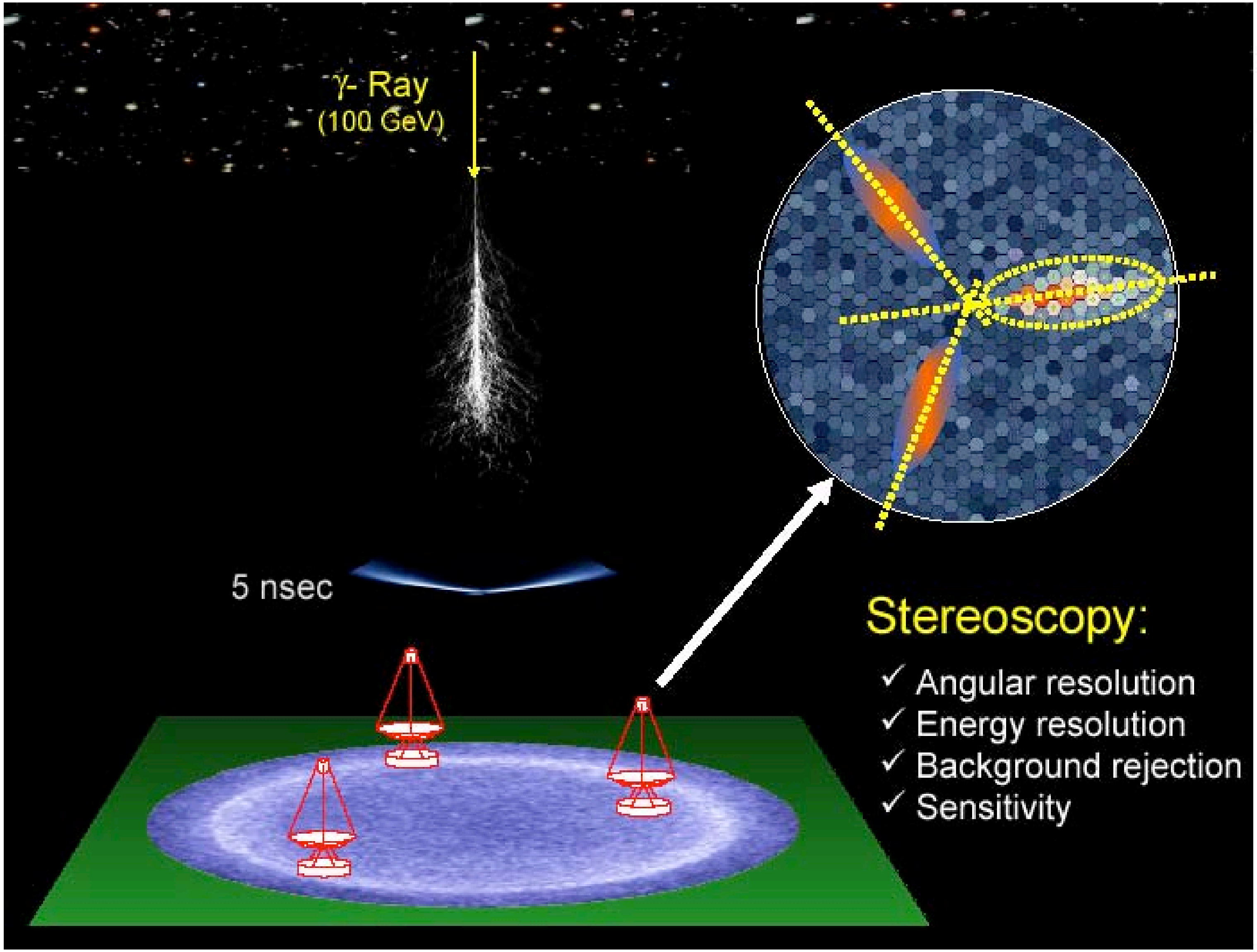

Various foregrounds need to be considered

• A γ–ray diffuse emission from the Milky Way itself is produced as primary cosmic rays interact on the atoms of the interstellar medium. This foreground results from the convolution

$$\Phi_\gamma^{\rm diffuse}(E) \; = \; \int_{\rm los} I_{\rm H}(E,s)\, n_{\rm H}(s)\, ds$$

between the gamma–ray emissivity per hydrogen atom and the hydrogen density.

$$I_{\rm H}(E_\gamma, s) \; = \; \int_{E_\gamma}^{+\infty} \sigma_{\rm pp}\,(E_{\rm p})\, \frac{dN_\gamma}{dE_\gamma}\, \Phi_{\rm p}\,(E_{\rm p}, s)\; dE_{\rm p}$$

$$\Downarrow$$

$$I_{\rm H}(E_\gamma, \odot) \; = \; \left(2 \times 10^{-35}\ {\rm GeV}^{-1}\, {\rm s}^{-1}\, {\rm sr}^{-1}\right)\, (E/1\, {\rm TeV})^{-2.73}$$

• In the case of **atmospheric Cerenkov telescopes (ACT)**, the dominant foreground arises from the CR high–energy electrons that impact on the upper atmosphere and generate electromagnetic showers

$$\Phi_{\rm e} \; = \; \left(6.4 \times 10^{-2}\ {\rm GeV}^{-1}\, {\rm cm}^{-2}\, {\rm s}^{-1}\, {\rm sr}^{-1}\right)\, (E/1\, {\rm GeV})^{-3.3\pm0.2}$$

• CR hadrons cannot be completely rejected and a few hadronic showers are misinterpreted as electromagnetic events

$$\Phi_{\rm had} \; = \; \left(1.8\ {\rm GeV}^{-1}\, {\rm cm}^{-2}\, {\rm s}^{-1}\, {\rm sr}^{-1}\right)\, (E/1\, {\rm GeV})^{-2.75}$$

Detection principle

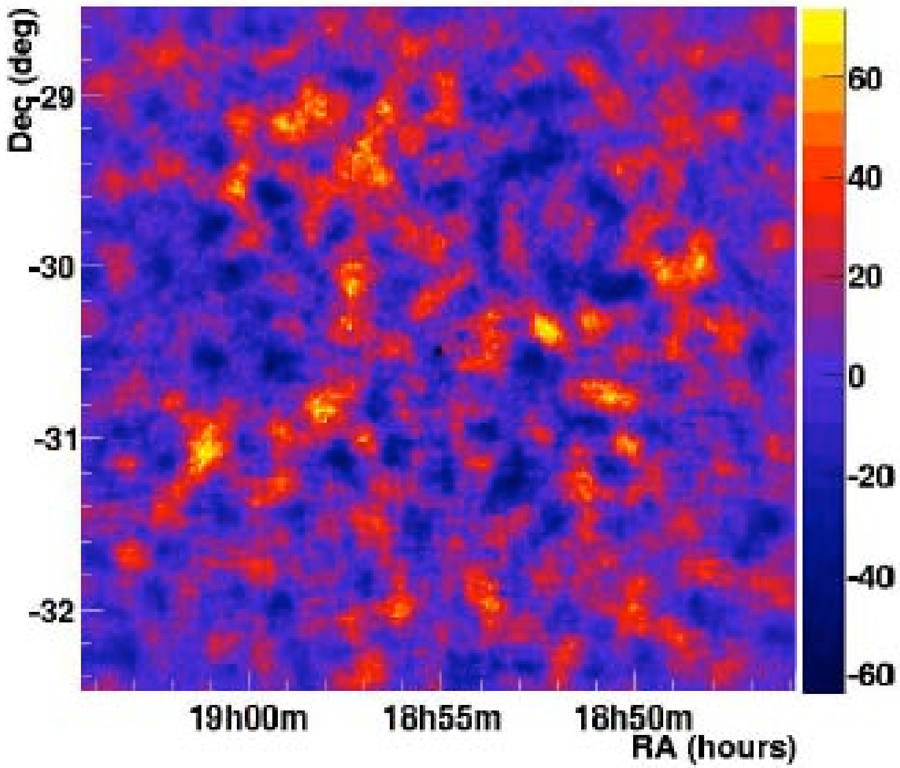

FOV of Sagittarius Dwarf Spheroidal

$$S_\gamma = N_\gamma^{\mathrm{ON}} - N_\gamma^{\mathrm{OFF}}$$

$$\Delta S_\gamma = \sqrt{N_\gamma^{\mathrm{ON}} + N_\gamma^{\mathrm{OFF}}} \simeq \sqrt{2\,N_\gamma^{\mathrm{ON}}}$$

Detection at the $5\,\sigma$ level means that $\dfrac{S_\gamma}{\Delta S_\gamma} = 5$

Galactic Center region

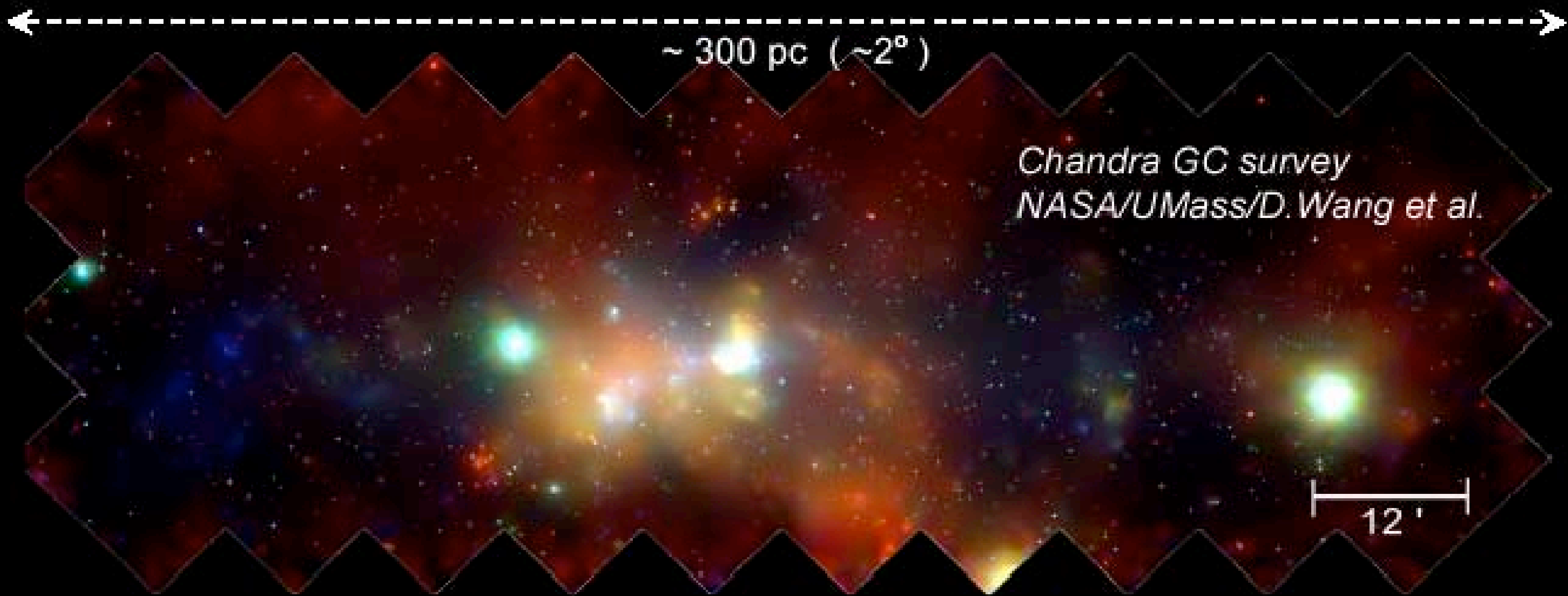

Astrophysics:
- full "zoo" of objects
- Pulsars and PWN
- Supernova remnants
- X-Ray binaries
- Molecular clouds

Bit more exotic:
- Supermassive BH Sgr A*
- INTEGRAL 511 keV line

Even more exotic:
- Dark Matter accumulation
- → Neutralino annihilation

HESS: Galactic Center

Galactic Centre is a very crowded region in all wave-lengths

<u>White contours:</u>
molecular cloud emission (CS line)

~ 3,500 diffuse γ
Significance = 14.6

SNR G 0.9+0.1
Sgr B
Sgr A*

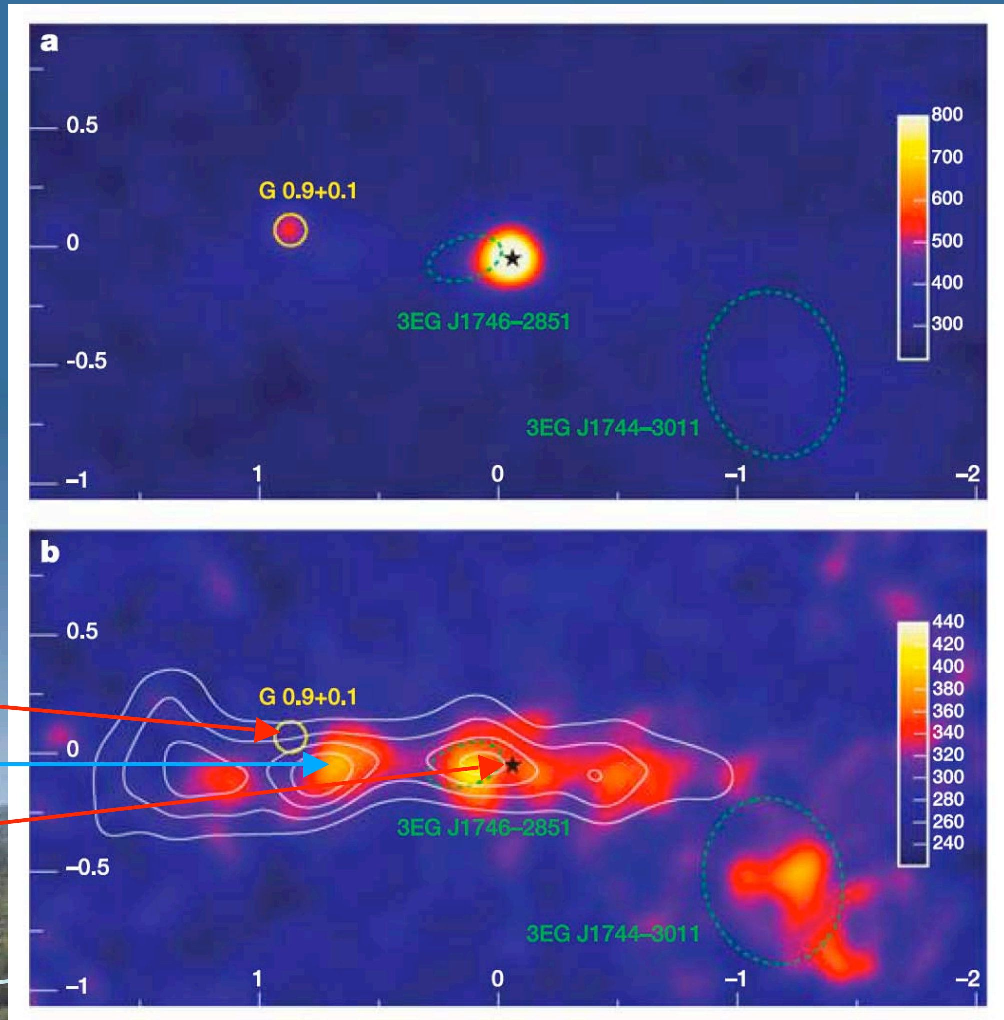

EGRET non-identifiéd sources

HESS, NATURE, vol.439, p.695, 2006

HESSJ1745-290: morphology

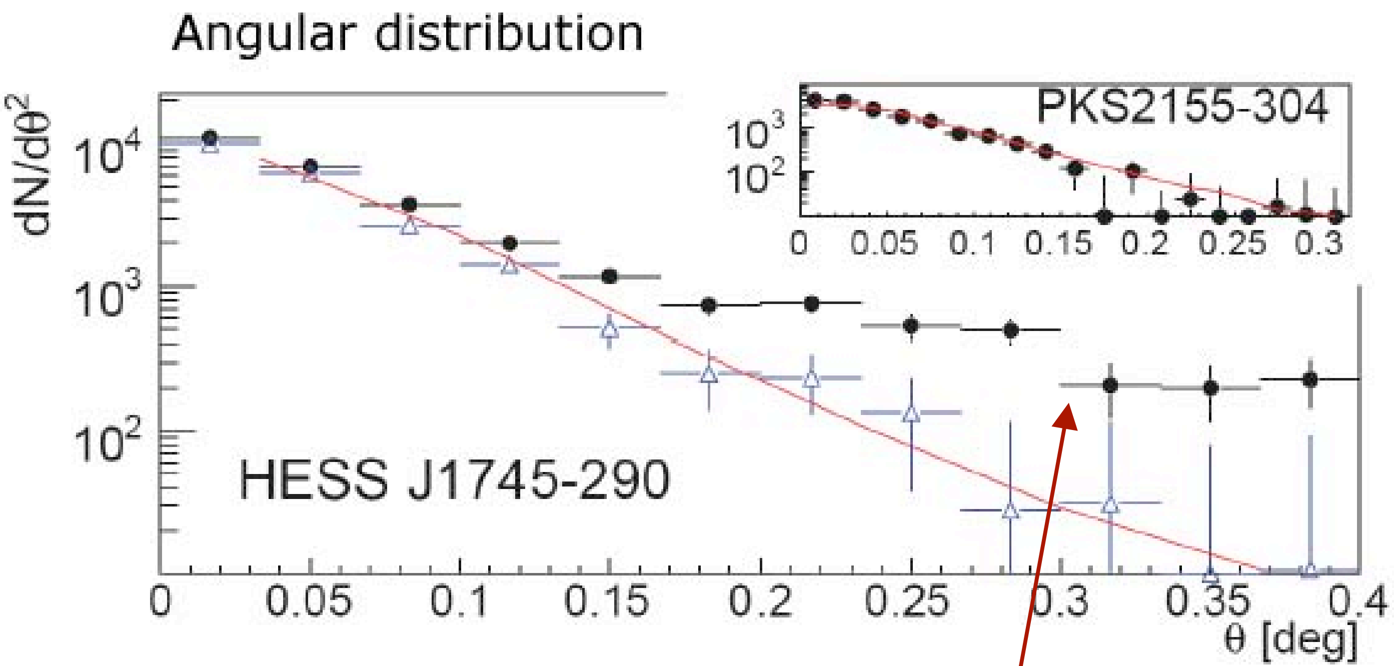

Well described by H.E.S.S. PSF for point like source

Source size: 0.12°

Diffuse component: 16%

H.E.S.S., PRL 97 (2006)

HESSJ1745-290: morphology

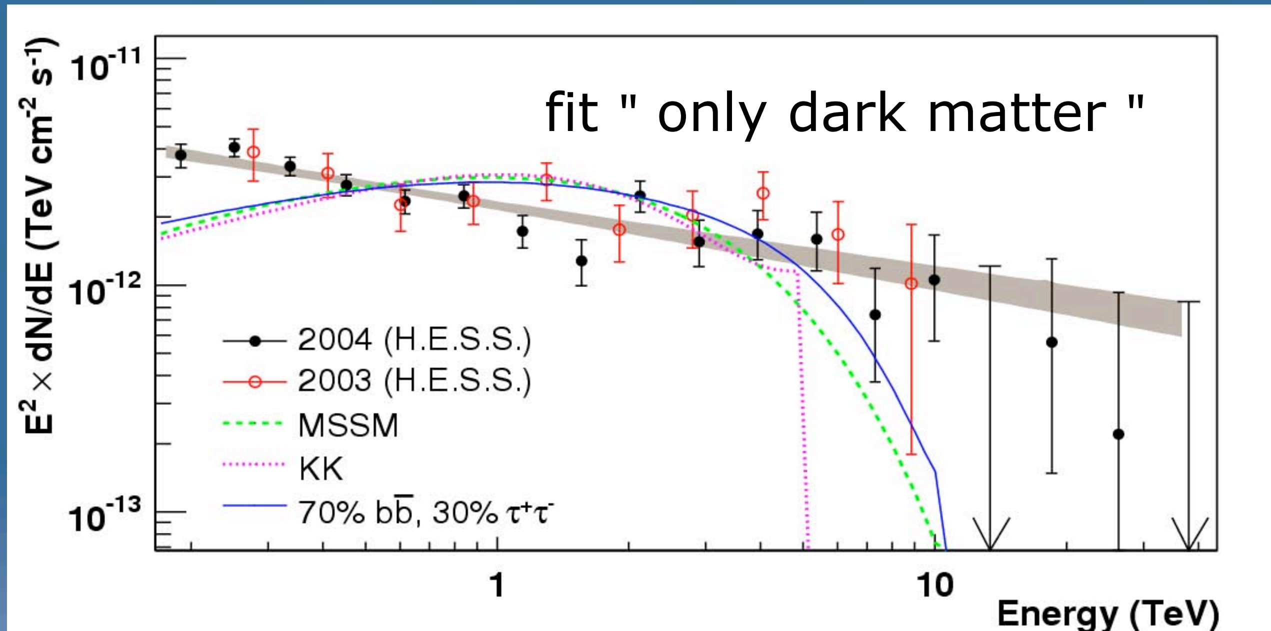

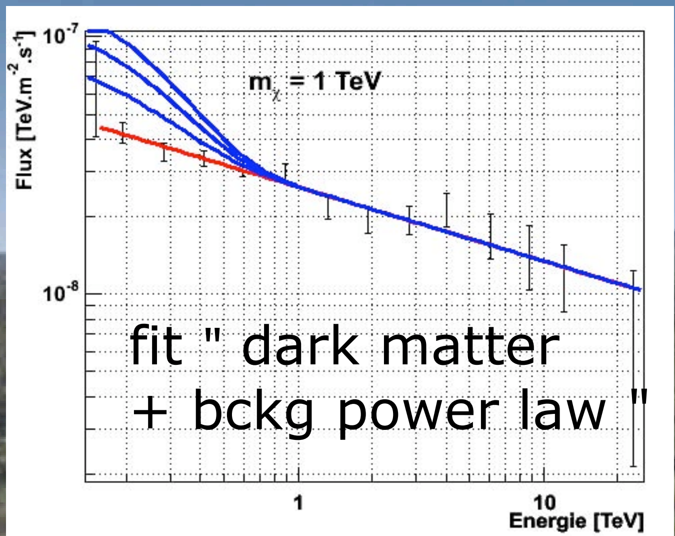

Data 2003/2004:

- Power Law Spectrum (E_{th} > 160 GeV) Γ=2.25±0.04±0.10
- Exponential cut-off limit E_{cut} > 9 TeV (95% CL)
- Diffuse emission included

HESS: Galactic Center

- Strong point-like source (0.1°) detected - HESSJ1745-290 at the position of Sgr A* with spectral index ~ 2.2
- Important Diffuse emission associated with molecular clouds spread over whole region with similar spectral index
- No line emission observed
- Need of uncomfortably high masses of neutralino or Kaluza-Klein particles
- Contribution of Dark Matter below 10% cannot be excluded

HESS will re-observe Galactic Centre with low energy threshold in phase II

Indirect Dark Matter Detection

Pierre Salati – Université de Savoie & **LAPTH**

1) The messengers of DM annihilation

2) High energy photons and the Galactic centre

3) Hunting for neutrinos in the ice cap

4) Cosmic ray transport : a short overview

5) TeV antiprotons : a new window

6) Uncertainties … propagation

1. accumulation of GeV-TeV mass neutralinos by the Sun and the Earth

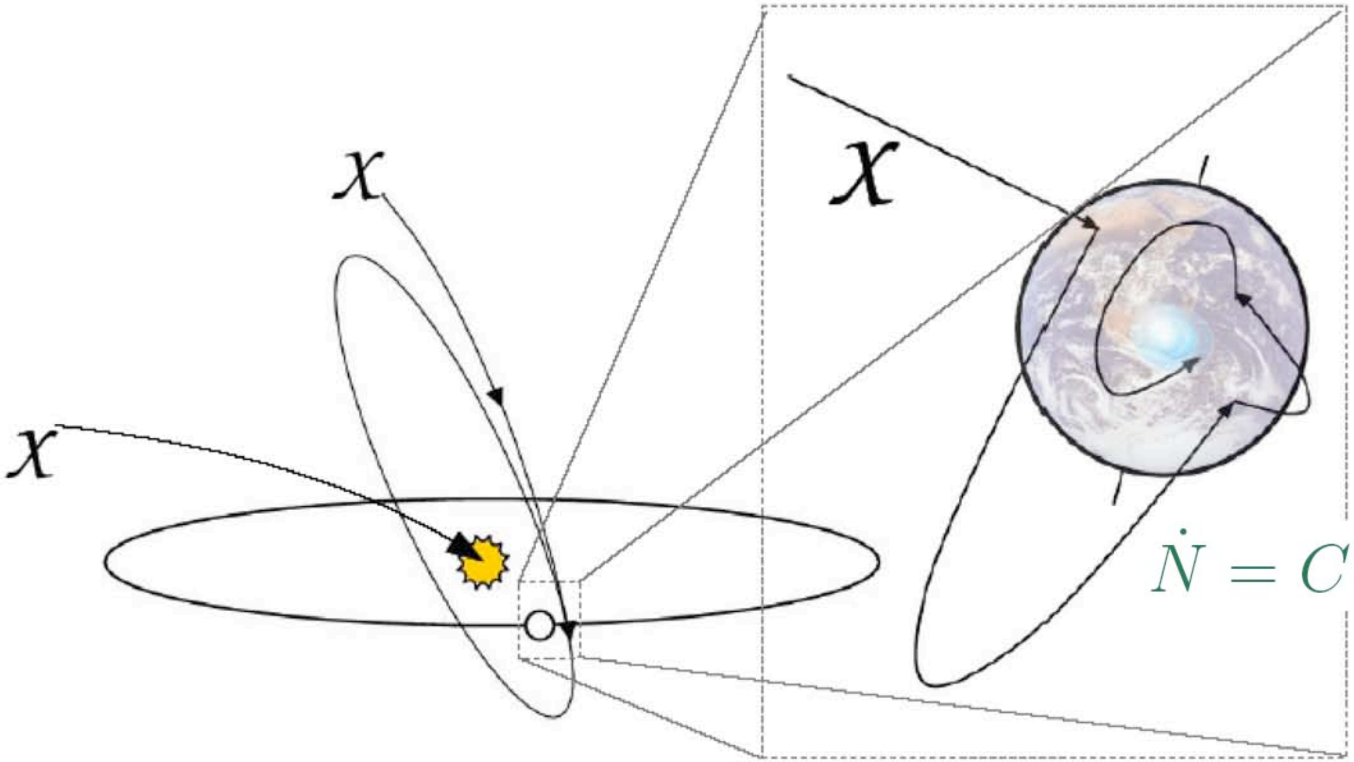

$$\dot{N} = C - C_A N^2$$

$$\Gamma_A = \frac{1}{2} C_A N^2 = \frac{1}{2} C \tanh^2(t/\tau) \text{ where } \tau = (C C_A)^{-1/2}$$

2. Neutralino-induced neutrinos

$$\chi\chi \to \begin{Bmatrix} q\bar{q} \\ l^+l^- \\ W, Z, H \end{Bmatrix} \to \nu$$

3. Atmospheric background

- atm. μ: absorbed by the Earth
- atm. ν: compare on/off source angular regions

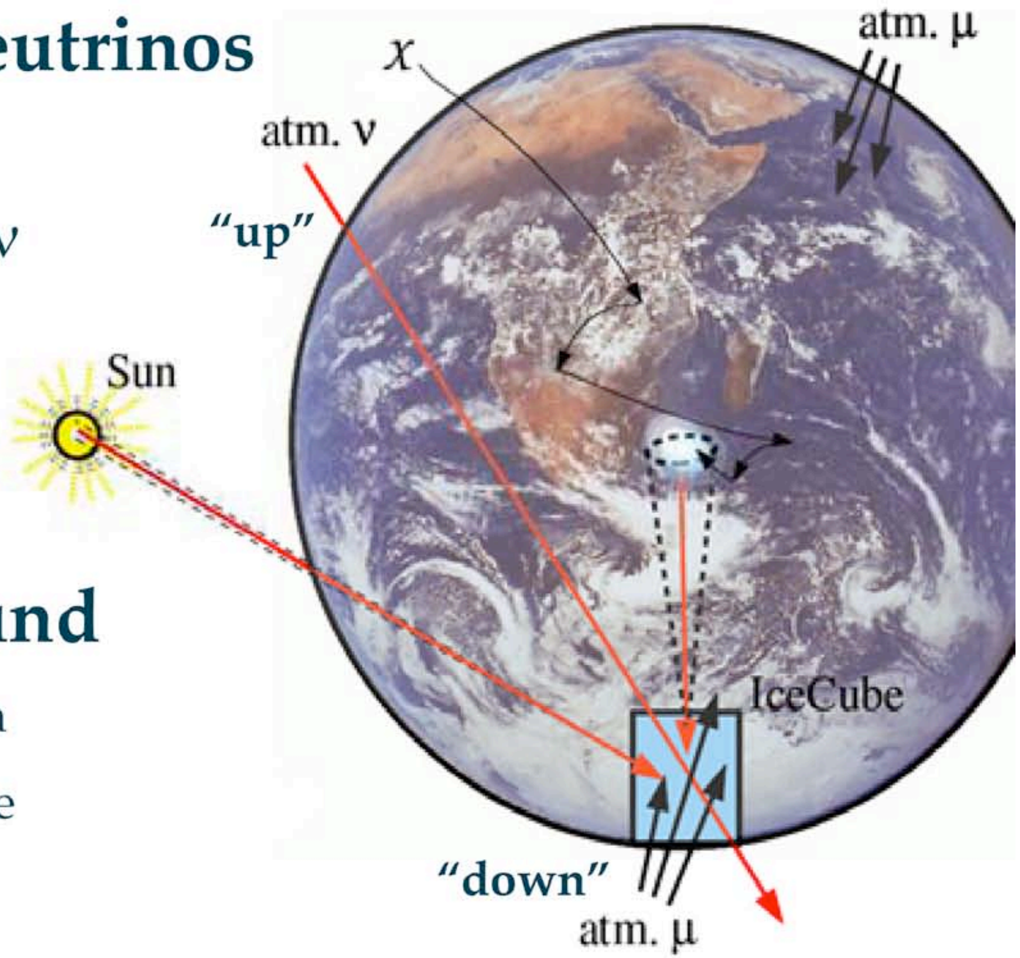

Large neutralino masses favored

$C \propto m_\chi^{-1}$

$\sigma(\nu_\mu \to \mu) \propto s \propto E_\nu \propto m_\chi$

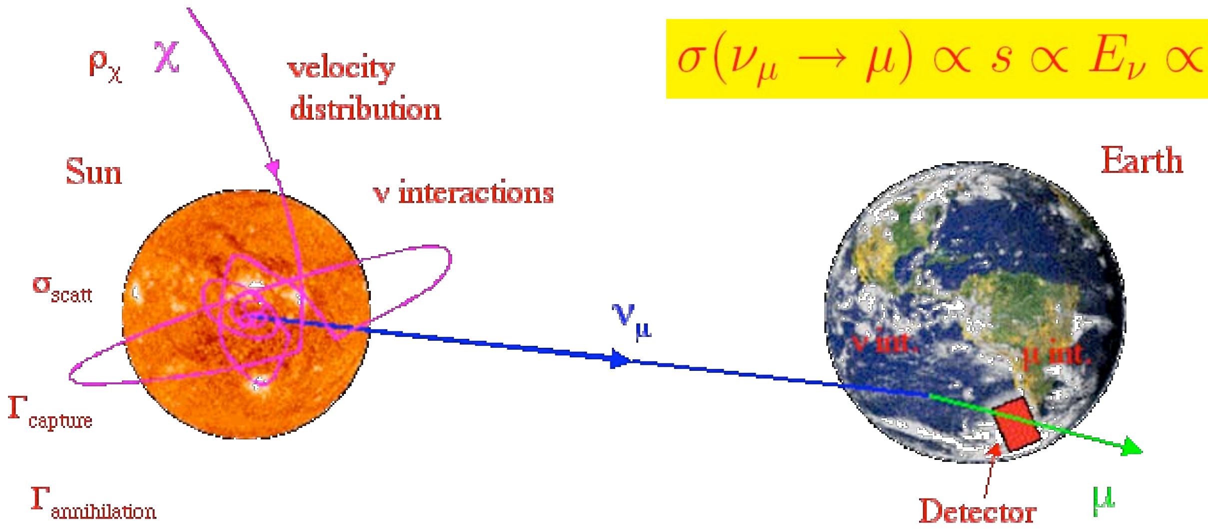

muon range $\propto E_\mu \propto m_\chi$

Up–going muons lose 1 GeV as they cross 4 meters of ice or water.

The fiducial volume for the neutrino–muon conversion increases with the neutrino energy.

Amundsen-Scott South Pole station

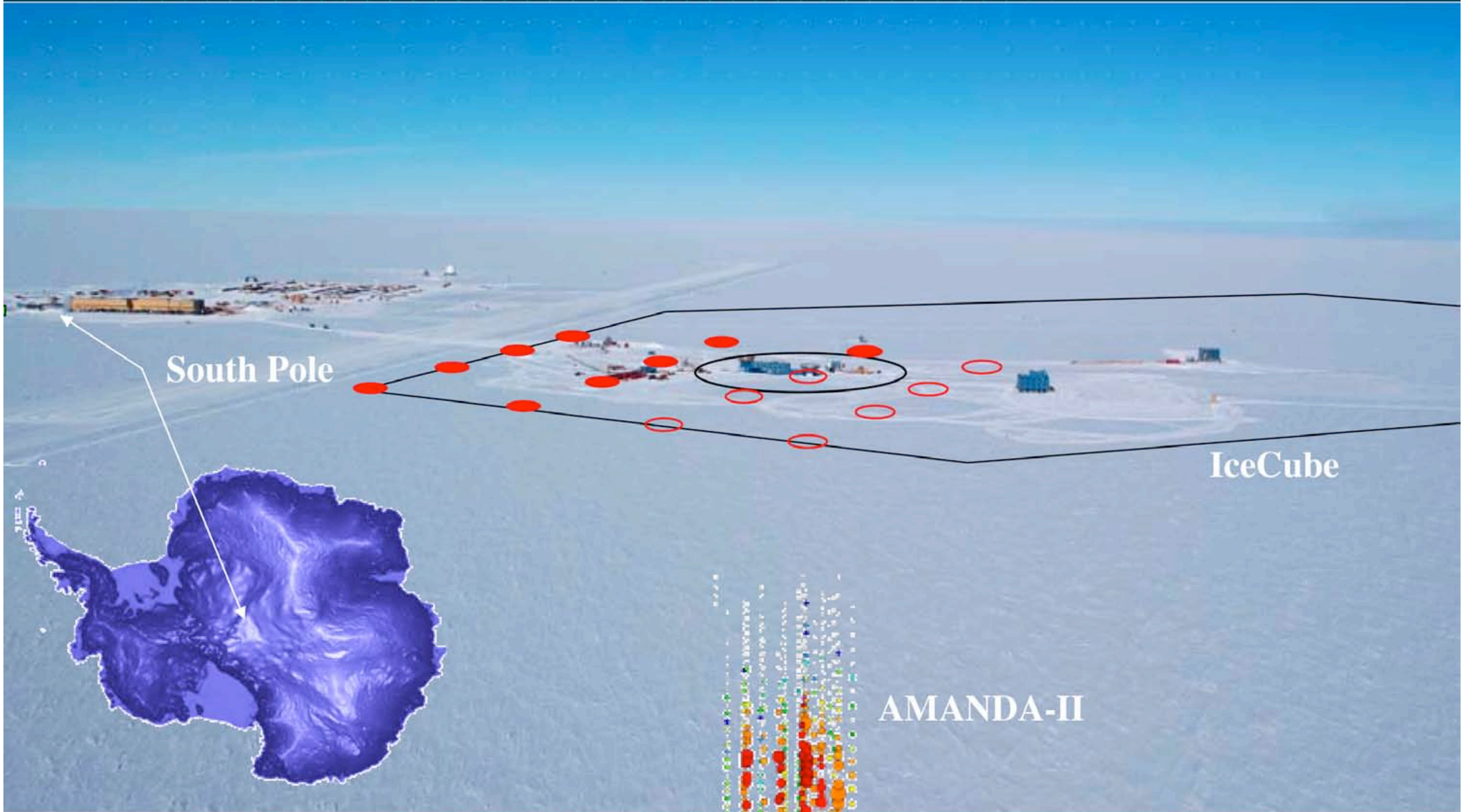

The IceCube neutrino detector

AMANDA-B10(B13): 1997-1999

- 302-428 OMs on 10-13 strings
- diameter ~120m, height ~500m

AMANDA-II: 2000-...

- 677 OMs on 19 strings
- diameter ~200m, height ~500m

IceCube: 2005-...

- 4800 OMs on 80 strings (when completed)
- feb 2006: 9 strings deployed
- diameter ~1000m, height ~1000m

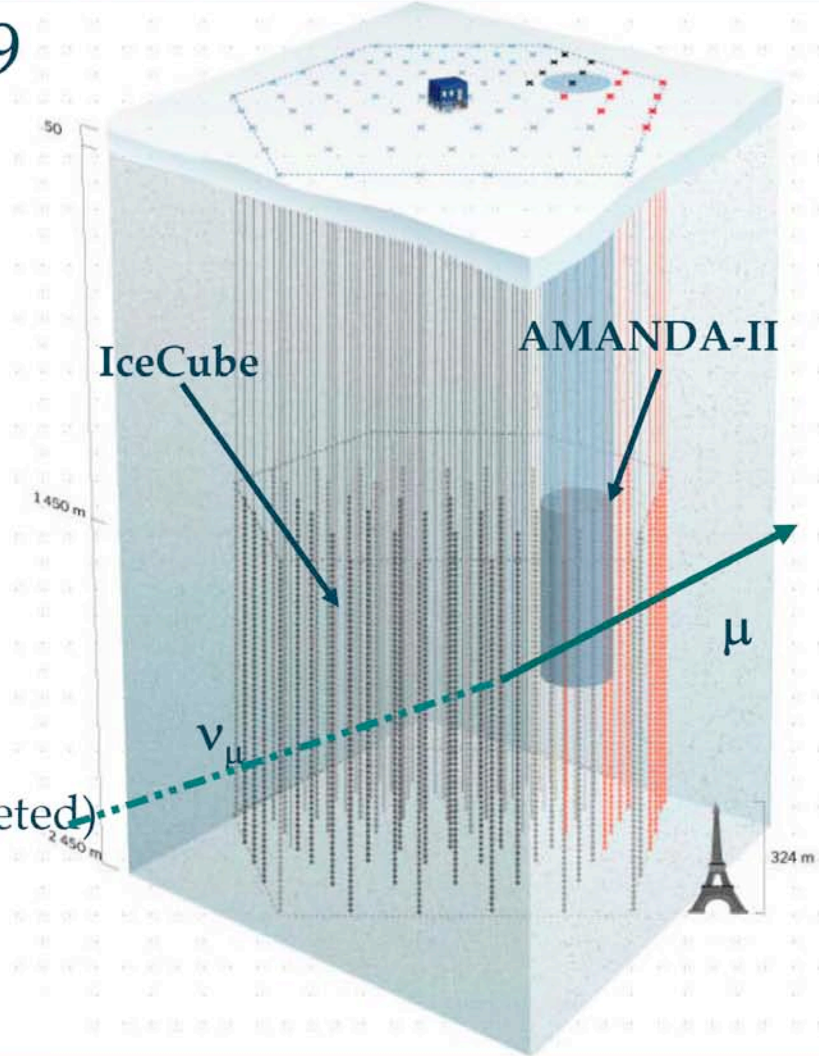

IceCube Deployment

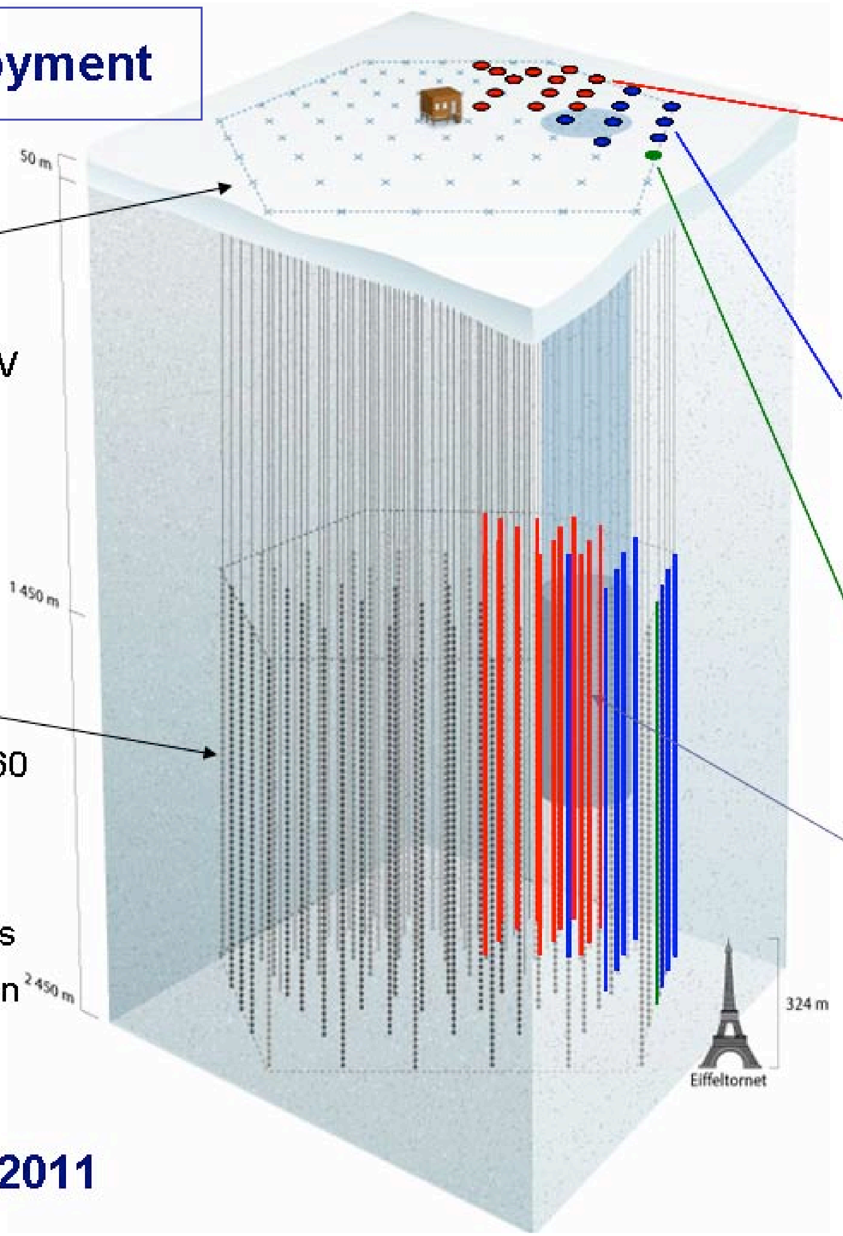

IceTop

Air shower detector

Threshold ~ 300 TeV

InIce

planned 80 strings of 60 optical modules each

17 m between modules

125 m string separation

Completion by 2011

2006-2007:

13 strings deployed

22 strings
1320 digital modules
52 surface detectors

2005-2006: 8 strings

2004-2005 : 1 string

First data in 2005
first upgoing muon: July 18, 2005

AMANDA
19 strings
677 modules

Neutrino detectors

AMANDA/IceCube – South Pole

SuperK Japan

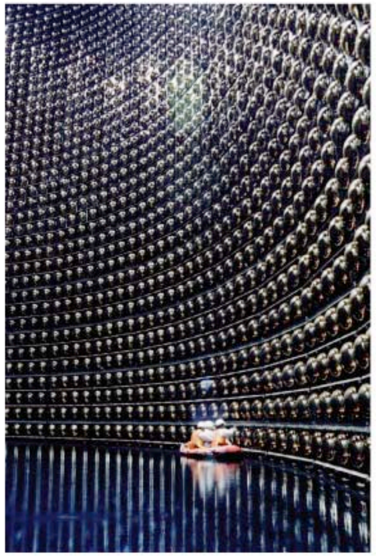

(a)

ANTARES France

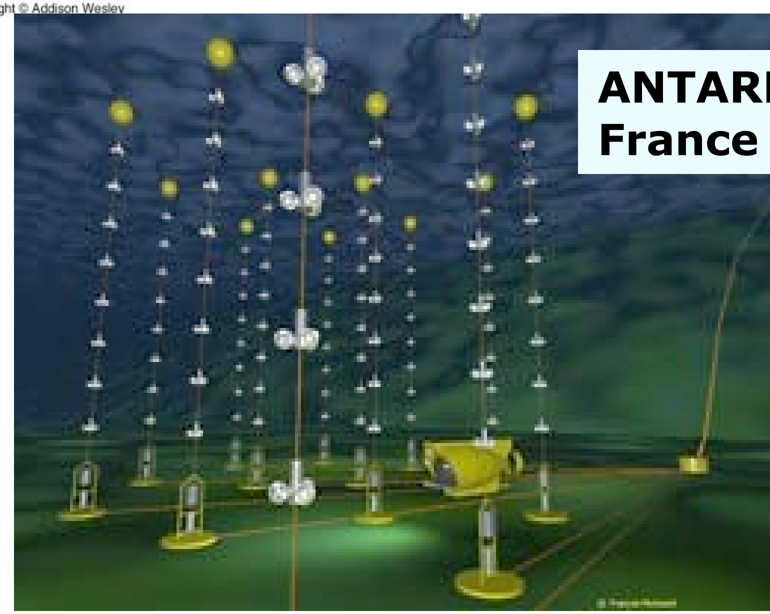

No excess of neutralino-induced neutrinos

Earth 1997-1999 **(subm. Astropart. Phys.)**

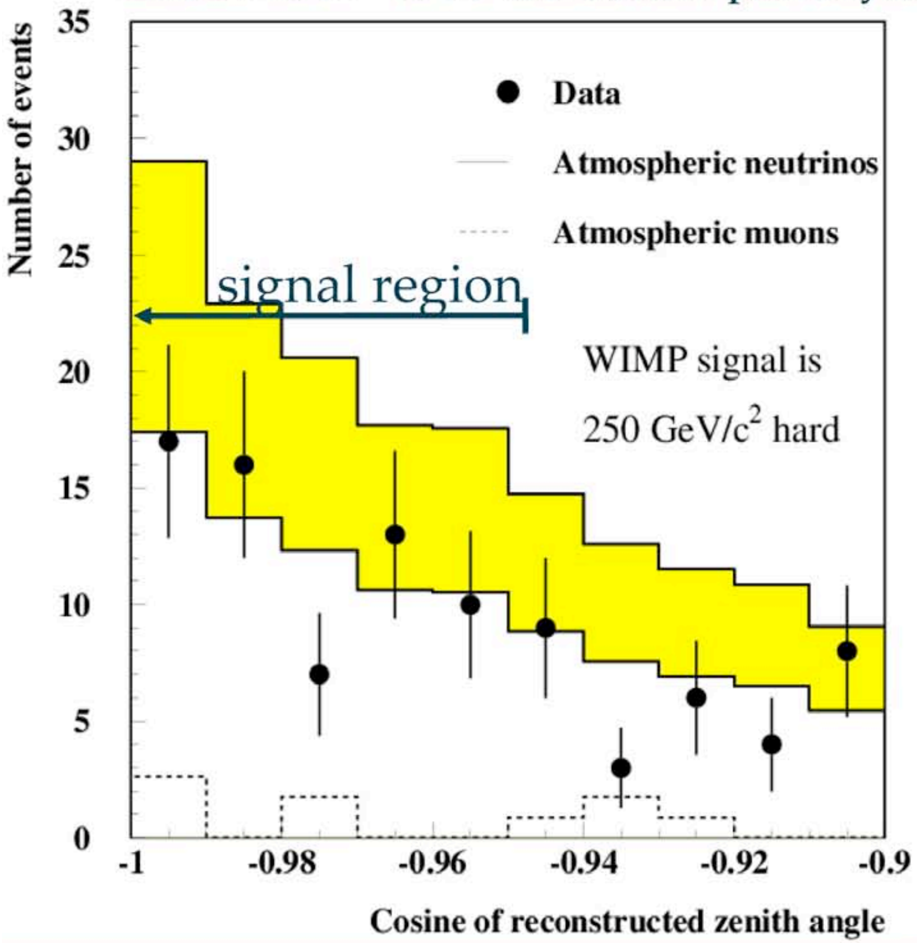

Sun 2001 **(Astropart. Phys. (2006) 459-466)**

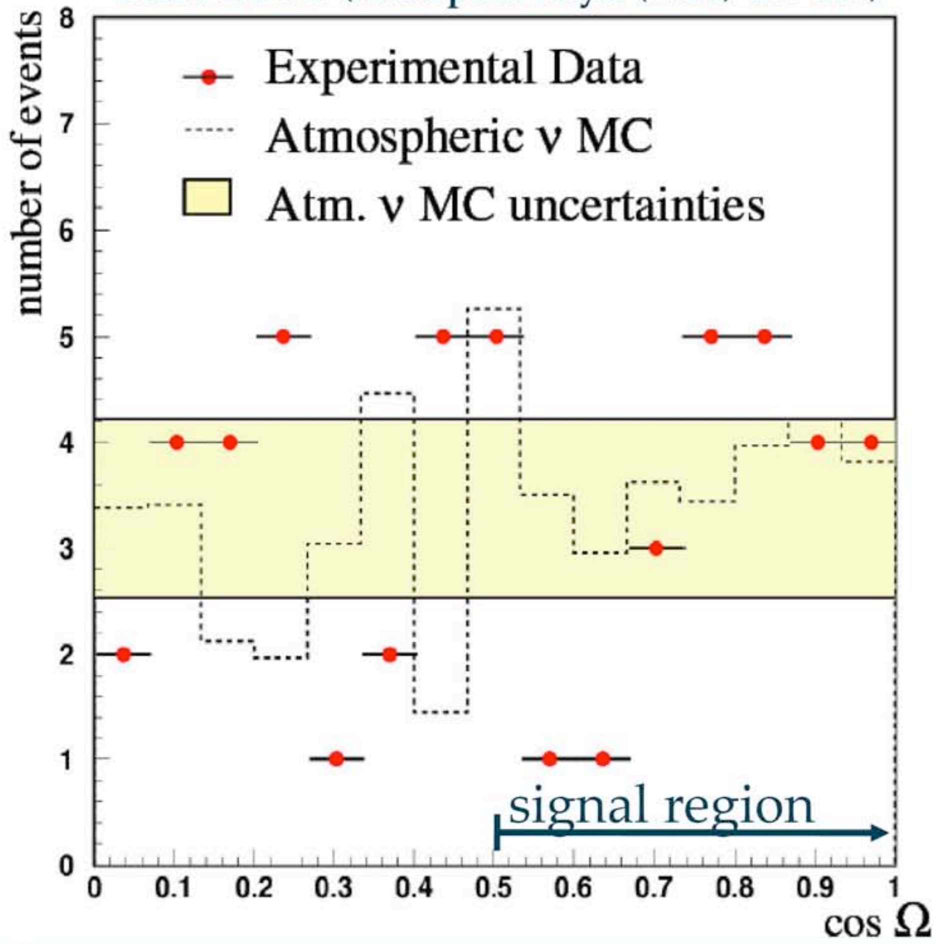

Muon flux limits – Earth '97-'99

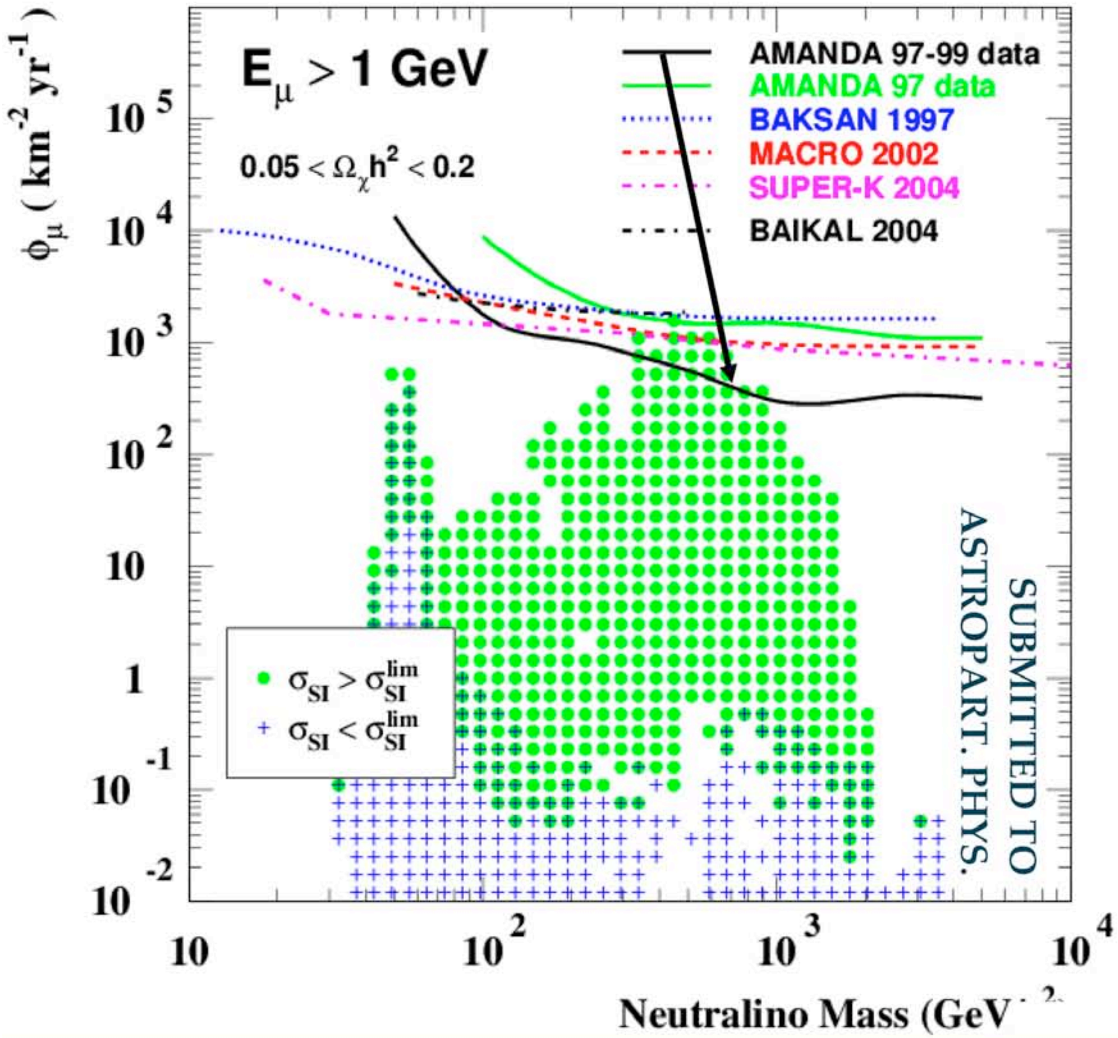

Improvement (wrt. '97)

- separate filter for each neutralino model
- more statistics

Muon flux limits - Sun 2001

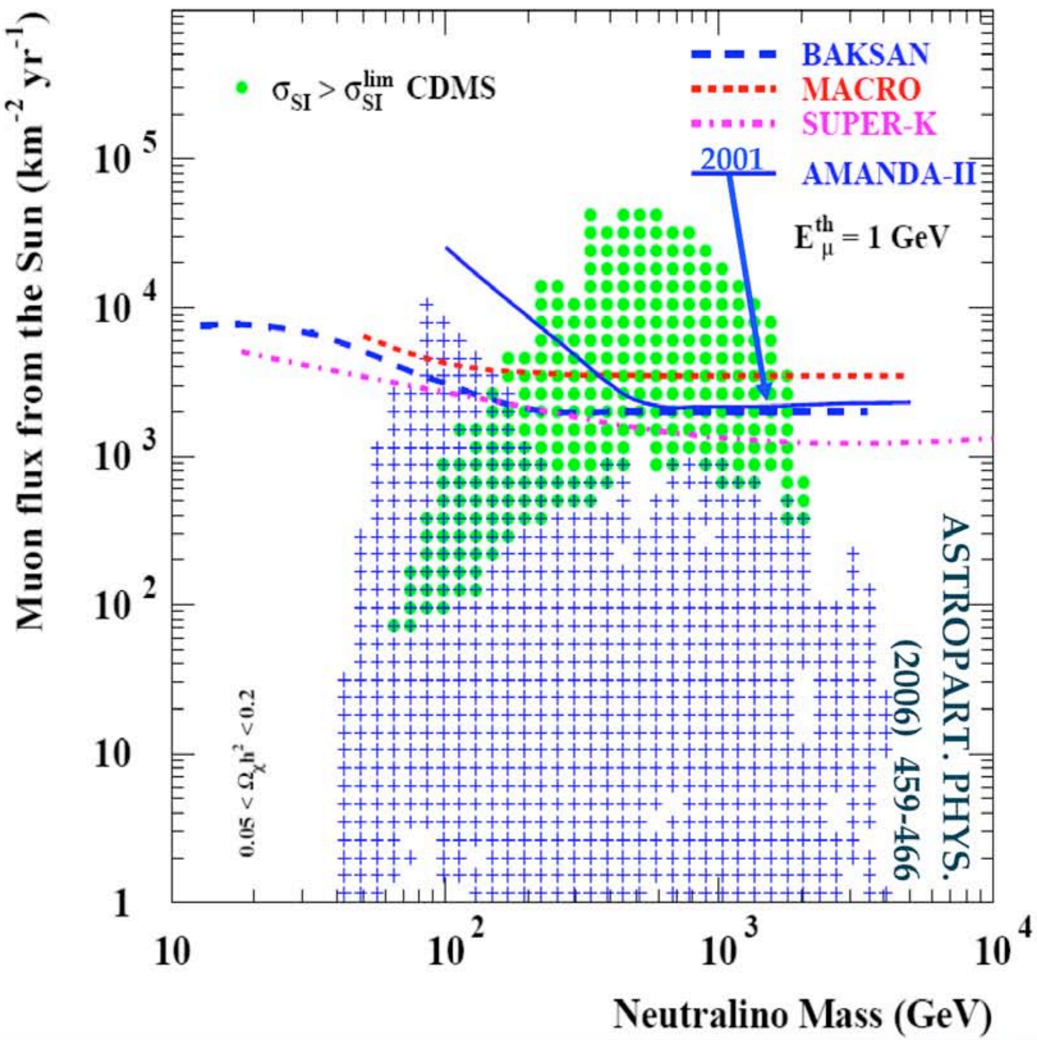

1st AMANDA solar neutralino result

- 200m diameter enables robust reconstruction of horizontal tracks
- competitive with only 144d lifetime

IceCube prospects

Earth

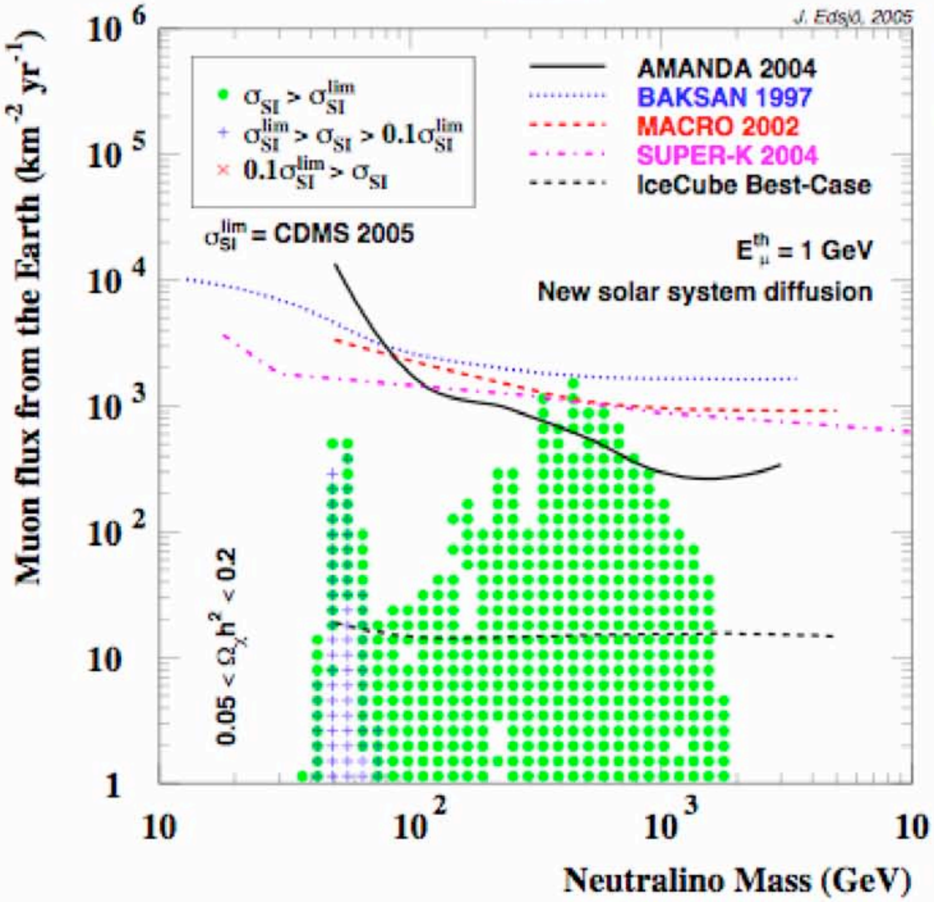

Sun

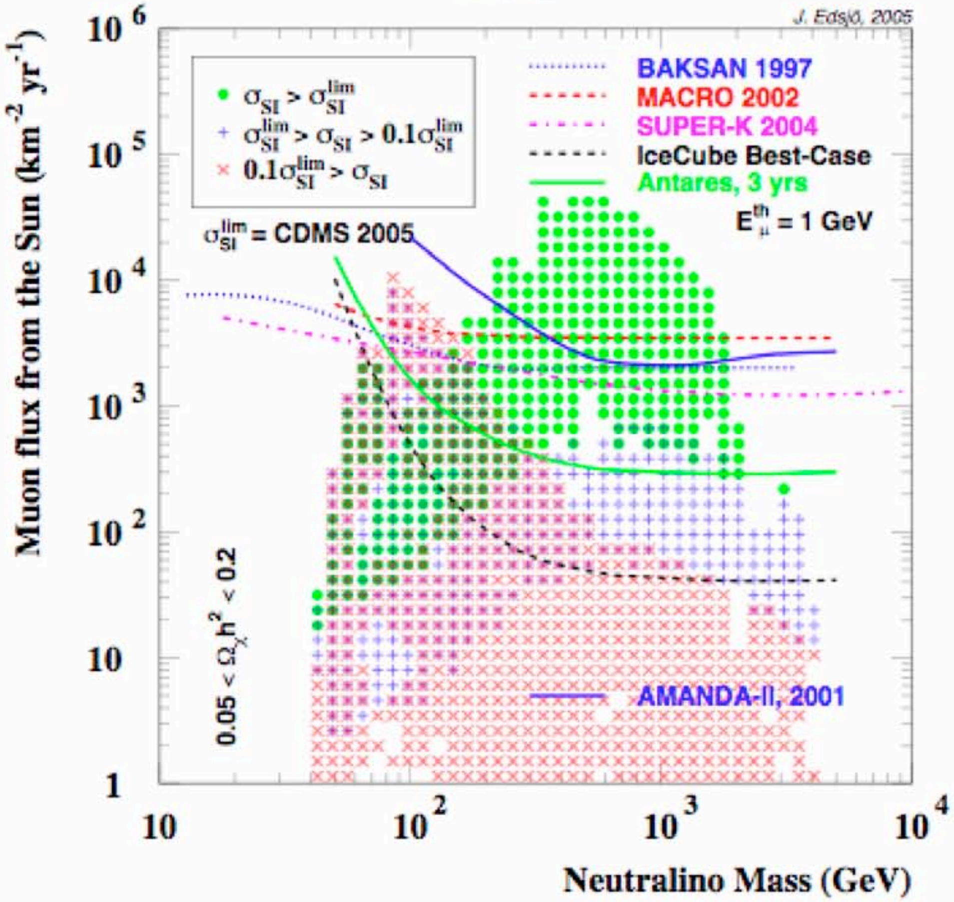

Conclusion & outlook

- No statistically significant excess of neutralino-induced neutrinos from the center of the Earth or the Sun observed
- Upper limits on the muon flux competitive with other indirect searches
- Additional AMANDA-II statistics is being analysed with improved techniques in searches for neutralinos and Kaluza-Klein
- IceCube analysis will soon start!

Indirect Dark Matter Detection

Pierre Salati – Université de Savoie & **LAPTH**

1) The messengers of DM annihilation

2) High energy photons and the Galactic centre

3) Hunting for neutrinos in the ice cap

4) Cosmic ray transport : a short overview

5) TeV antiprotons : a new window

6) Uncertainties i … propagation

Cosmology and Particle Physics Beyond the Standard Models – Cargese – August 7, 2007

Salient features of cosmic ray physics

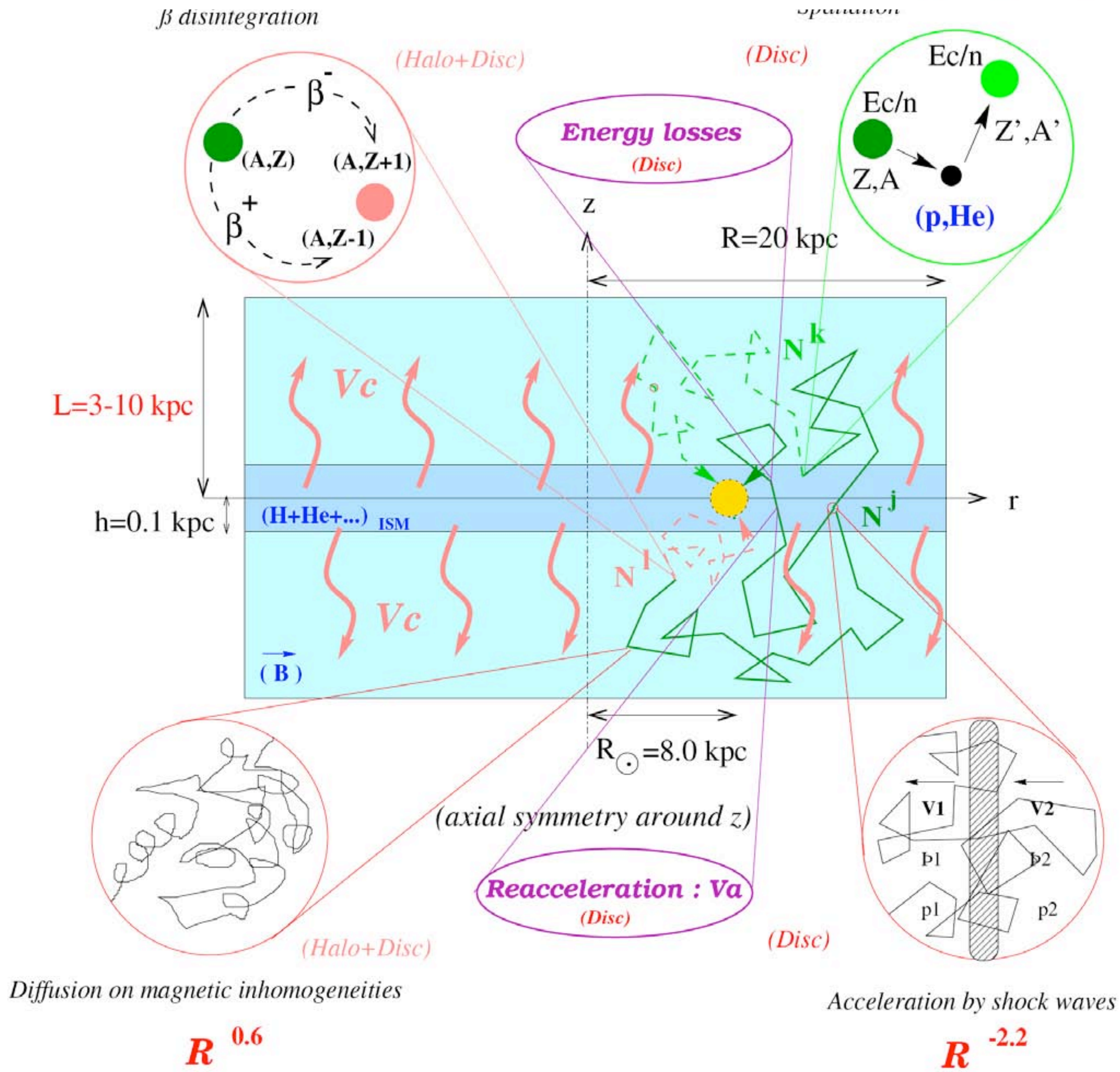

Cosmic–rays diffuse in space and energy

- Diffusion and convection in space

$$\vec{J} \;=\; -\,K\,\vec{\nabla}\Psi \;+\; \Psi\,\vec{V_C}$$

- Second order Fermi mechanism

$$J_E \;=\; b^{\rm loss}(E)\,\Psi \;-\; K_{EE}(E)\,\partial_E\Psi$$

- Steady state holds with $\partial_t\Psi = 0$

Thickness L

$$K(E) = K_0\,\beta \times \mathcal{R}^{\delta} \qquad \Downarrow \qquad K_{EE} = \frac{2}{9}{V_a}^2\frac{E^2\beta^4}{K(E)}$$

$$V_C\,\partial_z\Psi \;-\; K\,\Delta\Psi \;+\; \partial_E\left\{b^{\rm loss}(E)\,\Psi \;-\; K_{EE}(E)\,\partial_E\Psi\right\} \;=\; Q$$

THE ASTROPHYSICAL JOURNAL, 555:585–596, 2001 July 10

D. Maurin et al.

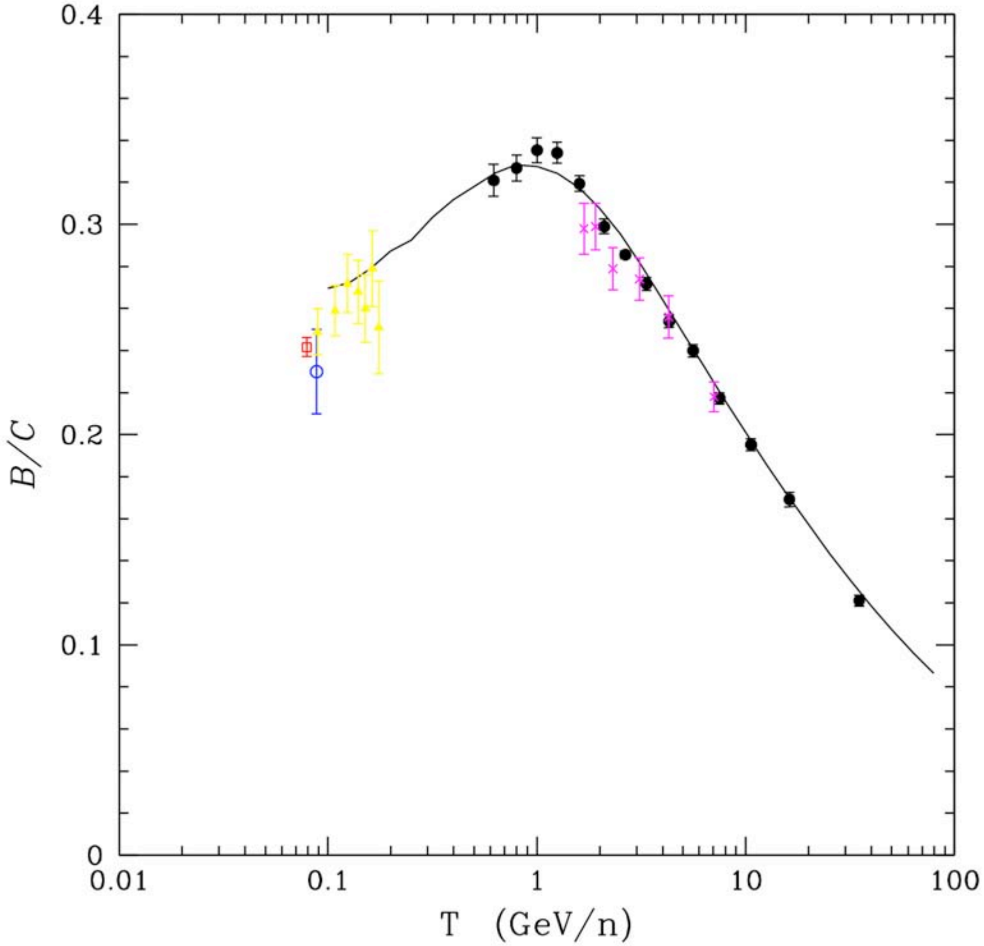

Fig. 3.— This curve displays the computed ratio of (^{10}B+^{11}B)/(^{12}C+^{13}C+^{14}C) for a configuration giving a reduced $\chi_r^2 \approx 1.3$. The experimental points are from HEAO-3 (solid circles), ISEE (triangles), IMP-8 (empty circle), VOYAGER (square) and balloons (crosses).

THE ASTROPHYSICAL JOURNAL, 555:585–596, 2001 July 10

D. Maurin et al.

$$K(E) = K_0\,\beta \times \mathscr{R}^{\delta}$$

Iso-χ^2 contours for B/C ($\chi^2 < 40$)

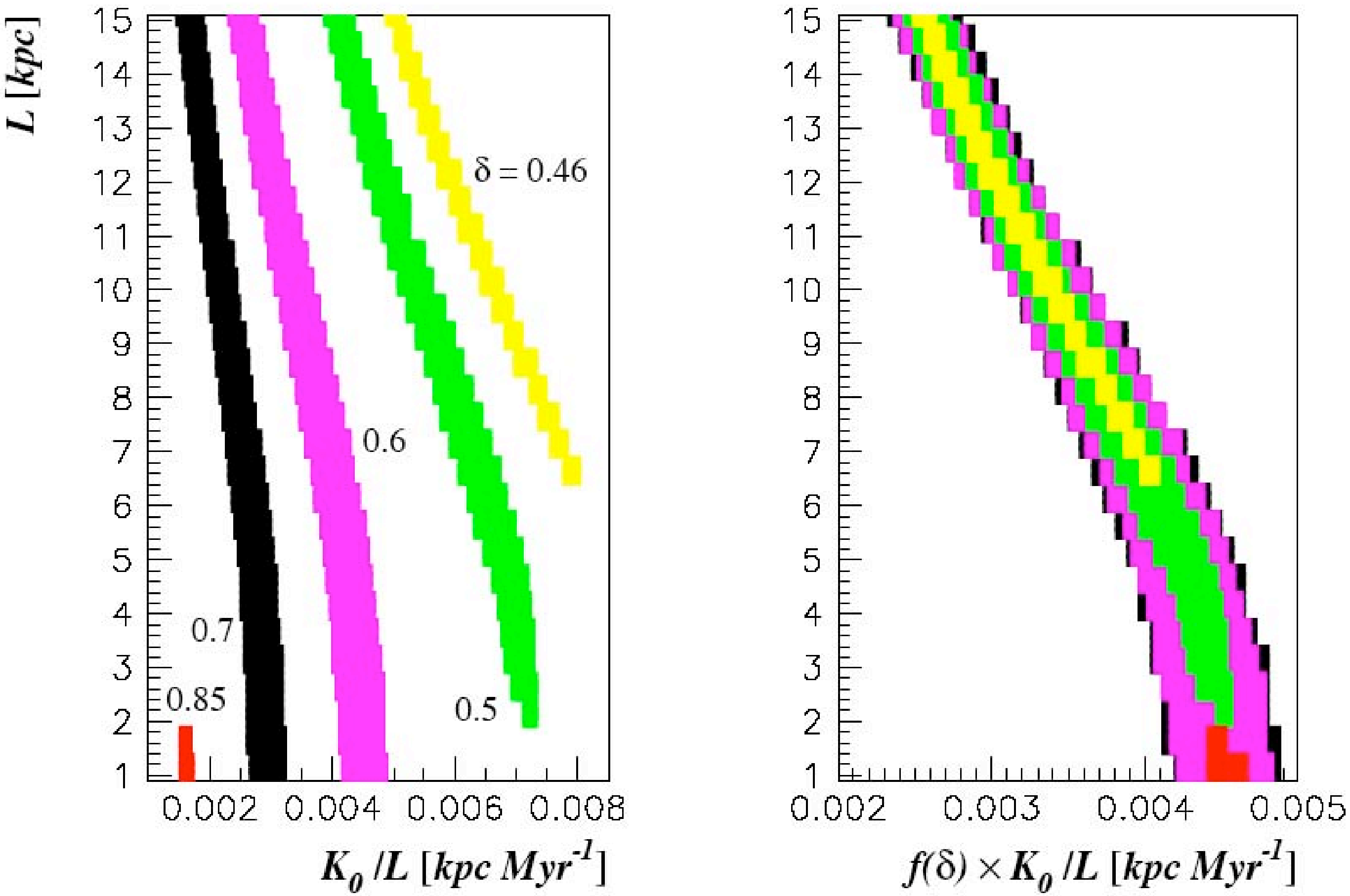

THE ASTROPHYSICAL JOURNAL, 555:585–596, 2001 July 10

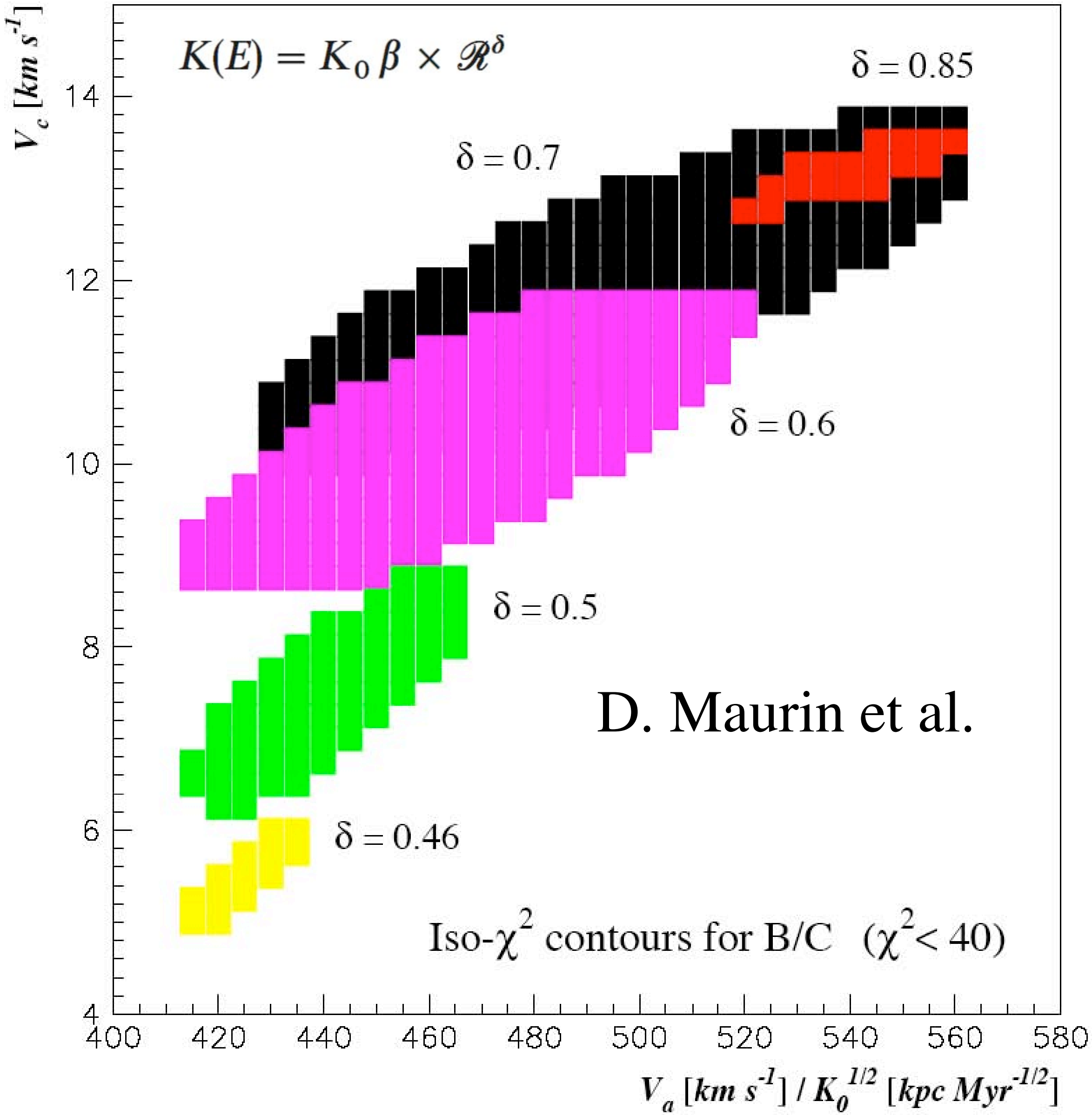

Transport of Cosmic Rays in Chaotic Magnetic Fields

F. Casse, M. Lemoine & G. Pelletier, PRD **D65** (2002) 023002

Magnetic turbulence $\delta\mathbf{B}(\mathbf{x}) = \int \frac{\mathrm{d}\mathbf{k}}{(2\pi)^3}\, e^{-i\mathbf{k}\cdot\mathbf{x}}\, \delta\mathbf{B}(\mathbf{k})$ whose power spectrum is defined by

$$\langle \delta\mathbf{B}(\mathbf{k})\delta\mathbf{B}^{\dagger}(\mathbf{k}')\rangle \;=\; (2\pi)^3\, \delta(\mathbf{k}-\mathbf{k}')\, S_{3\mathrm{d}}(\mathbf{k})$$

and follows between k_{min} and k_{max} the power law

$$S_{3\mathrm{d}}(\mathbf{k}) \propto k^{-\alpha}$$

The level of turbulence wrt to the homogeneous field $\mathbf{B}_0$ is defined by

$$\eta \;=\; \frac{\langle \delta\mathbf{B}^2\rangle}{\mathbf{B}_0^2 + \langle \delta\mathbf{B}^2\rangle}$$

Transport of Cosmic Rays in Chaotic Magnetic Fields

F. Casse, M. Lemoine & G. Pelletier, PRD **65** (2002) 023002

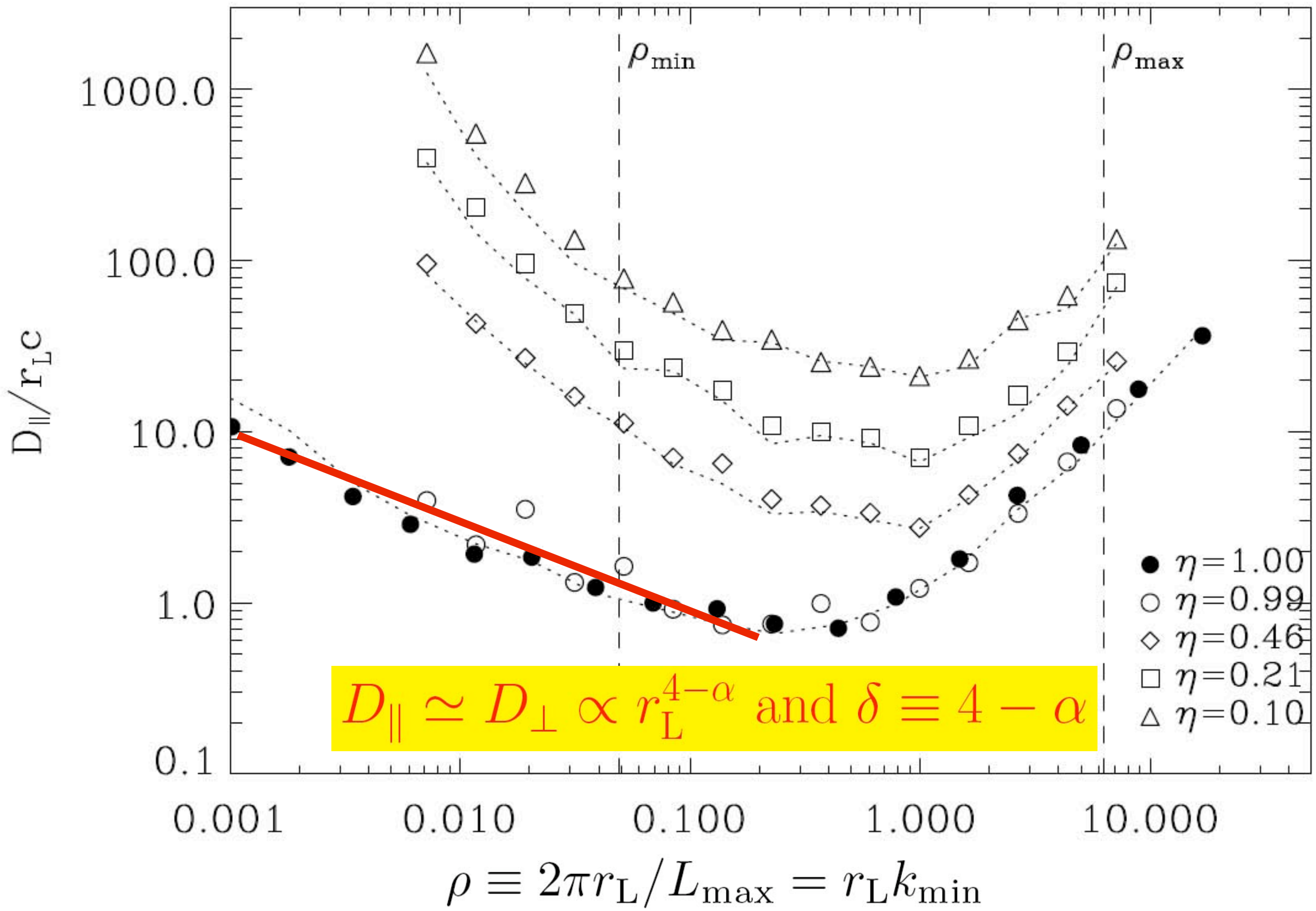

$\delta = 1/3$ (Kolmogorov) or $\delta = 1/2$ (Iroshnikov, Kraichnan)

A.M. Lionetto, A. Morselli & V. Zdravkovic, JCAP **0509** (2005) 010

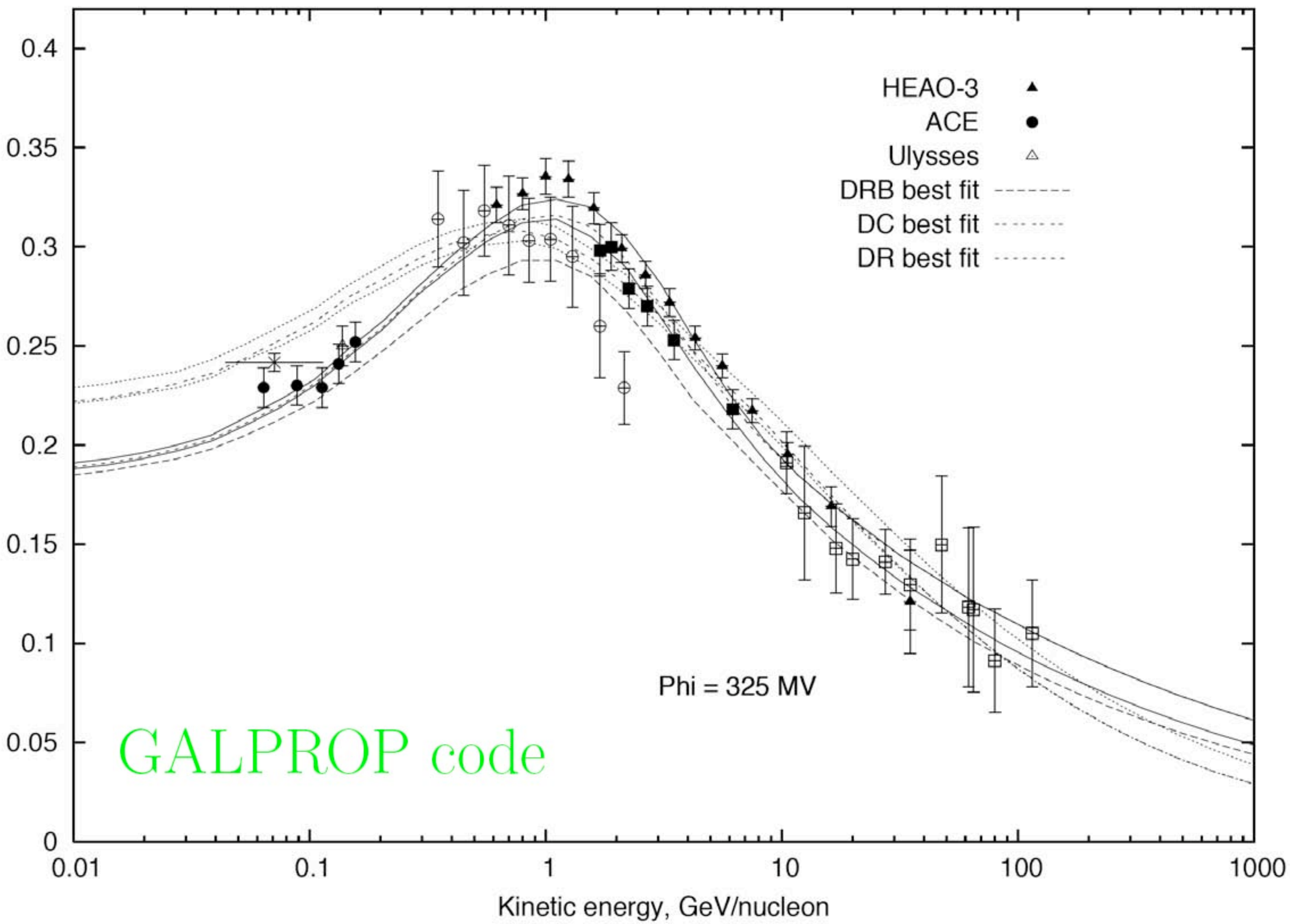

A.M. Lionetto, A. Morselli & V. Zdravkovic, JCAP **0509** (2005) 010

GALPROP code

Space Diffusion & Diffusive Reacceleration

Table 1. Allowed values for diffusion and reacceleration model propagation parameters.

par./val.	$z[Kpc]$	$D_0[cm^2 s^{-1}]$	δ	γ	$v_A[Kms^{-1}]$
minimal	3.0	$5.2\ 10^{28}$	0.25	2.35	22
best fit	4.0	$5.8\ 10^{28}$	0.29	2.47	26
maximal	5.0	$6.7\ 10^{28}$	0.36	2.52	35

Space Diffusion & Convective Wind

Table 2. Allowed values for the propagation parameters for diffusion convection model.

par./val.	$z[Kpc]$	$D_0[\frac{cm^2}{s}]$	δ_2	$\frac{dV_C}{dz}[\frac{Km}{skpc}]$	γ_1	γ_2
minimal	3.0	$2.3\ 10^{28}$	0.48	5.0	2.42	2.14
best fit	4.0	$2.5\ 10^{28}$	0.55	6.0	2.48	2.20
maximal	5.0	$2.7\ 10^{28}$	0.62	7.0	2.50	2.22

Indirect Dark Matter Detection

Pierre Salati – Université de Savoie & **LAPTH**

1) The messengers of DM annihilation

2) High energy photons and the Galactic centre

3) Hunting for neutrinos in the ice cap

4) Cosmic ray transport : a short overview

5) TeV antiprotons : a new window

6) Uncertainties i … propagation

Cosmology and Particle Physics Beyond the Standard Models – Cargese – August 7, 2007

Space diffusion dominates in the master equation

$$V_C\,\partial_z\Psi \;-\; K\,\Delta\Psi \;+\; \partial_E\left\{b^{\mathrm{loss}}(E)\,\Psi \;-\; K_{EE}(E)\,\partial_E\Psi\right\} \;=\; Q$$

Poisson equation $K\,\Delta\Psi + Q = 0$

$$\Downarrow$$

Long range with $G_{\bar{\mathrm{p}}}^{\mathrm{3D}}(r) \;=\; \dfrac{Q}{4\pi K r}$

- Evaporation at the vertical boundaries $\pm L$
- Leakage at the radial boundaries $R = 20$ kpc
- Evaporation from convective wind V_C
- Annihilations inside the MW gaseous disk
- Energy losses and mild diffusive reacceleration

Exercise – Level **[3]** *: Solving the previous CR diffusion equation with the Bessel expansion method allows to naturally implement a vanishing antiproton density at the radial boundary* $r = R$

$$\Psi\,(r, z, E) \;=\; \sum_{i=1}^{+\infty} P_i\,(z, E)\;J_0\,(\alpha_i\, r/R)\;\;, \tag{1}$$

where α_i *is the ith zero of the Bessel function* J_0*. Show that each Bessel transform* P_i *fulfills the relation*

$$V_C\,\partial_z P_i - K\,\partial_z^2 P_i + K \left\{ \frac{\alpha_i^2}{R^2} \right\} P_i = Q_i\,(z, E) \equiv \frac{2}{R^2}\,\frac{1}{J_1^2\,(\alpha_i)} \int_0^R r\,J_0 \left(\alpha_i\,\frac{r}{R} \right) Q\,(r, z, E)\;dr\;, \tag{2}$$

when energy losses and diffusive reacceleration are neglected. Integrate this equation along the vertical axis assuming that Q_i *is an even function of* z *and establish that*

$$P_i\,(0, E) = \frac{2}{\mathcal{A}_i} \int_0^L dz\;Q_i\,(z, E)\;e^{-\dfrac{V_C\,z}{2K}}\;\mathcal{F}_i(z)\;. \tag{3}$$

The coefficients $\mathcal{A}_i$ *that appear in the previous expression are given by*

$$\mathcal{A}_i(E) = V_C \;+\; K S_i \coth \left(\frac{S_i\,L}{2} \right)\;, \tag{4}$$

where $S_i^2 \;=\; (V_C/K)^2 \;+\; (2\,\alpha_i/R)^2$*, and the vertical functions* $\mathcal{F}_i(z)$ *are defined as*

$$\mathcal{F}_i(z) \;=\; \sinh \left\{ \frac{S_i}{2}\;(L - z) \right\} / \sinh \left\{ \frac{S_i}{2}\;L \right\}\;. \tag{5}$$

Exercise – Level [4] : *A completely different approach to describe the antiproton propagation through the diffusive halo relies on the existence of a Green function $G_{\bar{p}}$. Such a function translates the probability for an antiproton produced at point $S(x_S, y_S, z_S)$ to travel to the observer located at point $M(x, y, z)$. The antiproton energy spectrum is given by the convolution of the Green function $G_{\bar{p}}$ with the production rate Q*

$$\Psi(M, E) = \int d^3\mathbf{x}_S \;\; G_{\bar{p}}(M \leftarrow S, E) \; Q(S, E) \;\; . \tag{1}$$

The construction of the Green function for antiprotons is inspired from the positron case – see in particular the next section – with the difference that the antiproton energy does not change and that time is integrated out. Because the Milky Way is now pictured as an infinite slab of half-thickness L with a gaseous disk in the middle at $z = 0$, the antiproton propagation is invariant under a translation along the horizontal axis x or y. Neglect energy losses and diffusive reacceleration to show that

$$G_{\bar{p}}(\odot \leftarrow S, E) = \frac{e^{-z_S/r_w}}{2\pi K(E)} \;\; \sum_{n=1}^{+\infty} \frac{1}{C_n} \; \phi_n(0) \, \phi_n(z_S) \; K_0\left(\frac{r}{L}\sqrt{\epsilon_n}\right) \; . \tag{2}$$

The vertical functions ϕ_n are defined by

$$\phi_n(z) \;=\; \sin\left\{\xi_n\left(1 - \frac{z}{L}\right)\right\} \;, \tag{3}$$

where the coefficients ξ_n are solutions to the equation $\xi_n = n\,\pi \;-\; \tan^{-1}(p\,\xi_n)$. The parameter p is related to the convective scale $r_w \equiv 2K(E)/V_C$ through $p = r_w L$ whereas the scale C_n is defined by

$$\frac{C_n}{L} \;=\; 1 \;+\; \frac{1}{p}\left(\frac{\sin\xi_n}{\xi_n}\right)^2 \; . \tag{4}$$

In the argument of the modified Bessel functions of the second kind K_0 in Eq. (2), the ratio r/L is multiplied by a factor $\sqrt{\epsilon_n}$ where $\epsilon_n = \xi_n^2 \;+\; (L/r_w)^2$.

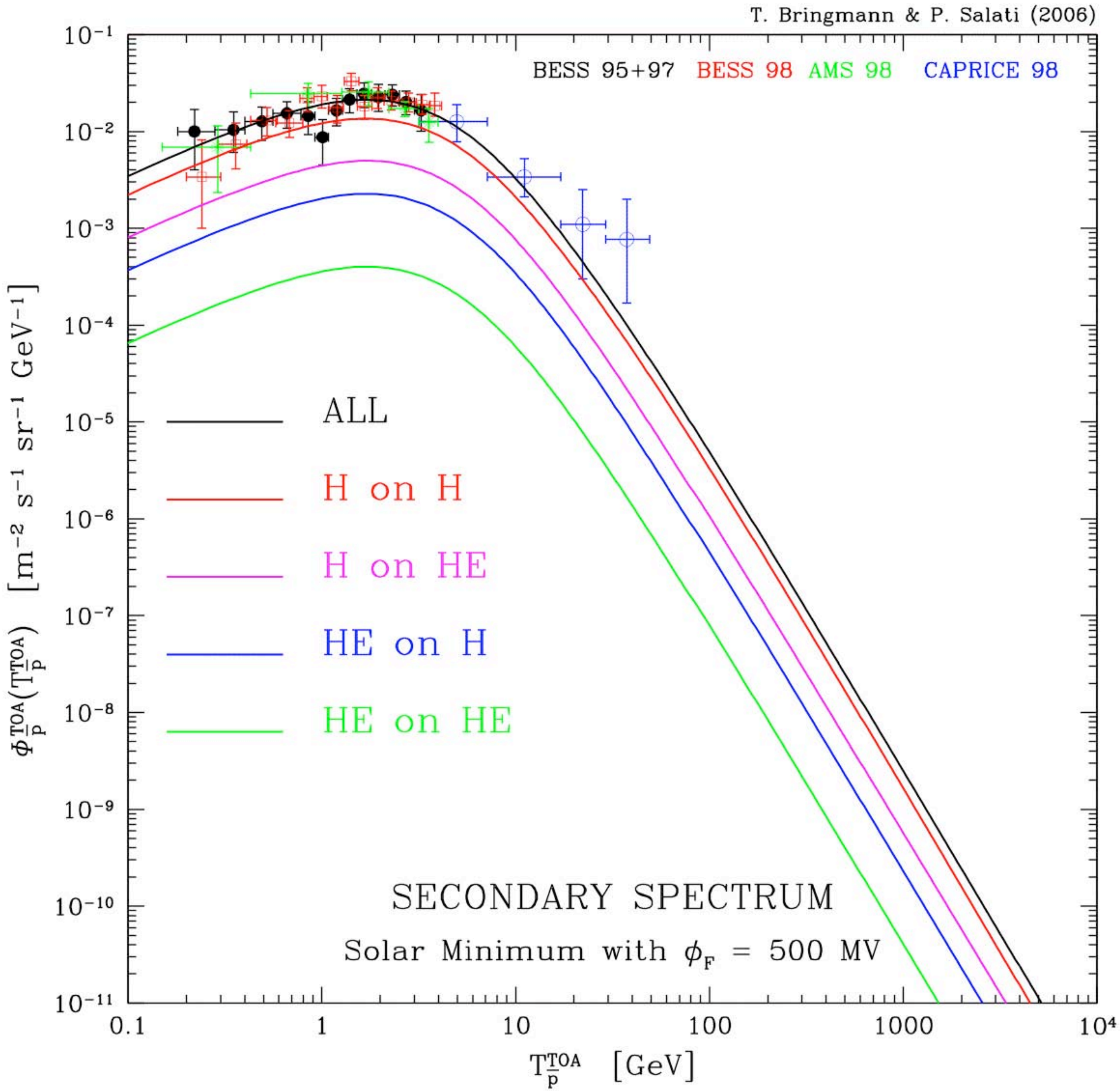

T. Bringmann & P. Salati (2006)
BESS 95+97
BESS 98
AMS 98
CAPRICE 98
ALL
H on H
H on HE
HE on H
HE on HE
SECONDARY SPECTRUM
Solar Minimum with ϕ_F = 500 MV
$\Phi_{\bar{p}}^{TOA}(T_{\bar{p}}^{TOA})$ [m^{-2} s^{-1} sr^{-1} GeV^{-1}]
$T_{\bar{p}}^{TOA}$ [GeV]
10^{-1}
10^{-2}
10^{-3}
10^{-4}
10^{-5}
10^{-6}
10^{-7}
10^{-8}
10^{-9}
10^{-10}
10^{-11}
0.1
1
10
100
1000
10^4

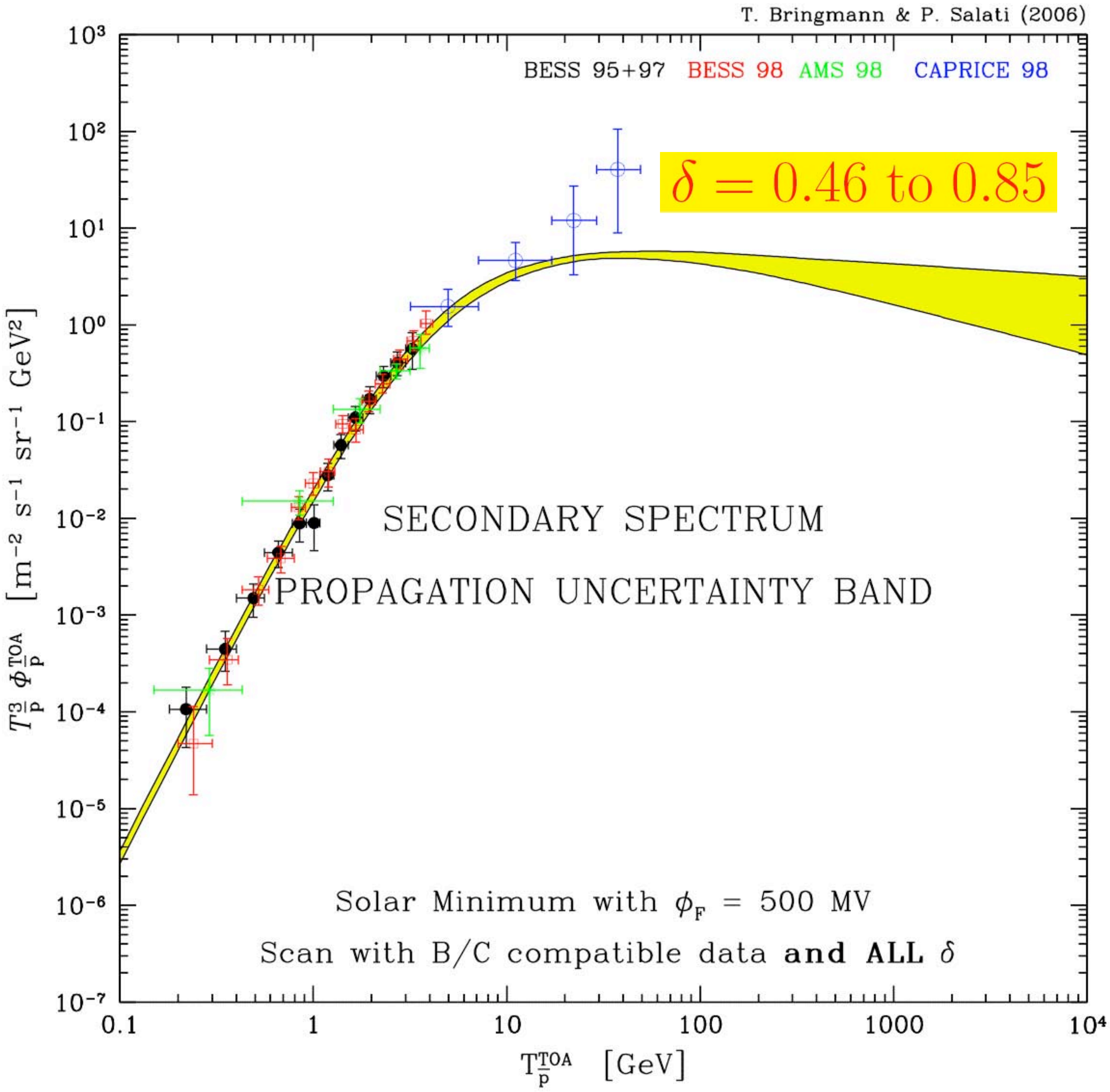

T. Bringmann & P. Salati (2006)
BESS 95+97 BESS 98 AMS 98 CAPRICE 98
$\delta = 0.46$ to 0.85
SECONDARY SPECTRUM
PROPAGATION UNCERTAINTY BAND
Solar Minimum with ϕ_F = 500 MV
Scan with B/C compatible data **and ALL** δ
$T^3_{\bar{p}} \, \Phi^{TOA}_{\bar{p}}$ [m^{-2} s^{-1} sr^{-1} GeV^2]
$T^{TOA}_{\bar{p}}$ [GeV]

CREAM

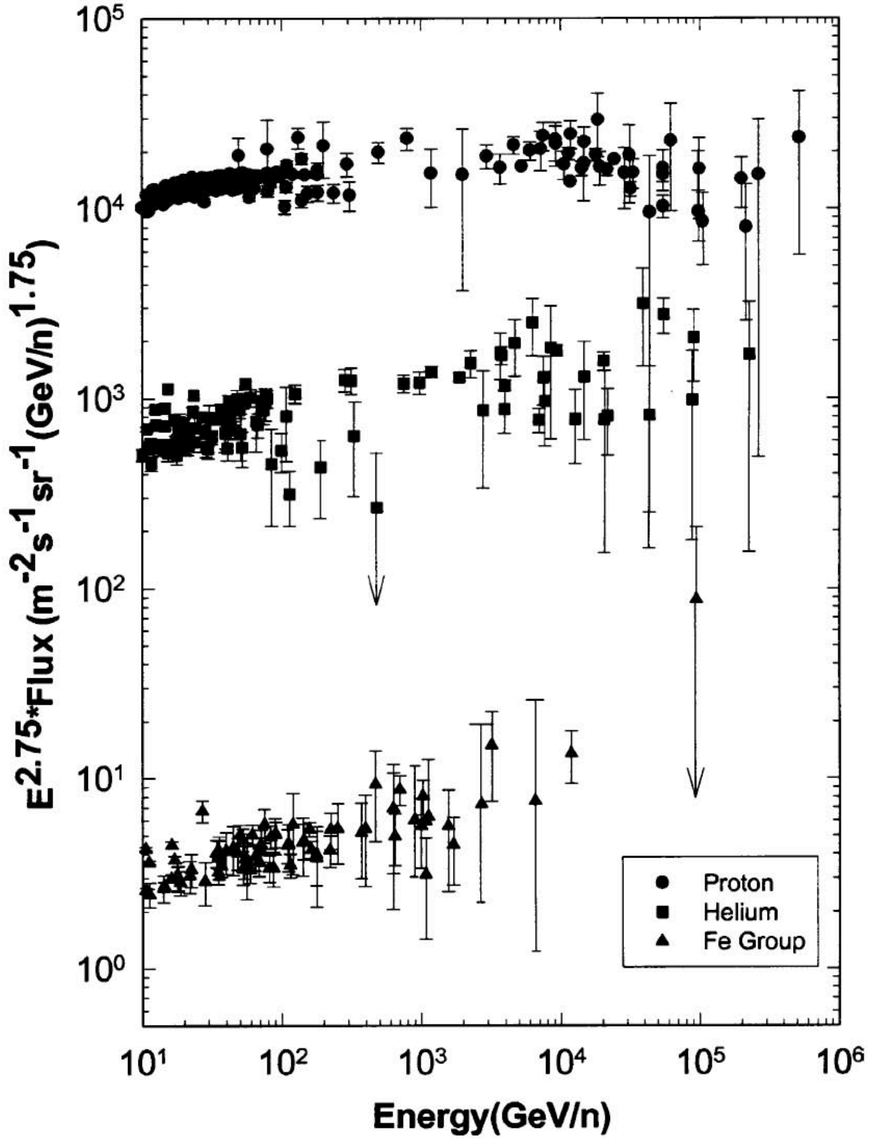

Fig. 1. Compiled data from direct measurements.

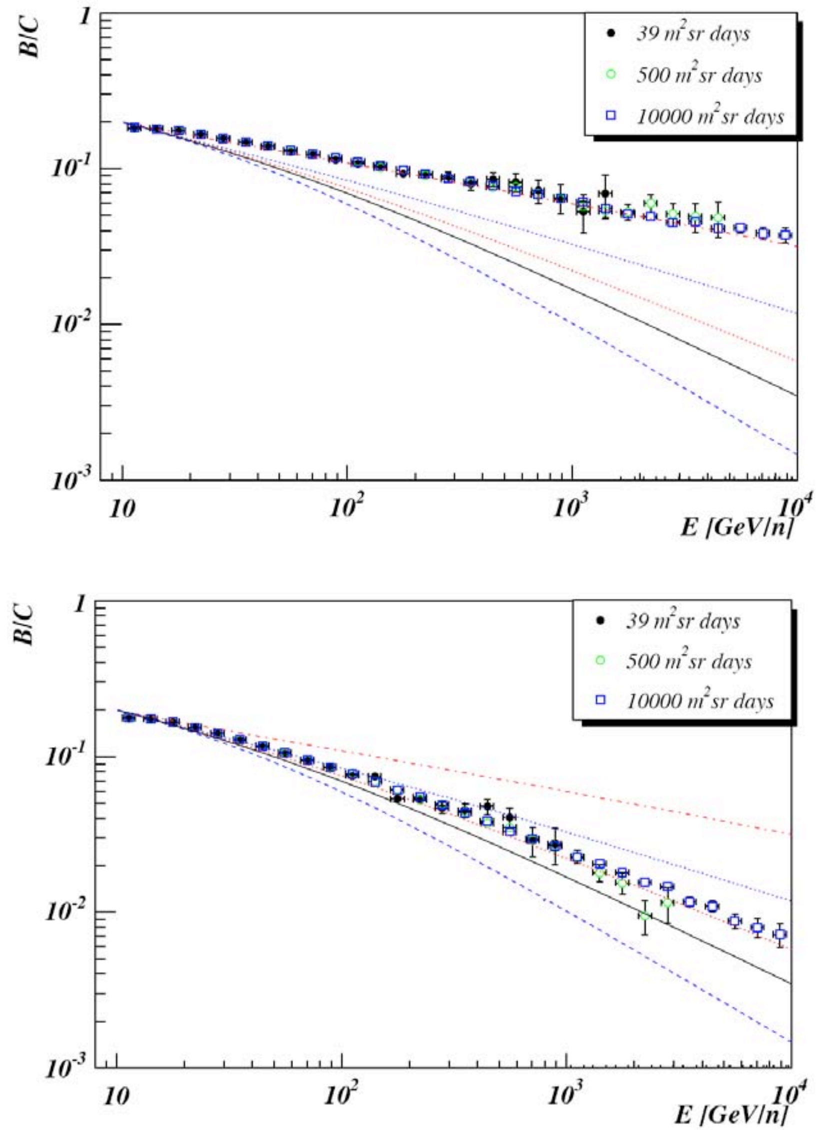

A. Castellina & F. Donato `astro-ph/0504149`

$$\rho_{\rm CDM}(\mathbf{r}) = \rho_{\rm s} \left(\frac{r_{\rm s}}{r}\right)^{\gamma} \left\{1 + \left(\frac{r}{r_{\rm s}}\right)^{\alpha}\right\}^{\frac{\gamma-\beta}{\alpha}}$$

Halo model	α	β	γ	$\rho_{\rm s}$ $[10^6 M_\odot \rm{kpc}^{-3}]$	$r_{\rm s}$ [kpc]
isothermal sphere	2	2	0	7.90	4
NFW 97 [37]	1	3	1	5.38	21.75
Moore 04 [38]	1	3	1.16	2.54	32.62
Moore 99 [39]	1.5	3	1.5	1.06	34.52

Case	δ	K_0 [kpc^2/Myr]	L [kpc]	V_C [km/s]	V_a [km/s]
max	0.46	0.0765	15	5	117.6
med	0.70	0.0112	4	12	52.9
min	0.85	0.0016	1	13.5	22.4

DM model	m	$\langle\sigma_{\rm ann}v\rangle$	$t\bar{t}$	$b\bar{b}$	$c\bar{c}$	$s\bar{s}$	$u\bar{u}$	$d\bar{d}$	ZZ	W^+W^-	HH	gg
LSP1.0	1.0	0.46	-	-	-	-	-	-	-	100	-	-
LKP1.0	1.0	1.60	10.9	0.7	11.1	0.7	11.1	0.7	0.5	1.0	0.5	0.5
LSP1.7	1.7	102	-	-	-	-	-	-	20.1	79.9	-	-
LKP1.7	1.7	0.55	11.0	0.7	11.1	0.7	11.1	0.7	0.5	0.9	0.5	0.5

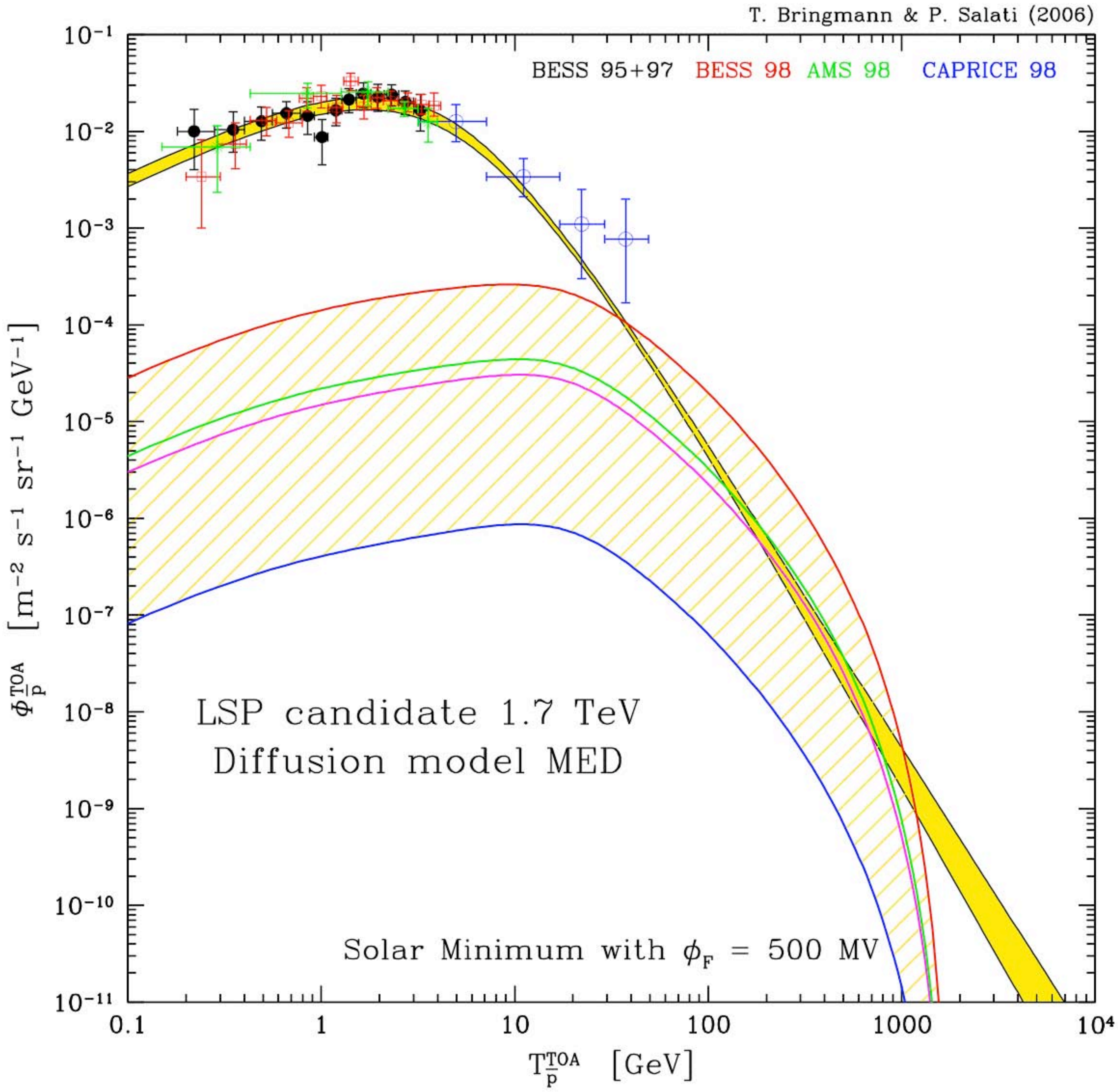
T. Bringmann & P. Salati (2006)
BESS 95+97
BESS 98
AMS 98
CAPRICE 98
LSP candidate 1.7 TeV
Diffusion model MED
Solar Minimum with ϕ_F = 500 MV
$\phi_{\bar{p}}^{TOA}$ [m^{-2} s^{-1} sr^{-1} GeV^{-1}]
$T_{\bar{p}}^{TOA}$ [GeV]
10^{-1}
10^{-2}
10^{-3}
10^{-4}
10^{-5}
10^{-6}
10^{-7}
10^{-8}
10^{-9}
10^{-10}
10^{-11}
0.1
1
10
100
1000
10^4

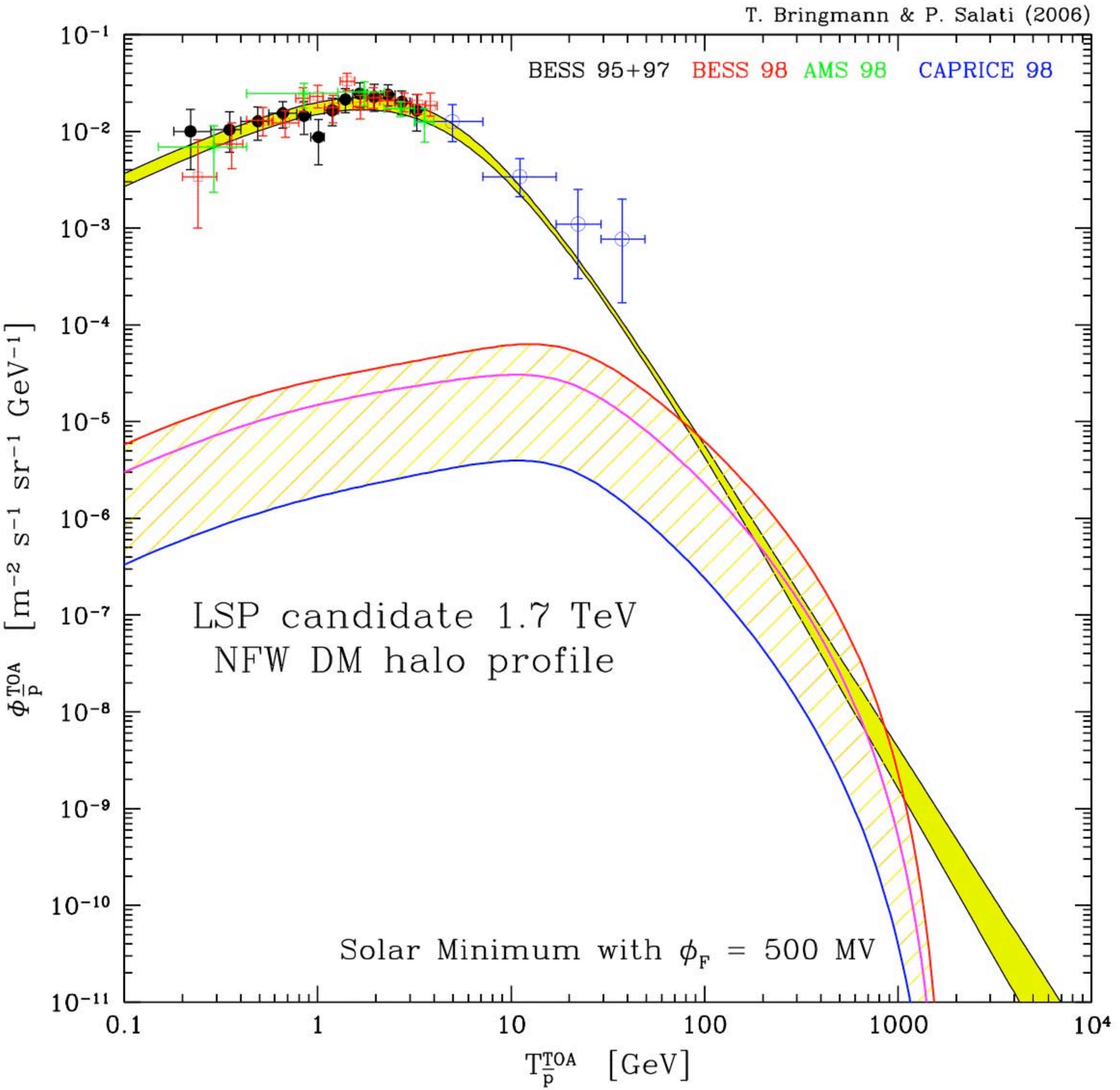

T. Bringmann & P. Salati (2006)
BESS 95+97
BESS 98
AMS 98
CAPRICE 98
LSP candidate 1.7 TeV
NFW DM halo profile
Solar Minimum with ϕ_F = 500 MV
$\phi_{\bar{p}}^{TOA}$ [m^{-2} s^{-1} sr^{-1} GeV^{-1}]
$T_{\bar{p}}^{TOA}$ [GeV]
10^{-1}
10^{-2}
10^{-3}
10^{-4}
10^{-5}
10^{-6}
10^{-7}
10^{-8}
10^{-9}
10^{-10}
10^{-11}
0.1
1
10
100
1000
10^4

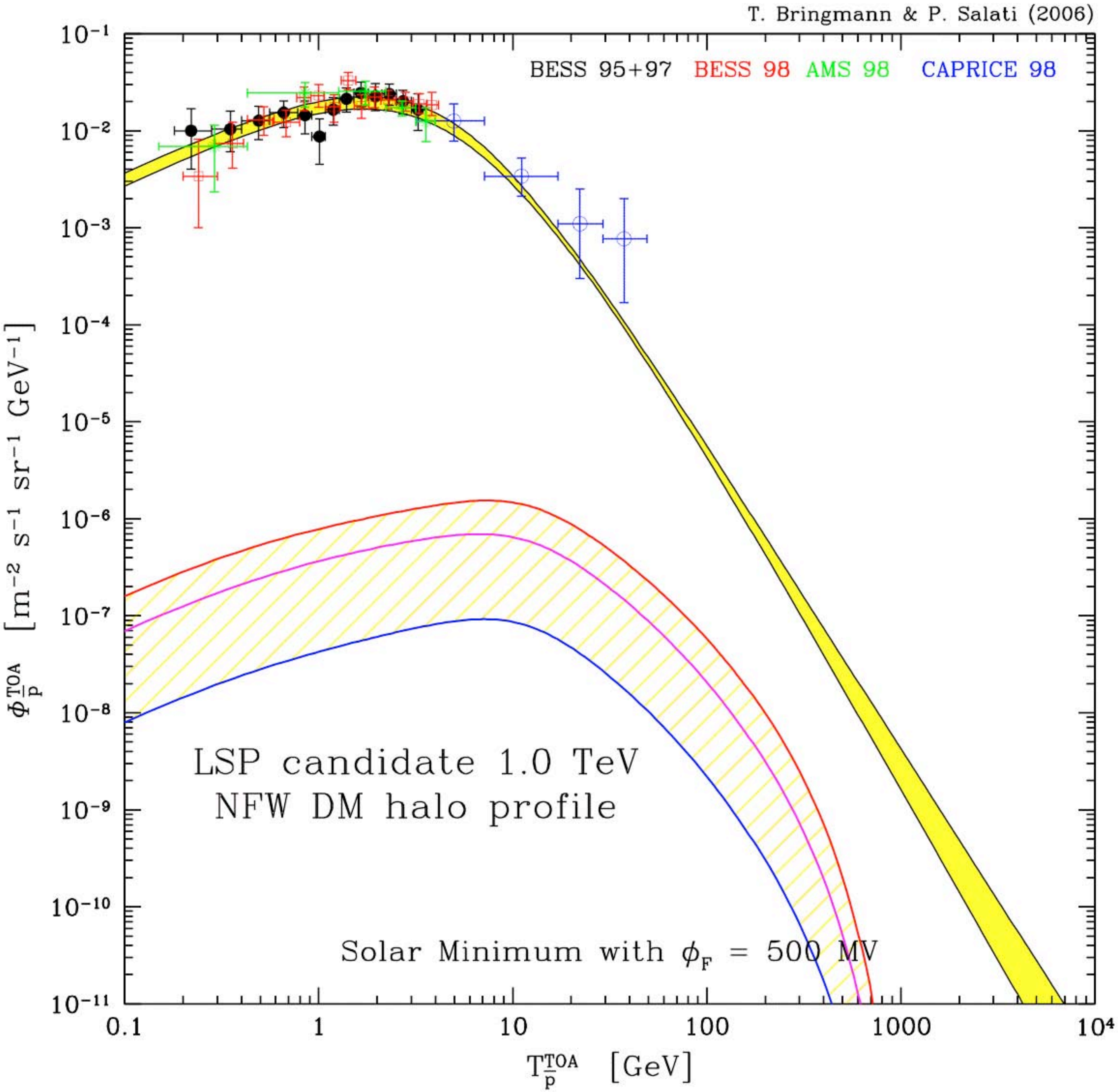

T. Bringmann & P. Salati (2006)
BESS 95+97
BESS 98
AMS 98
CAPRICE 98
LSP candidate 1.0 TeV
NFW DM halo profile
Solar Minimum with ϕ_F = 500 MV
$\Phi_{\bar{p}}^{TOA}$ [m^{-2} s^{-1} sr^{-1} GeV^{-1}]
$T_{\bar{p}}^{TOA}$ [GeV]
10^{-1}
10^{-2}
10^{-3}
10^{-4}
10^{-5}
10^{-6}
10^{-7}
10^{-8}
10^{-9}
10^{-10}
10^{-11}
0.1
1
10
100
1000
10^4

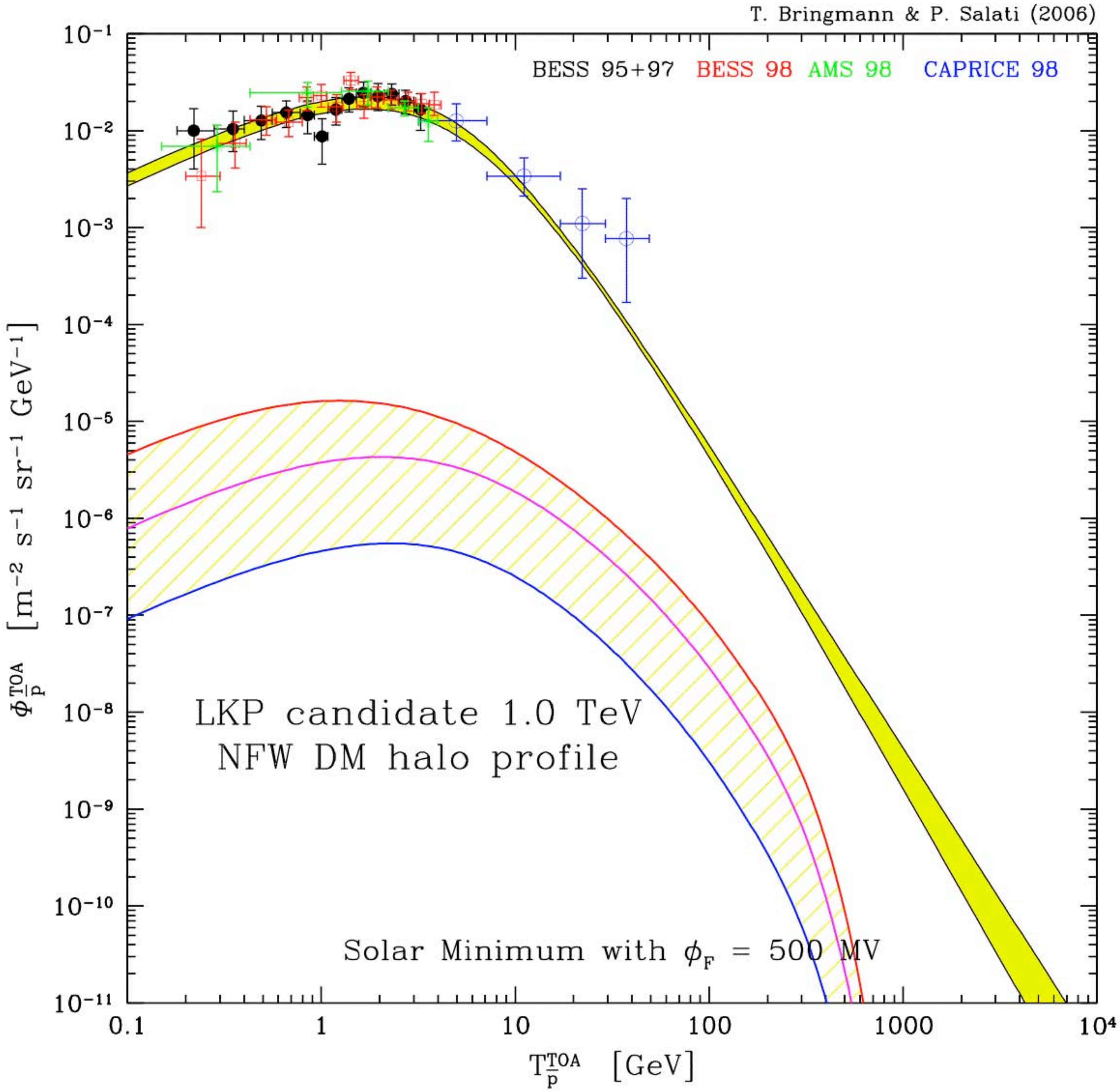

T. Bringmann & P. Salati (2006)
BESS 95+97
BESS 98
AMS 98
CAPRICE 98
LKP candidate 1.0 TeV
NFW DM halo profile
Solar Minimum with ϕ_F = 500 MV
$\Phi_{\bar{p}}^{TOA}$ [m^{-2} s^{-1} sr^{-1} GeV^{-1}]
$T_{\bar{p}}^{TOA}$ [GeV]
10^{-1}
10^{-2}
10^{-3}
10^{-4}
10^{-5}
10^{-6}
10^{-7}
10^{-8}
10^{-9}
10^{-10}
10^{-11}
0.1
1
10
100
1000
10^4

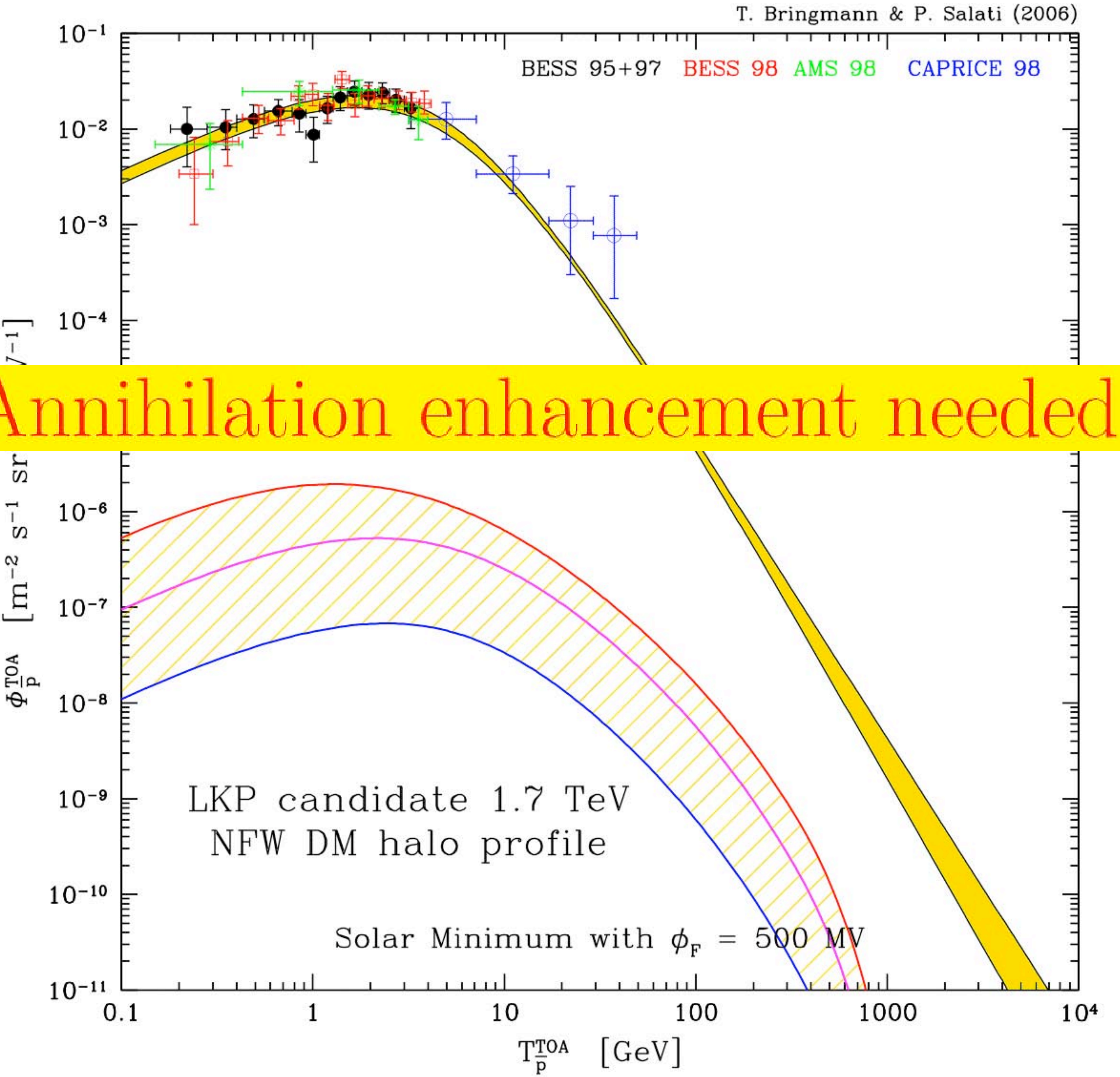

Annihilation enhancement needed !

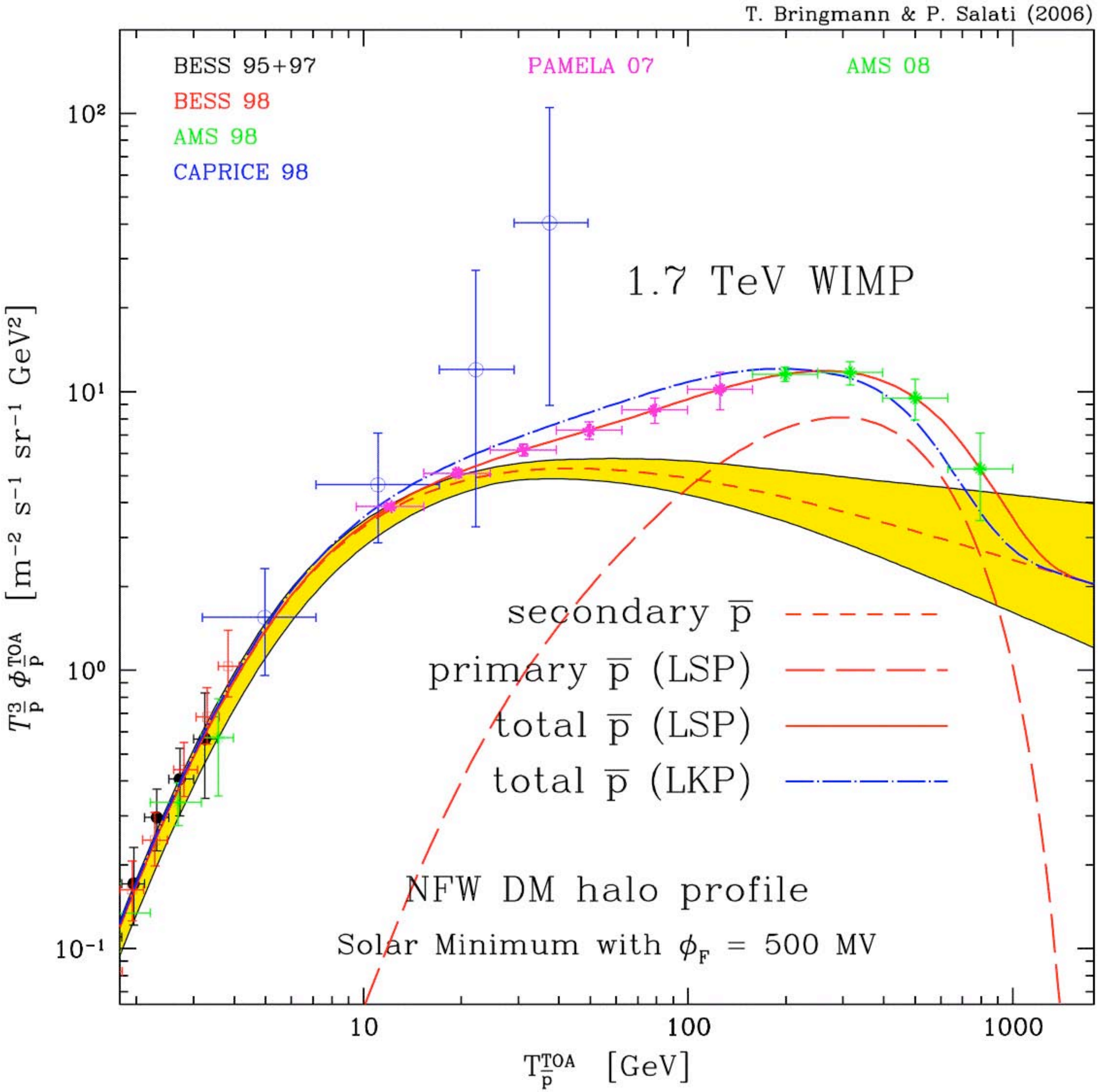

T. Bringmann & P. Salati (2006)
BESS 95+97
BESS 98
AMS 98
CAPRICE 98
PAMELA 07
AMS 08
1.7 TeV WIMP
secondary p̄
primary p̄ (LSP)
total p̄ (LSP)
total p̄ (LKP)
NFW DM halo profile
Solar Minimum with ϕ_F = 500 MV
$T_{\bar{p}}^3 \, \Phi_{\bar{p}}^{TOA}$ [m⁻² s⁻¹ sr⁻¹ GeV²]
$T_{\bar{p}}^{TOA}$ [GeV]
10
100
1000

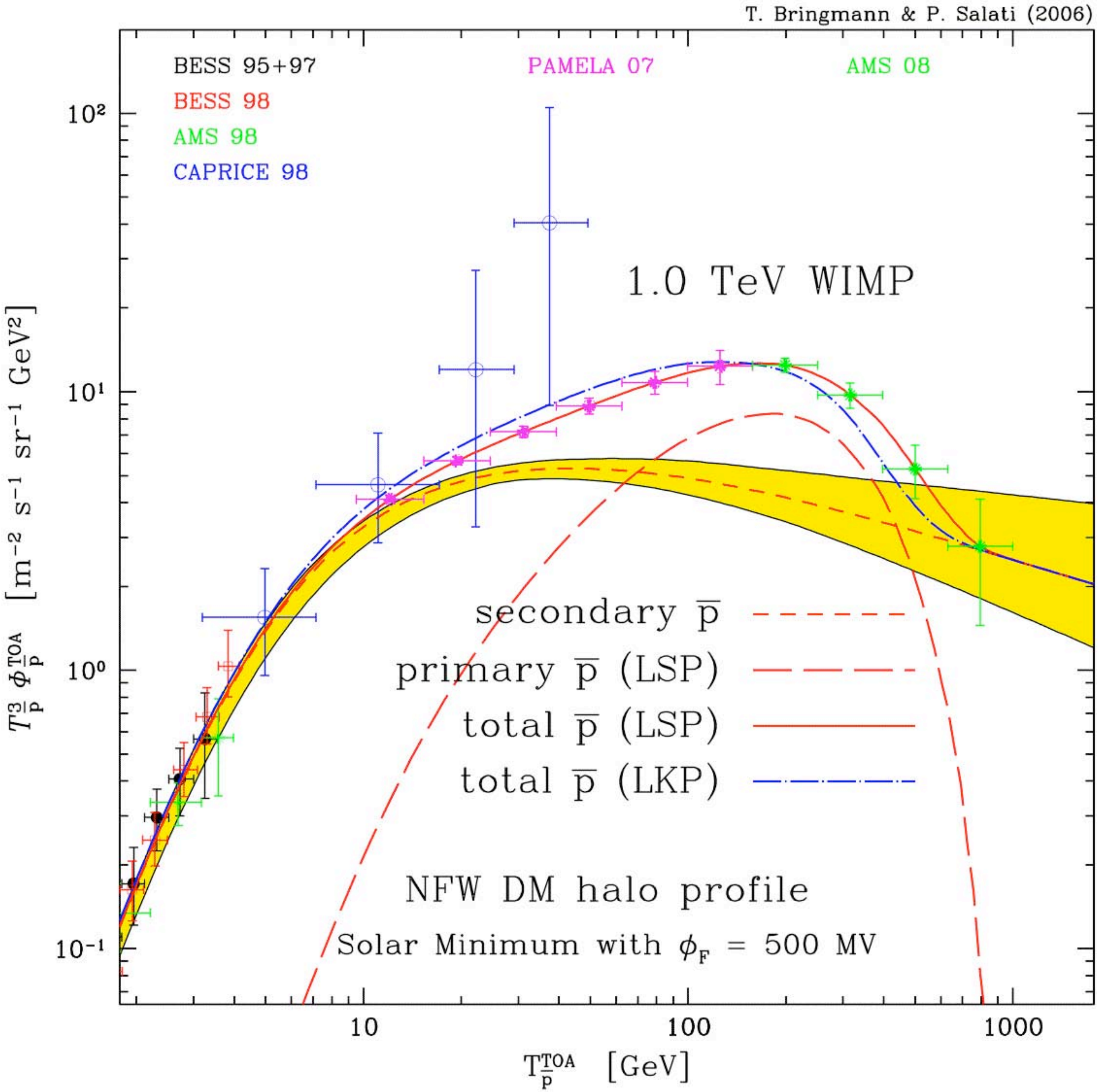
T. Bringmann & P. Salati (2006)
BESS 95+97
BESS 98
AMS 98
CAPRICE 98
PAMELA 07
AMS 08
1.0 TeV WIMP
secondary p̄
primary p̄ (LSP)
total p̄ (LSP)
total p̄ (LKP)
NFW DM halo profile
Solar Minimum with ϕ_F = 500 MV
$T^3_{\bar{p}}\ \phi^{TOA}_{\bar{p}}$ [m^{-2} s^{-1} sr^{-1} GeV^2]
$T^{TOA}_{\bar{p}}$ [GeV]
10
100
1000
10²
10¹
10⁰
10⁻¹

Indirect Dark Matter Detection

Pierre Salati – Université de Savoie & **LAPTH**

1) The messengers of DM annihilation

2) High energy photons and the Galactic centre

3) Hunting for neutrinos in the ice cap

4) Cosmic ray transport : a short overview

5) TeV antiprotons : a new window

6) Uncertainties i ropagation

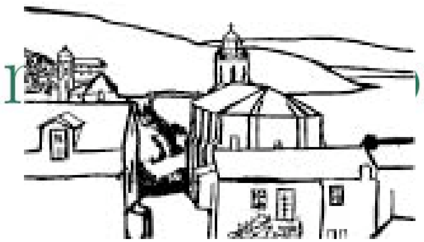

Cosmology and Particle Physics Beyond the Standard Models – Cargese – August 7, 2007

$$\frac{\partial \psi}{\partial t} - \vec{\nabla} \cdot \quad = Q(\vec{x}, E)$$

Energy losses dominate

IC on stellar light & CMB – synchrotron

$$K(E) = K_0 \left\{ \frac{E}{E_0} \right\}^{\delta} = K_0 \, \epsilon^{\delta}$$

$$b(E_{e^+}) = 10^{-16} E_{e^+}^2 \ \mathrm{s}^{-1}$$

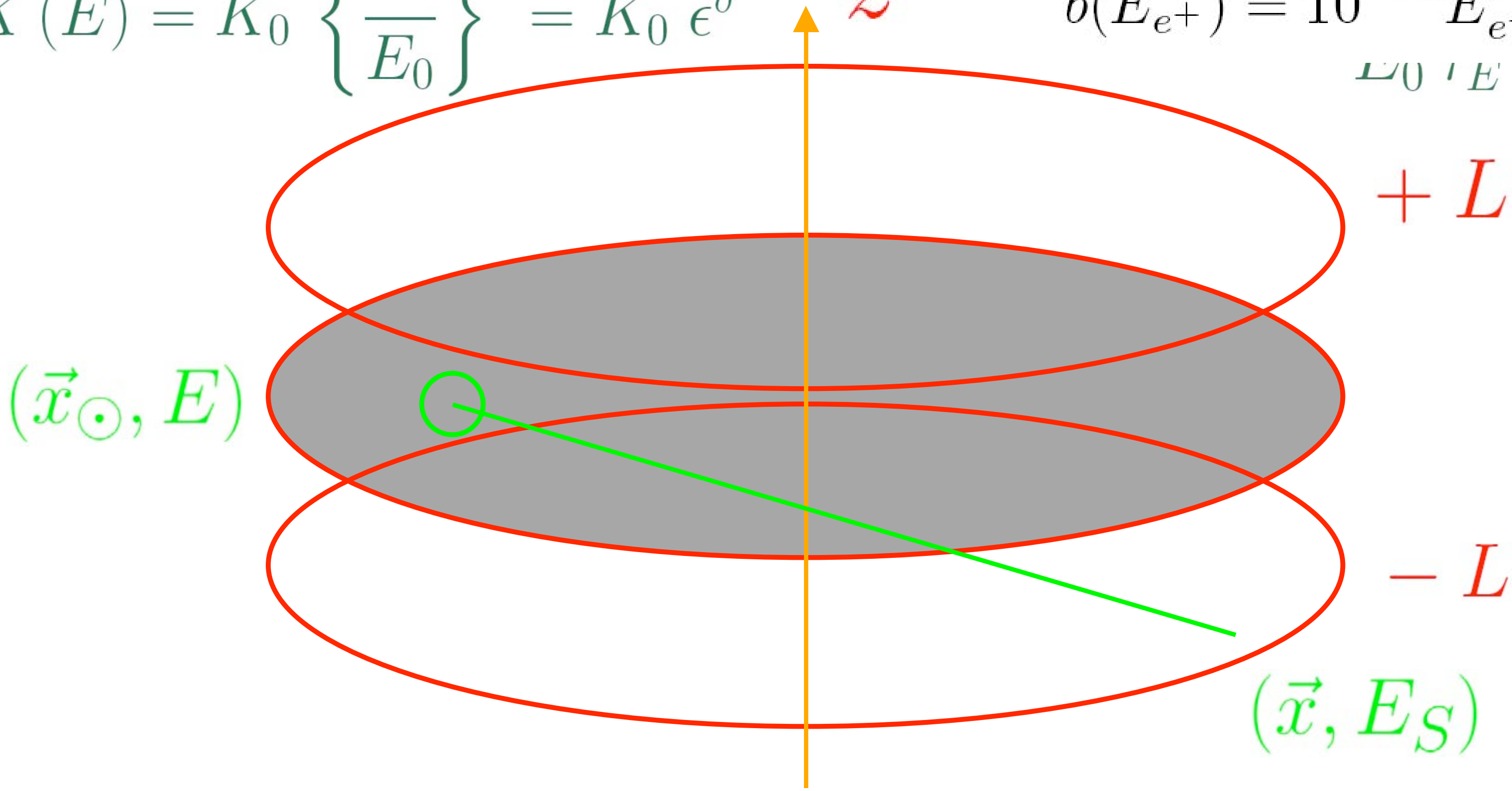

$$K_0 \, \epsilon^{\delta} \, \Delta \psi + \frac{\partial}{\partial \epsilon} \left\{ \frac{\epsilon^2}{\tau_E} \psi \right\} + Q = 0$$

Baltz & Edsjo trick

$$\tilde{\psi} = \epsilon^2 \, \psi \quad \text{and} \quad \tilde{Q} = \epsilon^{2-\delta} \, Q \quad \text{and} \quad \tilde{t}(E) = \tau_E \left\{ v(E) \; = \; \frac{\epsilon^{\delta-1}}{1-\delta} \right\}$$

pseudo–time $\tilde{t}$

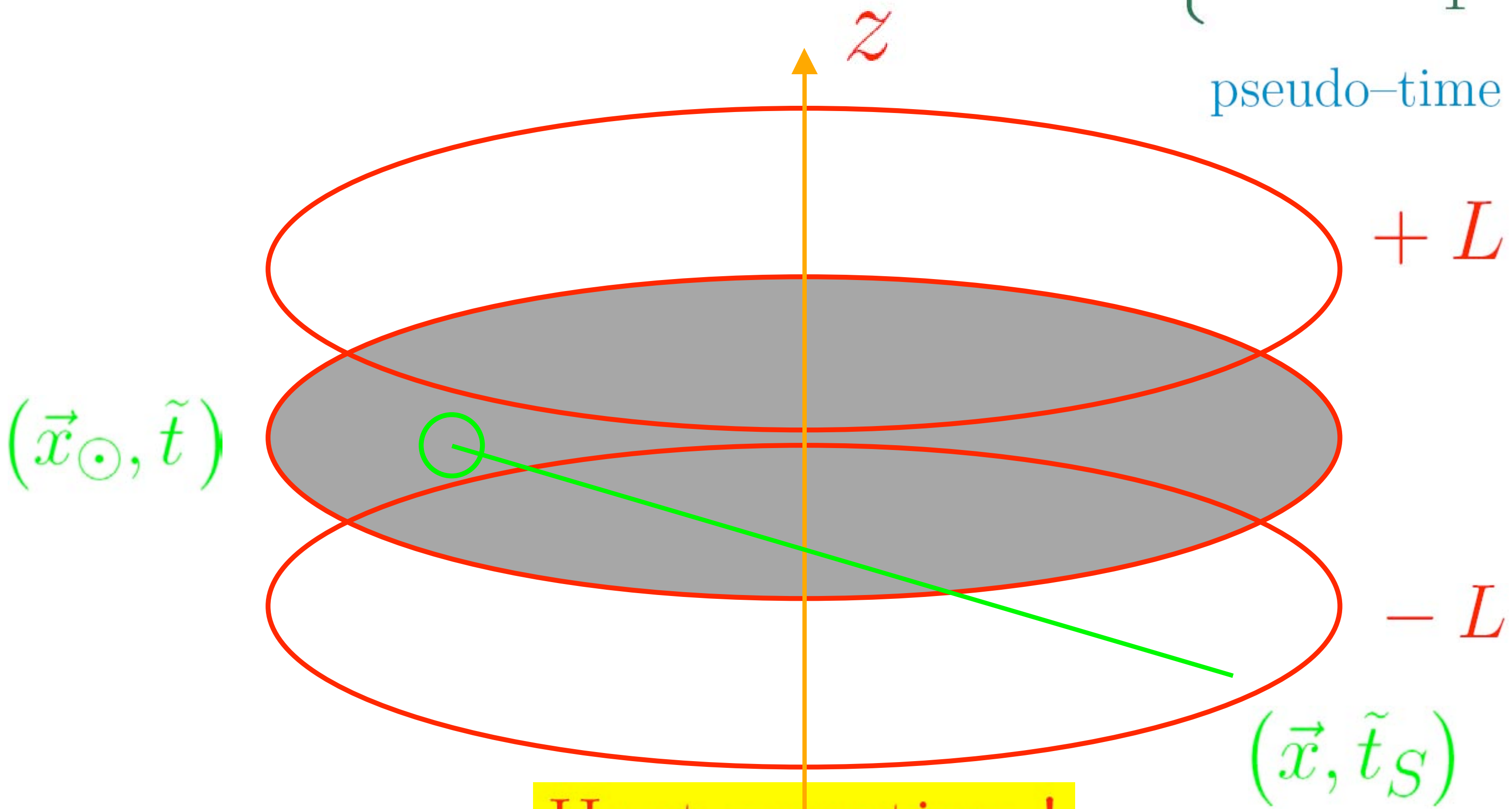

Heat equation !

$$\frac{\partial \tilde{\psi}}{\partial \tilde{t}} \; - \; K_0 \, \Delta \tilde{\psi} \; = \; \tilde{Q} \, (\vec{x}, \tilde{t}\,)$$

Positron propagator

$$E_S = 500\ \text{GeV} \quad \rightarrow \quad E = 450\ \text{GeV}$$

$$G_{e^+}\left(\vec{x}_\odot, E \leftarrow \vec{x}, E_S\right) \; = \; \frac{\tau_E}{E_0\,\epsilon^2}\,\tilde{G}\left(\vec{x}_\odot, \tilde{t} \leftarrow \vec{x}, \tilde{t}_S\right)$$

$$\tilde{\tau} = \tilde{t} - \tilde{t}_S$$

$$\tilde{G}\left(\vec{x}_\odot, \tilde{t} \leftarrow \vec{x}, \tilde{t}_S\right) \; = \; \left\{4\,\pi\,K_0\,\tilde{\tau}\,\right\}^{-3/2} \exp\left\{-\frac{r^2}{4\,K_0\,\tilde{\tau}}\right\}$$

Milky Way seen from above

Positron propagator

$$E_S = 500 \text{ GeV} \quad \rightarrow \quad E = 450 \text{ GeV}$$

$$G_{e^+}\left(\vec{x}_\odot, E \leftarrow \vec{x}, E_S\right) \;=\; \frac{\tau_E}{E_0\,\epsilon^2}\,\tilde{G}\left(\vec{x}_\odot, \tilde{t} \leftarrow \vec{x}, \tilde{t}_S\right)$$

$$\tilde{G}\left(\vec{x}_\odot, \tilde{t} \leftarrow \vec{x}, \tilde{t}_S\right) = \frac{\theta(r_S - r)}{V_S}$$

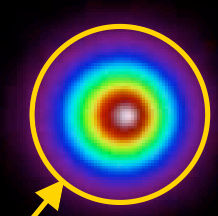

$$\tilde{\tau} = \tilde{t} - \tilde{t}_S$$

$$\frac{1}{V_S} = \int \tilde{G}^2\, d^3\vec{x}$$

Typical range $\lambda_{\rm D} = \sqrt{4\,K_0\,\tilde{\tau}}$

$$V_S = \left(\sqrt{2\pi}\,\lambda_{\rm D}\right)^3$$

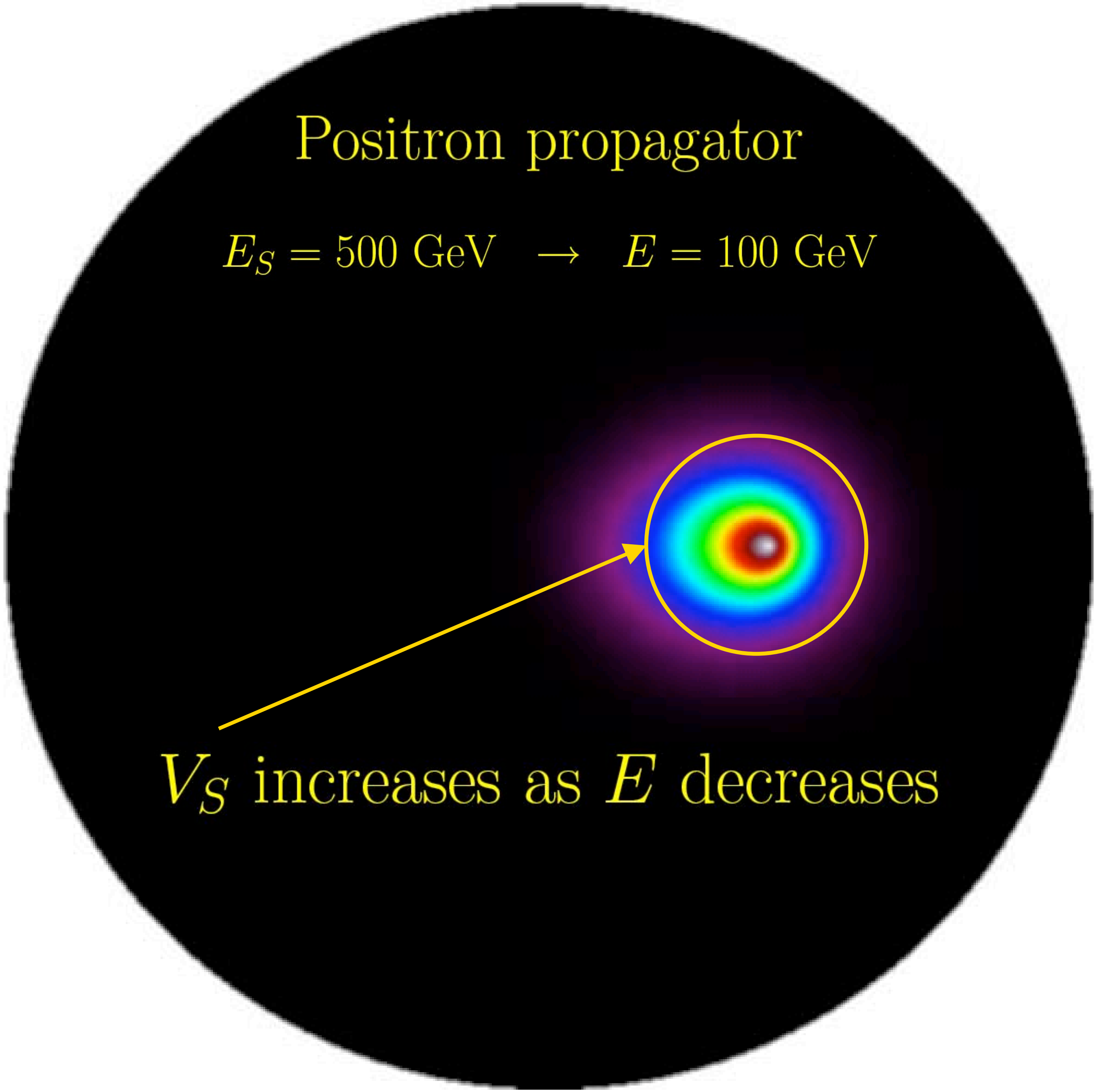
Positron propagator
$E_S = 500$ GeV $\rightarrow$ $E = 100$ GeV
V_S increases as E decreases

Positron injected at E_S

Observed at E_1 or E_2

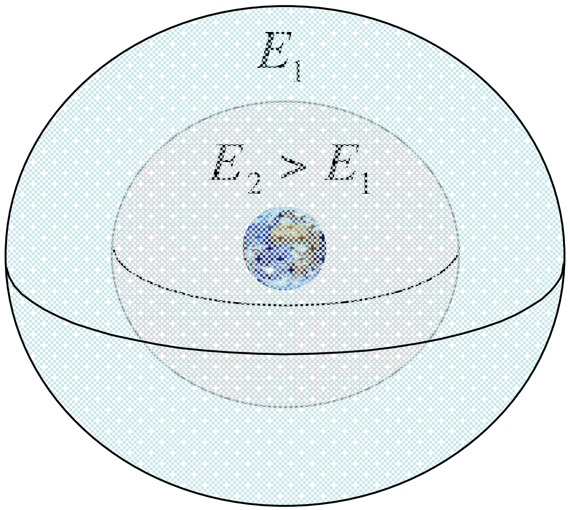

$$\lambda_D = \sqrt{4\,K_0\,\tilde{\tau}}$$

$$V_S = \left(\sqrt{2\pi}\,\lambda_D\right)^3$$

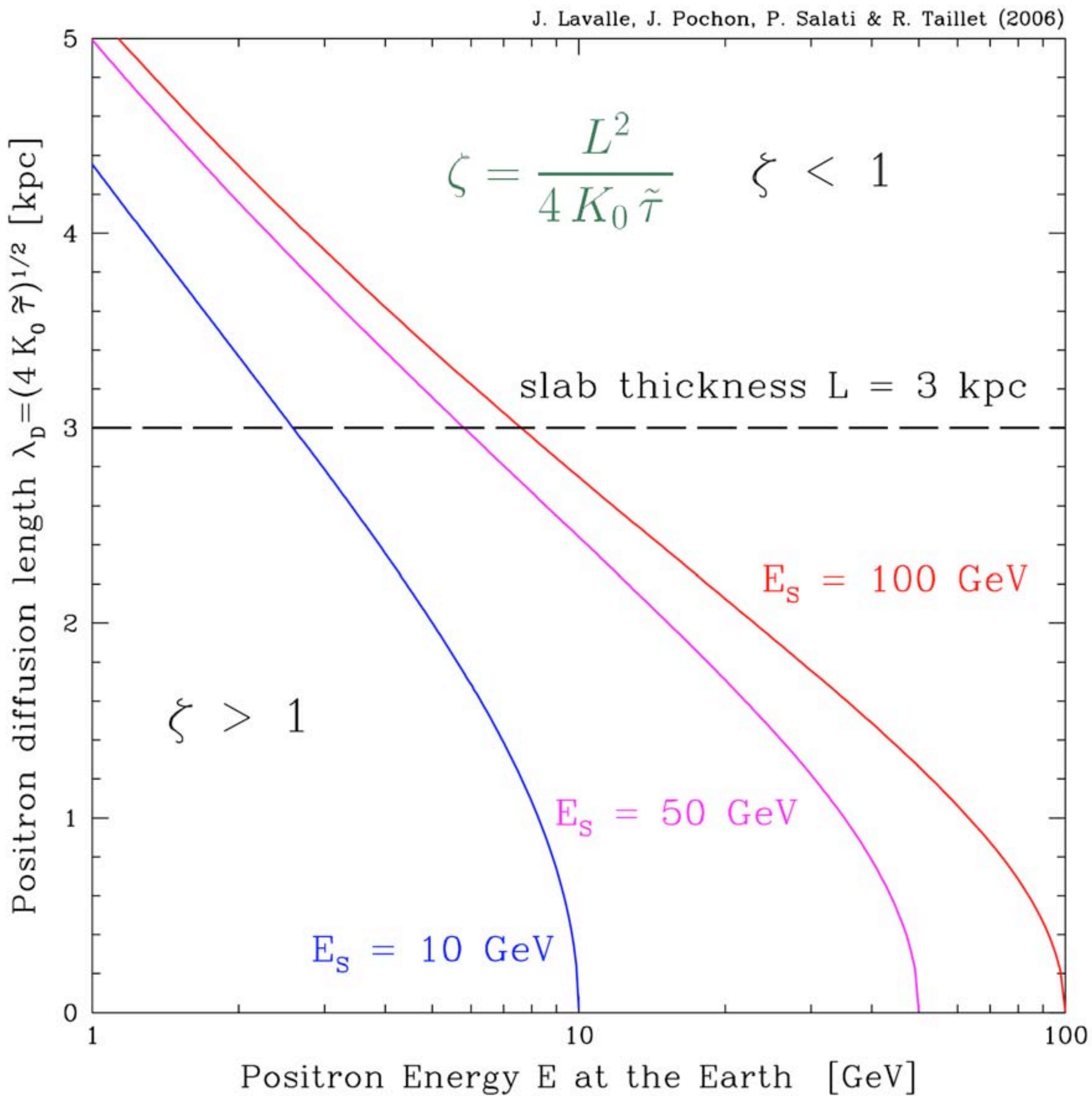

D. Hooper & J. Silk, PRD **71** (2005) 083503

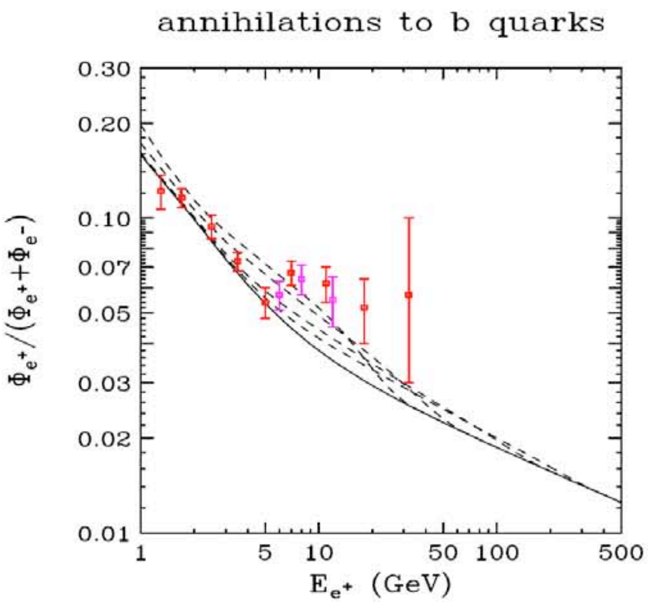

FIG. 6. The positron fraction in the cosmic ray spectrum from dark matter annihilations to b quark pairs. WIMP masses of 50, 100, 300 and 600 GeV were considered. A dark matter distribution with $BF = 5$ (see section III), $\rho(\text{local}) = 0.43\,\text{GeV/cm}^3$ and an annihilation cross section of $\sigma v = 10^{-25}\,\text{cm}^3/\text{s}$ was used.

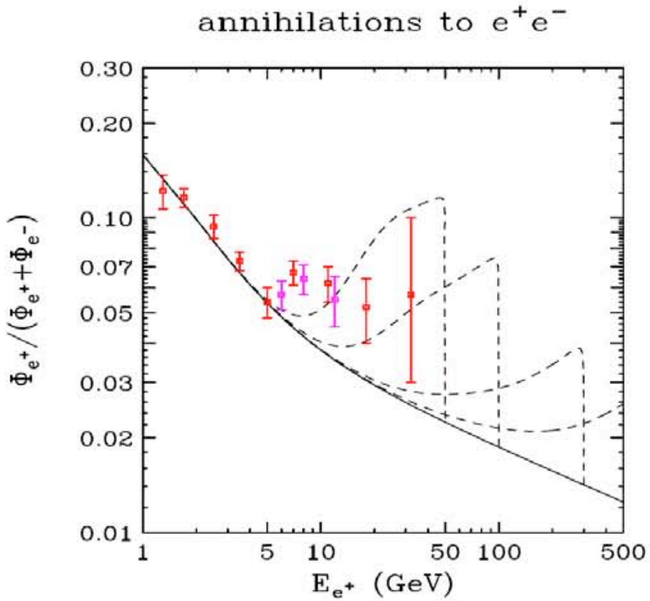

FIG. 8. The positron fraction in the cosmic ray spectrum from dark matter annihilations to e^+e^- pairs. WIMP masses of 50, 100, 300 and 600 GeV were considered. A dark matter distribution with $BF = 5$ (see section III), $\rho(\text{local}) = 0.43\,\text{GeV/cm}^3$ and an annihilation cross section of $\sigma v = 10^{-26}\,\text{cm}^3/\text{s}$ was used.

A.M. Lionetto, A. Morselli & V. Zdravkovic, JCAP **0509** (2005) 010

A consistent investigation is necessary !

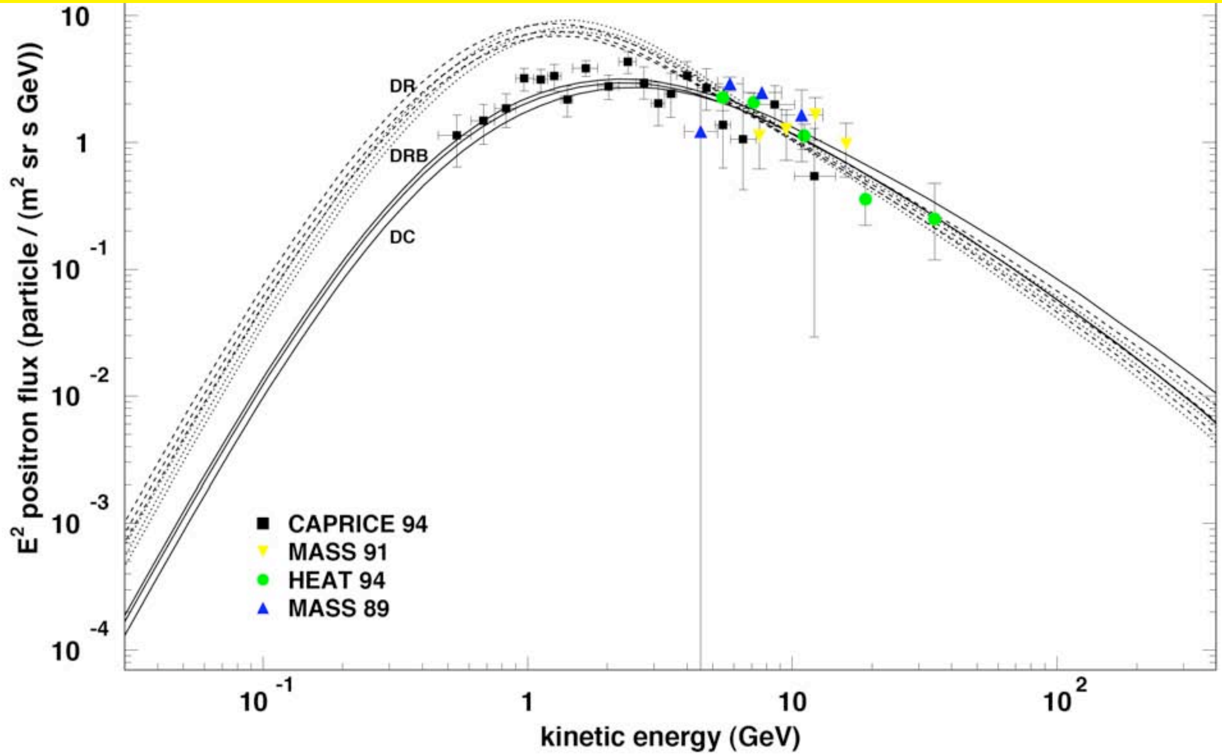

Figure 8. Total uncertainties of positron fluxes and spectra that correspond to the parameters of the best B/C fit for DC model (solid lines around the best fit curve, also solid), DR model (dashed lines around the best fit curve, also dashed) and DRB model (dotted lines around the best fit curve, also dotted). Experimental data are taken from [52]

Radial boundaries are accounted for with a Bessel expansion

$$\mathcal{I}(E \leftarrow E_S) = \int_{\rm DZ} \left\{ \frac{\rho_\chi}{\rho_\odot} \right\}^2 G_{\rm e^+}(\odot, E \leftarrow \mathbf{x}, E_S) \; d^3\mathbf{x}$$

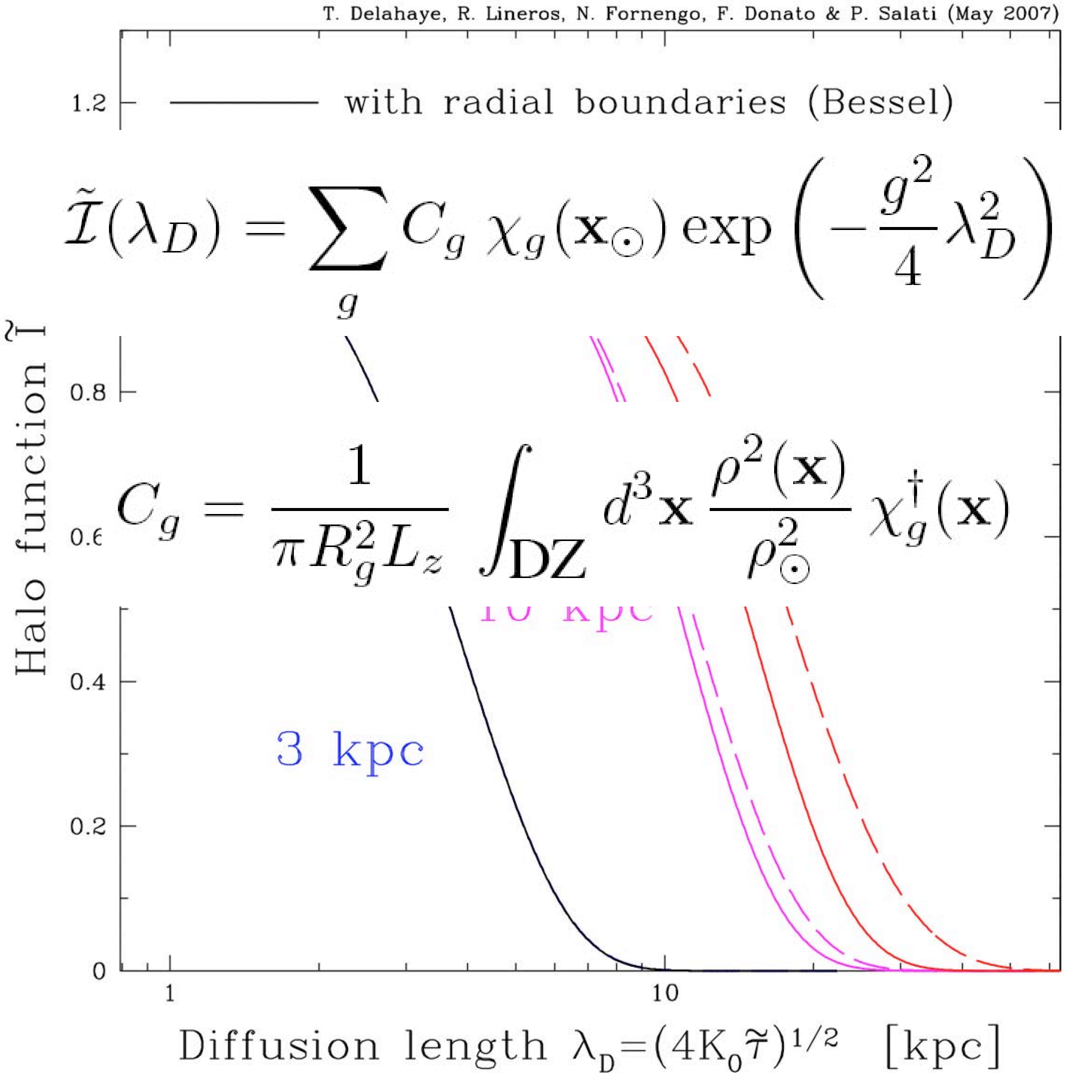

$$\tilde{\mathcal{I}}(\lambda_D) = \sum_g C_g \, \chi_g(\mathbf{x}_\odot) \exp\left(- \frac{g^2}{4} \lambda_D^2 \right)$$

$$C_g = \frac{1}{\pi R_g^2 L_z} \int_{\mathbf{DZ}} d^3\mathbf{x} \, \frac{\rho^2(\mathbf{x})}{\rho_\odot^2} \, \chi_g^\dagger(\mathbf{x})$$

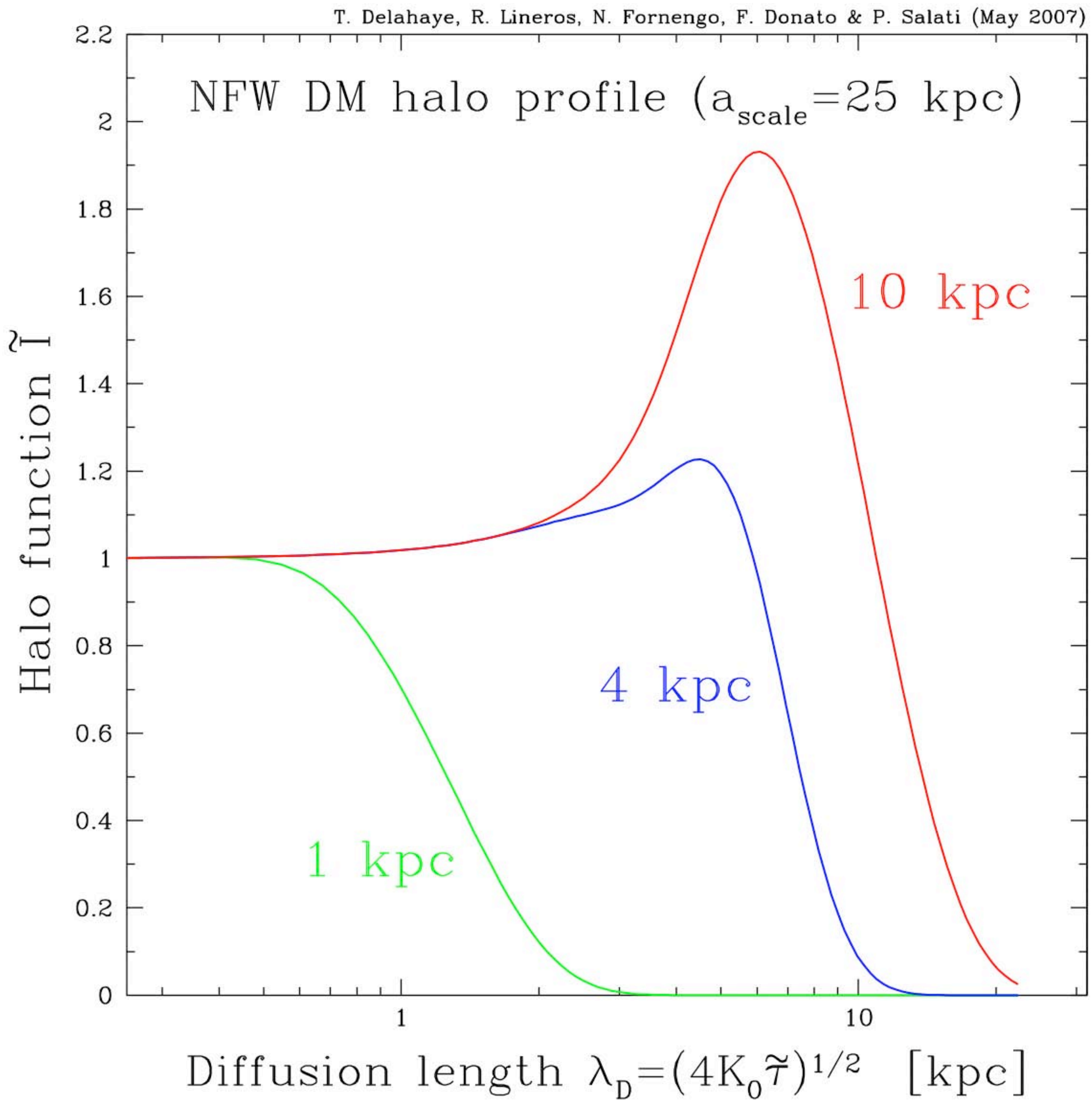

T. Delahaye, R. Lineros, N. Fornengo, F. Donato & P. Salati (May 2007)
NFW DM halo profile (a_scale=25 kpc)
10 kpc
4 kpc
1 kpc
Halo function Ĩ
Diffusion length λ_D=(4K_0τ̃)^1/2 [kpc]
2.2
2
1.8
1.6
1.4
1.2
1
0.8
0.6
0.4
0.2
0
1
10

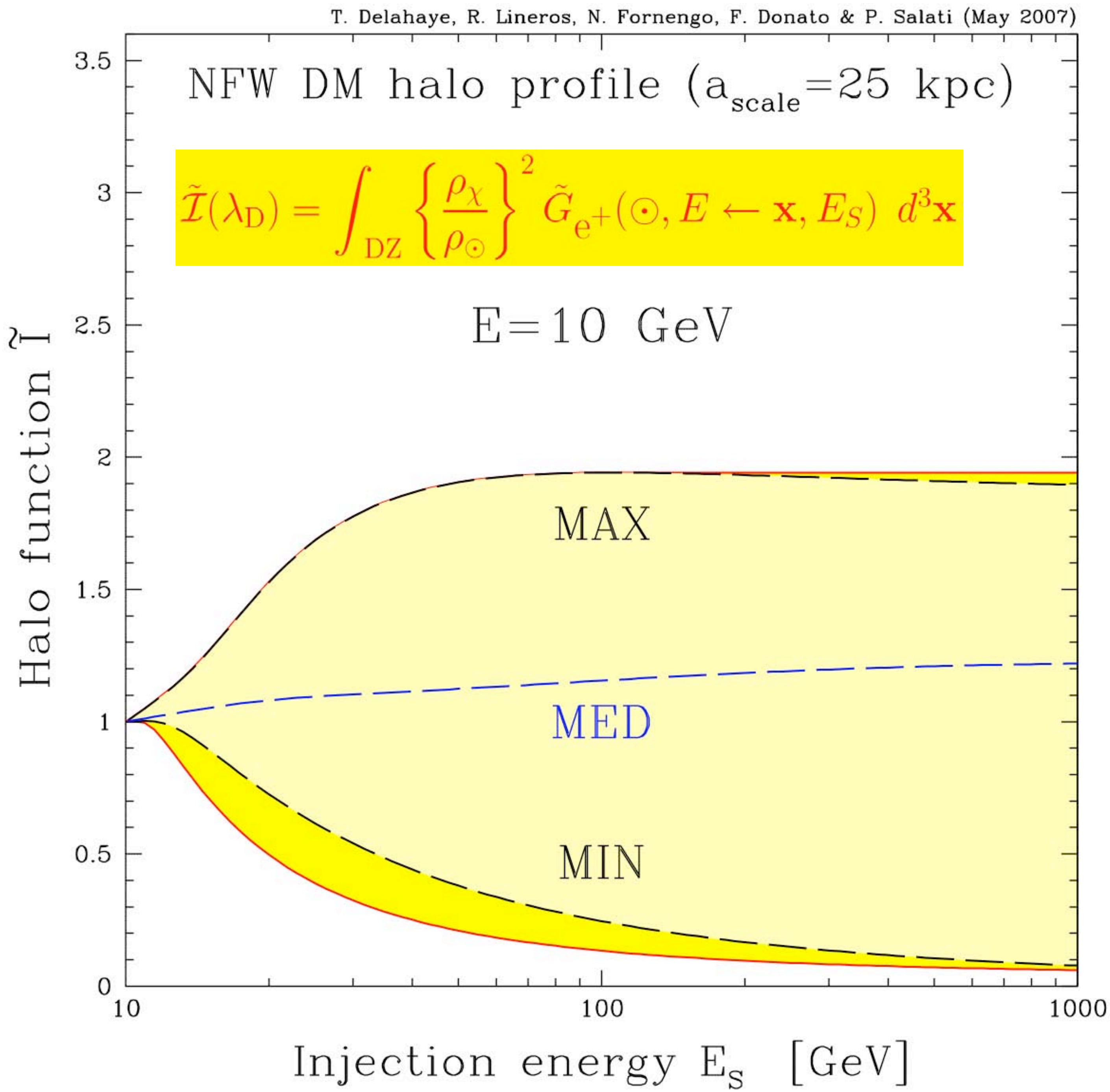
T. Delahaye, R. Lineros, N. Fornengo, F. Donato & P. Salati (May 2007)
NFW DM halo profile (a_{scale}=25 kpc)
$\tilde{\mathcal{I}}(\lambda_D) = \int_{DZ} \left\{ \frac{\rho_\chi}{\rho_\odot} \right\}^2 \tilde{G}_{e^+}(\odot, E \leftarrow \mathbf{x}, E_S) \, d^3\mathbf{x}$
E=10 GeV
MAX
MED
MIN
Halo function $\tilde{I}$
Injection energy E_S [GeV]
0
0.5
1
1.5
2
2.5
3
3.5
10
100
1000

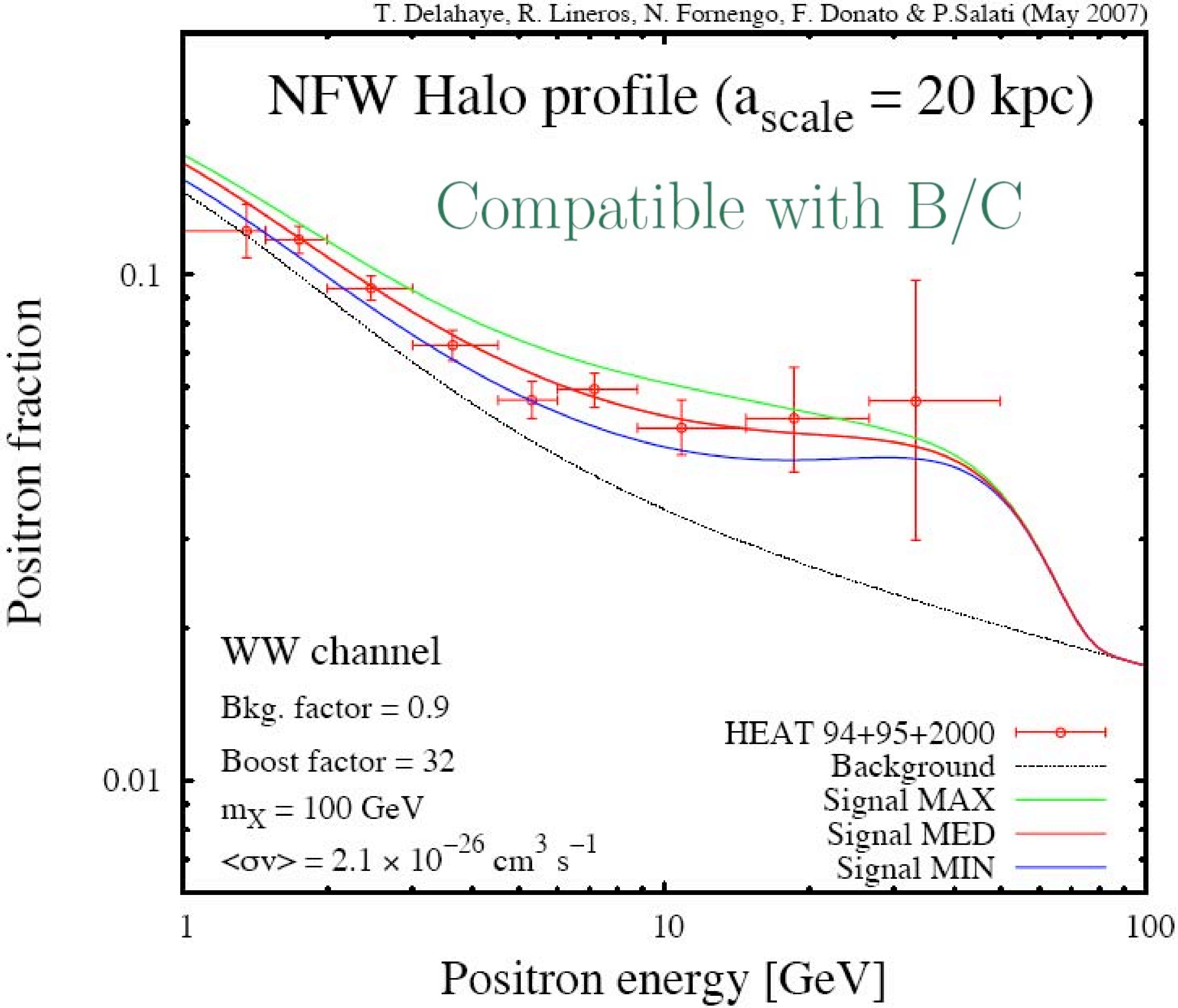

T. Delahaye, R. Lineros, N. Fornengo, F. Donato & P.Salati (May 2007)
NFW Halo profile (a_scale = 20 kpc)
Compatible with B/C
0.1
0.01
Positron fraction
WW channel
Bkg. factor = 0.9
Boost factor = 32
m_X = 100 GeV
<σv> = 2.1 × 10^-26 cm^3 s^-1
HEAT 94+95+2000
Background
Signal MAX
Signal MED
Signal MIN
1
10
100
Positron energy [GeV]